Award Number: W81XWH-09-2-0162

TITLE: Determination of Novel Strategies for Hastening Corneal Wound Healing and Reducing Tissue Inflammation

PRINCIPAL INVESTIGATOR: LTC Jose Capo-Aponte, OD, PhD (USAARL) and
                        Peter S. Reinach, PhD (SUNY)

CONTRACTING ORGANIZATION: ÚåæÁÖæ^æ{áÁÔ~|^äá\↔~^
                          ÁÁÁÁÁÁQá←æ}~~äÊÁÙNÁÁÏÎHÏIJ

REPORT DATE: October 2011

TYPE OF REPORT: Final

PREPARED FOR: U.S. Army Medical Research and Materiel Command
               Fort Detrick, Maryland 21702-5012

DISTRIBUTION STATEMENT:

     Approved for public release; distribution unlimited

The views, opinions and/or findings contained in this report are those of the author(s) and should not be construed as an official Department of the Army position, policy or decision unless so designated by other documentation.

REPORT DOCUMENTATION PAGE

Form Approved
OMB No. 0704-0188

1. REPORT DATE *(DD-MM-YYYY)*	2. REPORT TYPE	3. DATES COVERED *(From - To)*
10/18/2011	Final	21 Sep 2010-20 Sep 2011

4. TITLE AND SUBTITLE	5a. CONTRACT NUMBER
Determination of Novel Strategies for Hastening Corneal Wound Healing and Reducing Tissue Inflammation	W81XWH-09-2-0162
	5b. GRANT NUMBER
	5c. PROGRAM ELEMENT NUMBER

6. AUTHOR(S)	5d. PROJECT NUMBER
LTC Jose Capo-Aponte, OD, PhD	
	5e. TASK NUMBER
lqug(lecr qcr qpvgB wuftm {0b kn	
	5f. WORK UNIT NUMBER

7. PERFORMING ORGANIZATION NAME(S) AND ADDRESS(ES)	8. PERFORMING ORGANIZATION REPORT NUMBER
The Geneva Foundation Lakewood, WA 98496	

9. SPONSORING / MONITORING AGENCY NAME(S) AND ADDRESS(ES)	10. SPONSOR/MONITOR'S ACRONYM(S)
US Army Medical Research and Materiel Command Fort Detrick, MD 21702-5012	
	11. SPONSOR/MONITOR'S REPORT NUMBER(S)

12. DISTRIBUTION / AVAILABILITY STATEMENT

Approved for public release; distribution unlimited

13. SUPPLEMENTARY NOTES

14. ABSTRACT
The aim of this study is to uncover novel transient receptor potential protein vanilloid-1 (TRPV1)-linked cell signaling drug targets for more selective alleviation of trauma-induced corneal symptomology and faster restoration of normal vision. Dual specificity phosphatase (DUSP)5 and DUSP6 selectively control ERK pathway activity and proliferation in human corneal epithelial cells (HCEC). Capsaicin-induced increases in interleukin (IL)-6 and IL-8 occur primarily through phosphorylated JNK1. CB1 and TRPV1 activation induces increases in HCEC proliferation and migration through epidermal growth factor receptor (EGFR) transactivation leading to global mitogen activated protein kinase (MAPK) pathway stimulation. On the other hand, the TRPV1-mediated increases in IL-6 and IL-8 release are elicited through both EGF-dependent and EGFR-independent signaling pathways. Drug-induced modulation of transforming growth factor kinase 1 (TAK-1) activation is a potential target to selectively suppress dysregulated inflammation without compromising TRPV1 promotion of wound healing. In vivo studies demonstrated that TRPV1 activation accelerates epithelial wound healing response in a mice epithelial debridement wound healing model through stimulation of cell proliferation.

15. SUBJECT TERMS
TRPV1, EGF, DUSP, IL-6, IL-8, corneal healing

16. SECURITY CLASSIFICATION OF:			17. LIMITATION OF ABSTRACT	18. NUMBER OF PAGES	19a. NAME OF RESPONSIBLE PERSON USAMRMC
a. REPORT U	b. ABSTRACT U	c. THIS PAGE U	UU	113	19b. TELEPHONE NUMBER *(include area code)*

Standard Form 298 (Rev. 8-98)
Prescribed by ANSI Std. Z39.18

Table of Contents

Introduction
During the recent conflicts in Iraq and Afghanistan, 16% of all trauma encounters involve the eyes. The corneal epithelium is commonly damaged during ocular trauma, which compromises visual function. If epithelial integrity is not rapidly restored following severe injury, it can lead to corneal inflammation, opacification, perforation, ulceration and blindness. This undesirable wound healing outcome occurs because injury breaches epithelial barrier protective functions against damage caused by environmental insults/infections. We had previously identified transient receptor potential protein vanilloid-1 (TRPV1) channels as a novel drug target for reducing these sight threatening outcomes and hastening epithelial wound healing. The aim of this study is to uncover novel TRPV1-linked cell signaling drug targets for more selective alleviation of trauma-induced corneal symptomology and faster restoration of normal vision. The specific objectives were to: 1) determine in human corneal epithelial cells (HCEC) if TRPV1-induced increases in proinflammatory cytokine release are enhanced through loss of function of the protein phosphatase DUSP1/MKP-1 (dual specificity phosphatase-1/MAPK phosphatase MKP-1). Following DUSP1/MKP-1 lentiviral shRNA transduction, we will evaluate if TRPV1 activation of cell signaling and inflammatory cytokine expression are altered by DUSP1/MKP-1 knockdown; 2) determine in mice if corneal TRPV1 activation is sufficient to induce stromal inflammatory macrophage and polymorphonuclear (PMN) tissue infiltration.

Body
As reported in the interim Annual Report, dated Oct 2010, a no-cost extension was submitted to USAMRAA through T.R.U.E. Research Foundation on 20 Aug 2010 to allow continuance of the study and completion of all the experiments required to complete Objectives 1 and 2, that were slightly delayed due to the unexpected deployment of the study PI, LTC Capo-Aponte to Iraq in 2009. The approval for the no-cost extension was received on 3 Feb 2011. In addition, the T.R.U.E. Research Foundation, that manages our grand funds, went out of business in 7 Apr 2011, which forced the study to stop until USAMRAA approved a new award to the Geneva Foundation on 24 May 2011. Nevertheless, all planned experiments for Objectives 1 and 2 were completed during the time allocated by the no-cost extension (20 Sep 2011). Very significant results were obtained from our experiments resulting in three articles in peer-reviewed journals (one published, Appendix A; one in press, Appendix B; one submitted, Appendix C), four poster presentations (Appendices D-F) at the 2011 Association for Research in Vision and Ophthalmology Annual Meeting, and a book chapter (in press, Appendix G).

Key Research Accomplishments Objective 1: In addition to the accomplishments reported in the interim Annual Report submitted on October 2010, we determined during this performance period that in addition to corneal wounding, hypertonic stress also promotes increases in inflammatory cytokine (interleukin (IL)-6 and IL-8) release through TRPV1 signaling pathway activation in HCEC. Since current combat theaters of operations are located in very arid and extreme environments in which most Warfighters experience dry eye, it is expected that such extreme conditions will affect the corneal physiology and consequently the epithelial wound healing process. For these studies, Ca^{2+} signaling was measured in

fura2-AM-loaded HCEC using a single-cell fluorescence imaging system. Western blot analysis was used to evaluate the phosphorylation status of epidermal growth factor receptor (EGFR), extracellular signal-regulated kinases (ERK), p38 mitogen activated protein kinase (MAPK) and nuclear factor (NF)-κB. ELISA was used to assess the effect of TRPV1 activation on the release of proinflammatory and chemoattractant cytokines (i.e., IL-6 and IL-8). We found that hypertonic stress elicited Ca^{2+} transients 2-fold above baseline that were suppressed by the TRPV1-selective antagonists capsazepine and JYL1421 (Appendix A, Fig. 1A). Such transients were enhanced by prostaglandin E2, PGE2 (Appendix A, Fig. 1B). Hypertonicity-induced EGFR transactivation was suppressed by preincubating HCEC with capsazepine, matrix metalloproteinase 1 (MMP1) inhibitor (i.e., TIMP-1), broad-spectrum MMP inhibitor (i.e., GM6001), heparin-bound (HB)-EGF release inhibitor (i.e., CRM 197), or EGFR inhibitor (i.e., AG1478) (Appendix A, Figs. 2A and 2B). ERK and p38 MAPK and NF-κB activation after EGFR transactivation occurred in medium tonicity and in a time-dependent manner (Appendix A, Figs. 3A and 3B). Hypertonicity, mimicking tear film levels described in dry eye patients, induced increases in IL-6 and IL-8 release. They were suppressed by exposure to either capsazepine, AG 1478, ERK inhibitor PD98059, p38 inhibitor SB203580, or NF-κB inhibitor PDTC (Appendix A, 4A and 4B). It is known that NF-κB activation mediates a host of physiological responses that include increases in proinflammatory cytokine release, however, we showed that increases in IκB-α phosphorylation (p-IκB-α) occurred in a tonicity-dependent manner after 1 hr exposure to either 300 (isosmotic), 375, or 450 mOsm medium (Appendix A, Figs. 5A and 5B). Here declines of p-IκB-α formation elicited by the suppression of EGFR, ERK, and p38 MAPK confirm that EGFR and its linked MAPK signaling contribute to NF-κB activation. However, these individual declines did not reach the baseline level, suggesting potential signaling pathways in addition to those linked with EGFR affect NF-κB activity (Appendix A, Figs. 6, 7A, and 7B). More recent results revealed that TRPV1-linked signaling also includes another parallel pathway which through transforming growth factor kinase 1 (TAK1) elicits NF-κB activation (see below). Accordingly, we now know that the inflammatory response to TRPV1 activation is dependent on a maximal level of NF-κB activation only achievable through EGFR transactivation in combination with TAK1 activation. This realization indicates that inflammatory responses to injury may be better controlled through drug control of TAK1 activation.

EGFR phosphorylation or protein kinase C (PKC) stimulation enhances corneal epithelial cell proliferation. Cell proliferation is needed to maintain corneal transparency and vision. To determine in HCEC the involvement of changes in ion transport activity induced through MAPK activation by EGF or PKC, we delineated the cause and effect relationships between ERK1/2 and Na^+,K^+,Cl^- cotransporter 1 (NKCC1) phosphorylation (Appendix B, Fig. 1). Here NKCC1 inhibition by bumetanide suppressed EGF and PDBu-induced increases in cell proliferation. Furthermore, the roles of NF-κB and ERK1/2 were evaluated in mediating negative feedback control of ERK1/2 and NKCC1 phosphorylation through modulating DUSP1 and DUSP6 expression levels. Intracellular Ca^{2+} rises induced by EGF elicited NKCC1 phosphorylation through ERK1/2 activation (Appendix B, Fig. 2). Furthermore, bumetanide suppressed EGF-induced NKCC1 phosphorylation, transient cell swelling and cell proliferation. This cause and effect relationship was similar to that induced by PKC stimulation (Appendix B, Fig. 3). NKCC1 activation occurred through time-dependent increases in protein-protein interaction between ERK1/2 and NKCC1, which were proportional to EGF concentration. ERK1/2 activation by EGF is dependent on Ca^{2+} influx since clamping intracellular Ca^{2+} levels with a chelator, BAPTA, obviated MAPK activation (Appendix B, Fig. 6). In addition, we showed that DUSP6 upregulation obviated EGF and PKC-induced NKCC1 phosphorylation (Appendix B, Fig. 9). NF-κB inhibition by PDTC prolonged ERK1/2 activation through GSK-3 inactivation leading to declines in DUSP1 expression levels (Appendix B, Fig.

10). This response is modulated by changes in DUSP1- and DUSP6-mediated negative feedback control of ERK1/2-induced NKCC1 phosphorylation. These results indicate that the control of cell volume by growth factor receptors is essential for them to induce increases in cell proliferation subsequent to corneal epithelial injury.

We further characterized the signaling pathways mediating TRPV1-induced increases in inflammatory cytokine (IL-6) and chemoattractant (IL-8) release in HCEC. For these studies, SV40 immmortalized HCEC were transduced with lentiviral vectors to establish stable JNK1, NF-κB1 and DUSP1 shRNAmir sublines. Then immunoblotting assessed the extent of suppression of NF-κB1 and DUSP1 expression. In these sublines, changes in TRPV1-induced cell signaling were evaluated by ELISA measuring IL-6 and IL-8 release from cell cultures. We found that capsaicin, a selective TRPV1 agonist, induced time-dependent activation of transforming growth factor activated kinase 1 (TAK1) and MAPK cascades followed by IκBα phosphorylation and rises in IL-6 and IL-8 release (Appendix C, Figs. 1A and 1D). All responses were blocked by the TAK1 inhibitor 5z-7-oxozeaenol (5z-OX) (Appendix C, Figs. 1B and 1C). Ablation of either JNK1 or NF-κB1 expression abolished increased IL-6 and IL-8 release (Appendix C, Figs. 2C and 3B, respectively). However, JNK1 knockdown only partially suppressed capsaicin-induced NF-κB activation while 5z-OX eliminated it (Appendix C, Fig. 4A). On the other hand, loss of NF-κB1 expression diminished capsaicin-induced JNK1 activation as a result of increases in DUSP1 expression whereas PKCδ expression concomitantly declined (Appendix C, Figs. 4B and 4C). In contrast, in the DUSP1 knockdown subline, IL-6 and IL-8 release by capsaicin was augmented due to enhanced and prolonged JNK1 phosphorylation (Appendix C, Figs. 5B and 5C). We also found that capsaicin induced protein-protein interactions between TAK1, TRPV1 and CB1 are required for modulation of TRPV1-induced increases in IL-6 and IL-8 release in HCEC (Appendix D). This was determined by coimmunoprecipating HCEC lysates with either anti TRPV1, TAK1, CB1 or TAB1 (TGF-β-activated protein kinase 1-binding protein 1) antibodies followed by Western blotting with an appropriate antibody to probe for protein-protein interactions. Changes in I-κBα phosphorylation status provided readout of NF-κB activation. ELISA determined the individual effects of TRPV1 and CB1 activation as well as TAK1 inhibition on IL-6 and IL-8 release. The results indicate that 10 μM capsaicin or 5 μM WIN55,212-2 induced transient TAK1 activation through interactions with TRPV1 and CB1. Costimulation of TRPV1 and CB1 induced a smaller increase in TAK1 activation than that obtained from sole TRPV1 stimulation of TAK1 with capsaicin. TRPV1 activation resulted in protein-protein interaction with TAB1 which through its phosphatase activity may shape TAK1 phosphorylation. Okadaic acid, a phosphatase inhibitor, augmented and prolonged TAK1 phosphorylation indicating that TRPV1 and CB1 induce TAK1 phosphorylation. These effects were eliminated by either 5 μM capsazepine or a CB1 antagonist, AM251, respectively. Receptor-induced TAK1, JNK1/2, I-κBα phosphorylation and increases in IL-6 and IL-8 release were fully blocked by a selective TAK1 inhibitor, 10 nM 5z-OX.

Furthermore, we showed that CB1 activation reduces TRPV1-induced responses in HCEC (Appendix E). This finding is consistent with evidence for protein-protein interaction between TRPV1 and CB1 as well as their immunocytochemical co-localization. The CB1 agonist/ antagonist pair: WIN55,212-2 and AM251 were used along with the mixed endogenous TRPV1/CB1 agonist, anandamide (AEA) to characterize functional interaction between CB1 and TRPV1. The TRPV1 agonist/antagonist pair: capsaicin and capsazepine were also used. ELISA determined proinflammatory cytokine release. TRPV1 channel activity was characterized with the planar-patch clamp technique. The results show that coimmunoprecipitation analysis of HCEC identified protein-protein interaction between CB1 and TRPV1. Capsaicin (10 μM)-induced 2.1, 2.5, 1.8-fold increases in IL-6, IL-8 and TNF-α

3

release, respectively. Joint CB1/TRPV1 activation with 10 µM AEA induced rises that were 30-50% smaller than those obtained by capsaicin alone. However, these rises induced by AEA were even larger than those obtained with capsaicin through blocking AEA activation of CB1 with AM251. Capsaicin in HCEC induced 2.1-fold increases in cation channel current at a holding potential of 0 mV. This response to capsaicin could be suppressed during exposure to WIN55,212-2.

Lastly, rapid corneal epithelium wound healing is needed to reestablish its protective barrier properties to decrease tight junctional permeability by increasing translayer electrical resistance. However the effects of CB1 stimulation on tight junctional permeability have not been determined in HCEC. We characterized the effects of CB1 activation on translayer electrical resistance during exposure to a hypertonic stress described in some types of dry eye disease (Appendix F). SV40-immortalized HCEC were seeded on 0.4 µm pore size Transwell® inserts. They were air lifted and reached confluence after about 5 days. Transepithelial layer electrical resistance (TEER) assessed tight junctional integrity. Our results show that after 5 hr exposure to a 300 mOsm isotonic medium, TEER slightly declined to reach 200 ± 3.7 (n=3) ohm*cm^2 and remained stable during the subsequent 15 hr. On the other hand, replacement at 5 hr with a 375 mOsm medium caused TEER to initially fall by 31% with partial restoration to a level at 20 hr that was still 16% below the isotonic control. However, inclusion of the mixed CB1/TRPV1 agonist (i.e., AEA), at concentrations ranging from 1 to 10 µM, in the 375 mOsm medium, hastened complete TEER restoration to its isotonic control level. Recovery occurred as early as 5 hr after imposition of this stress. Under isotonic conditions, 1 µM AEA blocked the initial 31% decline in the baseline TEER. In 375 mOsm medium, the TEER decreased from 20% to 25% despite the presence of either 10 or 20 µM AEA if HCEC were instead pre-exposed for 30 min to either 5µM or 10 µM AM251, a selective CB1 antagonist. Furthermore, in isotonic medium, AM251 prevented TEER recovery from its 5 hr suppressed level to its baseline levels. The TEER in isotonic medium was unchanged with either 5 or 10 µM AM251. These results suggest that during exposure of HCEC to a hypertonic stress simulating tear film osmolarity in some types of dry eye disease, TEER initially declined and failed to fully recover with time. However, CB1 activation by AEA instead caused the TEER to fully recover more rapidly to its isotonic level. These AEA effects were solely due to CB1 activation since AM251 fully inhibited both of them. Taken together, endocannabinoids may have therapeutic potential in reducing declines in epithelial barrier function occurring in some types of dry eye disease.

All data were analyzed using Origin software and comparisons of each of the experimental conditions were made with the controls for each experiment. Each repetition had its own control. Student t-test (unpaired) was applied to determine significance of the means ± SD for each experimental series repeated in triplicate and $P < 0.05$ was considered as significant.

Research Accomplishments for Objective 2: In order to assess the role of TRPV1 activation in mediating an epithelial wound healing response, we compared the rapidity of wound healing in a homozygous TRPV1$^{-/-}$ (knock out, KO) mouse strain with that in its wildtype (WT) counterpart. Different types of corneal wound healing models have been developed by other investigators for this purpose. One type is referred to as the epithelial debridement model. With this model, an epithelial area whose diameter is frequently 2 mm is delineated with a trephine under anesthesia. The circumscribed area is then surgically removed with a knife. Wound closure is monitored by staining the corneal surface with a dye which such as fluorescein. The size of the stained area is a reflection of the remaining unhealed epithelial wound. In order to assess the wound closure area rates, we compared

4

declines in the size of the stained area with time in the WT and KO mice. We found in this epithelial debridement wound healing model using TRPV1 gene ablated mice (i.e., KO) that the wound healing response was delayed relative to that in the WT. We previously reported that after 30 hr the wound had completely closed in the WT since there was no evident green staining whereas in the KO even after 36 hr there was still detectable staining (Appendix H, Figs. A and B). As wound healing is a consequence of increases in both cell proliferation and migration, we assessed the contribution by cell proliferation to wound healing kinetics. We compared the intensity of anti-BrdU antibody staining in the two different genotypes (i.e., KO and WT). It was evident at 24 hr that there was more staining in the WT than in the KO, which suggests that TRPV1 activation by injury accelerates wound healing through stimulation of cell proliferation (Appendix H, Fig. C). In this study, we found that TRPV1 activation makes a double-edge contribution through EGFR transactivation to stimulate wound healing. The promotional effect is elicited through increases in cell proliferation and migration. On the other hand, its activation counters healing through increases in expression levels of IL-6 and IL-8. Such increases can be associated in vivo with compromised visual acuity due to chronic inflammation, which impedes or even prevents wound healing in response to severe injury. In order to validate the importance of TRPV1 activation by epithelial debridement to wound closure, we compared the wound healing response by making a 2.5 mm wound in WT mice. Their eyes (N=96) were organ cultured for up to 36 hr and exposed to either: a) 10 µM capsaicin; b) 0.5 µM SB366791 (TRPV1 antagonist); c) capsaicin and 0.5 µM SB366791 (Appendix I). The rates of wound closure were compared to the untreated control and assessed based on time-dependent declines in fluorescein staining. The results indicate that in the capsaicin treated group wound closure was complete already whereas it was delayed in the control and the SB366791 treated groups. Only at 30 hr was wound closure reached in both the control and SB366791 groups. At 24 hr there was slightly more staining in the SB366791 group than in the control group. On the other hand, at 18 hr the wound area in the capsaicin treated group was smaller than in those mice eyes incubated instead with both capsaicin and SB366791. Taken together, these results further substantiate our mouse eye results and those obtained with HCEC that TRPV1 activation by injury induces through EGFR transactivation increases in cell proliferation and migration that make an essential contribution to wound closure.

In Objective 2, we also assessed if there is an inflammatory response to epithelial debridement. This was done by performing immunohistochemistry to assess if corneal TRPV1 activation is sufficient to induce stromal inflammatory macrophage and PMN tissue infiltration. To make this assessment, we probed for PMN and macrophage stromal infiltration from the periphery during the wound healing response induced by epithelial debridement. This evaluation entailed using myeloperoxidase to stain for stromal PMN cell density and F4/80 to determine macrophage infiltration. Our results indicate that at no time point was it possible to detect any increases in their levels during wound healing. Therefore, epithelial debridement is a relatively mild injury, which is not severe enough to induce a chronic inflammatory response. In other words, epithelial debridement does not lead to sufficient TRPV1 activation to elicit a dysregulated inflammatory response. The inflammation, if any induced by epithelial debridement, is self-limiting and resolves itself prior to wound closure. However, we found that CB1 activation in the WT blocks neutrophil infiltration. CB1 activation has this effect since in the CB1 heterozygous and homozygous KO mice wound closure in the debridement model is delayed compared to that in the WT. This delay suggests that loss of CB1 suppressive function on neutrophil infiltration delays epithelial migration. Its suppressive role is evident since in the CB1 KO at 10 hr following injury show myeloperoxidase staining whereas in the WT no staining is evident (Appendix J) and wound closure was slightly faster than in the CB1 KO (Appendix K). We would like to characterize the role of TRPV1 activation in affecting the

rates of wound closure in a more damaging mouse wound healing model (such as an alkaline burn model as we originally proposed, but was rejected by one of the original grant reviewers). Based on our in vitro studies with HCEC, we hypothesize that a more severe injury is required to induce a dysregulated inflammatory response. Once we have established such a more severe injury model, it will be possible to assess the individual roles of TRPV1 activation on corneal resident and infiltrating inflammatory cells in inducing upregulation of proinflammatory and chemoattractant cytokines that severely compromise wound healing outcome. Such studies are needed to identify novel downstream cell signaling drug targets for reducing the complications arising from dysregulated inflammation without compromising endogenous endovanilloid-induced TRPV1 stimulation leading to increases in cell proliferation and migration.

Key Research Outcomes:
- We developed HCEC sublines expressing shRNAs for inhibition of DUSP1, DUSP6, JNK1, and NFκB gene expression (DUSP1[i], DUSP6[i], JNK[i], and NFκB[i]).
- We developed an over-expressed DUSP6 HCEC subline (DUSP6^{+}).
- We determined that ERK1/2 and NKCC1 phosphorylation induced by EGF receptor or PKC activation in HCEC.
- We determined that NKCC1 activation occurred through time-dependent increases in protein-protein interaction between ERK1/2 and NKCC1, which were proportional to EGF concentration.
- We determined that EGF receptor and PKC activation induce increases in HCEC proliferation through ERK1/2 interaction with NKCC1.
- We determined that NF-κB and ERK1/2 mediate negative feedback control of ERK1/2 and NKCC1 phosphorylation through modulating DUSP1 and DUSP6 expression levels.
- We determined that TRPV1 agonists induced time-dependent activation of TAK1 and MAPK cascades followed by IκBα phosphorylation and rises in IL-6 and IL-8 release.
- Corneal epithelial debridement is a relatively mild injury, which is not severe enough to induce a chronic inflammatory response; therefore it does not lead to sufficient TRPV1 activation to elicit a dysregulated inflammatory response.

Reportable Outcomes
- Pan, Z., Wang, Z., Yang, H., Zhang, F., Reinach, P.S. 2011. TRPV1 Activation Is Required for Hypertonicity-Stimulated Inflammatory Cytokine Release in Human Corneal Epithelial Cells. *Investigative Ophthalmology and Vision Science*. 52;1:485-93.
- Wang, Z., Bildin, V., Yang, H., Capó-Aponte, Yand, Y., Reinach, P.S. 2011. Dependence of Corneal Epithelial Cell Proliferation on Modulation of Interactions Between ERK1/2 and NKCC1. *Cellular Physiology and Biochemestry*. 27: xx (in press).
- Wang, Z., Yang, Y., Yang, H., Capó-Aponte, J.E., Tachado, S.D., Wolosin, J.M. Reinach, P.S. NFκB Feedback control of JNK1 Activation Modulates TRPV1-induced Increases in IL-6 and IL-8 Release by Human Corneal Epithelial Cells. *Molecular Vision*. Submitted Aug 2011.
- Wang, Z., Yang, H., Capó-Aponte, J.E., Parekh, N., Reinach, P.S. 2011. Tak1 Interactions with TRPV1 and CB1 Control IL-6 and IL-8 Release in Human Corneal Epithelial Cells. ARVO Abstract 416/D1063.
- Yang, H., Mergler, S., Wang, Z., Varadaraj, K., Kumari, S.S., Reinach, P.S. 2011. CB1 Activation Reduces TRPV1-induced Responses in Human Corneal Epithelial Cells ARVO Abstract 2053/D1060.

- Yuan, J., Zhang, F., Yang, H., Reinach, P.S. 2011. CB1 Receptor Activation Elicits Human Corneal Epithelial Layer Barrier Function Restoration During Exposure To A Hypertonic Stress. ARVO Abstract 4393.
- Zan, P, Capó-Aponte, J.E., Reinach, P.S. 2011. Book Chapter: Transient Receptor Potential (TRP) Channels in the Eye, in *Ophthalmology*. Publisher: InTech (in press).

Conclusions
- Hypertonic stress-elicited TRPV1 channel stimulation mediates increases in a proinflammatory cytokine IL-6 and a chemoattractant IL-8 by eliciting EGFR transactivation, MAPK, and NF-κB activation. Selective drug modulation of either TRPV1 activity or its signaling mediators may yield a novel approach to suppressing inflammatory responses occurring in dry eye syndrome.
- EGF receptor and PKC activation induce increases in HCEC proliferation through ERK1/2 interaction with NKCC1. This response is modulated by changes in DUSP1- and DUSP6-mediated negative feedback control of ERK1/2-induced NKCC1 phosphorylation.
- TRPV1 activation elicits increases in IL-6 and IL-8 release through two TAK1-dependent signaling pathways leading to NF-κB activation. One of them depends on JNK1 activation while the other is JNK1-independent.
- Positive feedback control of JNK1 activation by NF-κB is required for capsaicin to elicit IL-6 and IL-8 rises. NF-κB mediates such regulation through changes in DUSP1 expression, which in turn modulate JNK1 phosphorylation. NF-κB may control DUSP1 expression by altering PKCδ expression.
- Endocannabinoids may have therapeutic potential in reducing declines in epithelial barrier function occurring in some types of dry eye disease.
- Drug-induced modulation of TAK-1 activation is a potential target to selectively suppress dysregulated inflammation without compromising TRPV1 promotion of wound healing.
- Corneal epithelial debridement is a relatively mild injury, which is not severe enough to induce a chronic inflammatory response; therefore it does not lead to sufficient TRPV1 activation to elicit a dysregulated inflammatory response.

Appendix
A. Pan, Z., Wang, Z., Yang, H., Zhang, F., Reinach, P.S. 2011. TRPV1 Activation Is Required for Hypertonicity-Stimulated Inflammatory Cytokine Release in Human Corneal Epithelial Cells. Investigative Ophthalmology and Vision Science. 52;1:485-93.
B. Wang, Z., Bildin, V., Yang, H., Capó-Aponte, Yand, Y., Reinach, P.S. 2011. Dependence of Corneal Epithelial Cell Proliferation on Modulation of Interactions Between ERK1/2 and NKCC1. Cellular Physiology and Biochemestry. 27: xx (in press).
C. Wang, Z., Yang, Y., Yang, H., Capó-Aponte, J.E., Tachado, S.D., Wolosin, J.M. Reinach, P.S. NFκB Feedback control of JNK1 Activation Modulates TRPV1-induced Increases in IL-6 and IL-8 Release by Human Corneal Epithelial Cells. Molecular Vision. Submitted Aug 2011.
D. Wang, Z., Yang, H., Capó-Aponte, J.E., Parekh, N., Reinach, P.S. 2011. Tak1 Interactions with TRPV1 and CB1 Control IL-6 and IL-8 Release in Human Corneal Epithelial Cells. ARVO Abstract 416/D1063.

E. Yang, H., Mergler, S., Wang, Z., Varadaraj, K., Kumari, S.S., Reinach, P.S. 2011. CB1 Activation Reduces TRPV1-induced Responses in Human Corneal Epithelial Cells ARVO Abstract 2053/D1060.
F. Yuan, J., Zhang, F., Yang, H., Reinach, P.S. 2011. CB1 Receptor Activation Elicits Human Corneal Epithelial Layer Barrier Function Restoration During Exposure To A Hypertonic Stress. ARVO Abstract 4393.
G. Zan, P., Capó-Aponte, J.E., Reinach, P.S. 2011. Book Chapter: Transient Receptor Potential (TRP) Channels in the Eye, in *Ophthalmology*. Publisher: InTech (in press).
H. Unpublished data showing wound closure of TRPV1 KO and WT mice after epithelial debridement.
I. Unpublished data showing wound closure of untreated control and drug-inhibited TRPV1 WT mice after epithelial debridement.
J. Unpublished data showing myeloperoxidase staining in CB1 KO and WT mice after epithelial debridement.
K. Unpublished data showing wound closure in the CB1 KO mice after epithelial debridement.

Appendix A

TRPV1 Activation Is Required for Hypertonicity-Stimulated Inflammatory Cytokine Release in Human Corneal Epithelial Cells

Zan Pan,[1,2] Zheng Wang,[1] Hua Yang,[1] Fan Zhang,[1] and Peter S. Reinach[1]

PURPOSE. To determine whether hypertonic stress promotes increases in inflammatory cytokine release through transient receptor potential vanilloid channel type 1 (TRPV1) signaling pathway activation in human corneal epithelial cells (HCECs).

METHODS. Hyperosmotic medium was prepared by supplementing isotonic Ringers solution with sucrose. Ca^{2+} signaling was measured in fura2-AM–loaded HCECs using a single-cell fluorescence imaging system. Western blot analysis evaluated the phosphorylation status of EGFR, ERK, p38 MAPK, and nuclear factor (NF)-κB. ELISA assessed the effect of TRPV1 activation on the release of IL-6 and IL-8.

RESULTS. A 450 mOsm hypertonic stress elicited 2-fold Ca^{2+} transients that were suppressed by the TRPV1-selective antagonists capsazepine and JYL 1421. Such transients were enhanced by PGE2. Hypertonicity-induced EGF receptor (EGFR) transactivation was suppressed by preincubating HCECs with capsazepine, matrix metalloproteinase 1 (MMP1) inhibitor TIMP-1, broad-spectrum MMP inhibitor GM 6001, heparin-bound (HB)-EGF inhibitor CRM 197, or EGFR inhibitor AG 1478. ERK and p38 MAPK and NF-κB activation after EGFR transactivation occurred in tonicity and in a time-dependent manner. Hypertonicity-induced increases in IL-6 and IL-8 releases were suppressed by exposure to capsazepine, AG 1478, ERK inhibitor PD 98059, p38 inhibitor SB 203580, or NF-κB inhibitor PDTC.

CONCLUSIONS. Hypertonic stress–elicited TRPV1 channel stimulation mediates increases in a proinflammatory cytokine IL-6 and a chemoattractant IL-8 by eliciting EGFR transactivation, MAPK, and NF-κB activation. Selective drug modulation of either TRPV1 activity or its signaling mediators may yield a novel approach to suppressing inflammatory responses occurring in dry eye syndrome. (*Invest Ophthalmol Vis Sci.* 2011;52: 485–493) DOI:10.1167/iovs.10-5801

The superficial corneal epithelial layer protects the cornea from losses in tissue transparency and deturgescence resulting from environmental insults. This barrier function maintenance is dependent on the continuous renewal of corneal epithelial cells and the integrity of tight junctions between the superficial epithelial cells in this layer. One environmental stress that can compromise corneal epithelial barrier function is exposure to hyperosmotic tear film, which occurs in dry eye disease.[1,2] Increases in tear osmolarity promote ocular surface inflammation by activating proinflammatory cytokine release and enhancing inflammatory cell infiltration. These tear gland dysfunction and tear film instability; thus, corneal erosion and opacification may ensue. Although therapeutic approaches such as hypotonic or isotonic artificial tears provide symptomatic relief in dry eye disease patients by lowering their tear osmolarity,[3,4] development of drugs that can effectively suppress receptor-mediated inflammation is limited.

Emerging evidence indicates that the transient receptor potential vanilloid family members mediate responses to osmotic stress. TRPV channels function as a trans-plasma membrane ion entry pathway composed of six transmembrane-spanning subunits in the form of a tetramer. There are seven members (TRPV1-TRPV7) in this subfamily. Only 2 of 7 members have been documented to be activated by osmotic challenges. Our earlier study reveals TRPV4 contributes to hypo-osmosensing mechanism and initiates regulatory volume decrease in HCECs. Similar findings have been made in rat neurons, HaCaT cells, and human airway smooth muscle cells.[5–8] However, exposure to hyperosmotic challenges does not induce TRPV4 channel activation in HCECs and some other tissues.[8–10]

Some studies have identified TRPV1 as a hyperosmotic sensor. Liu et al.[11] found that hypertonicity sensitized capsaicin induced Ca^{2+} transients and enhanced TRPV1 translocation to plasma membrane in rat trigeminal neurons. Sharif et al.[12] and Yokoyama et al.[13] revealed that an N-terminal variant of the TRPV1 channel is required for hyperosmotic sensing but not for hypertonicity-induced regulatory volume increase in arginine vasopressin (AVP)-releasing neurons in supraoptic nucleus. On the other hand, it remains uncertain whether TRPV1 serves as a hyperosmotic sensor to stimulate fluid intake.[14,15] In addition, there is limited information regarding the role of TRPV1 hyperosmosensor in nonneuronal tissues. In HCECs, TRPV1 activation by capsaicin induces increases in IL-6 and IL-8 release through mitogen-activated protein kinase (MAPK) pathway stimulation.[16] As increases in IL-6 and IL-8 contribute to inflammation occurring in dry eye disease, it is possible that TRPV1 activation by hypertonicity can contribute to these increases.

The signaling mechanism through which hypertonic stress increases proinflammatory cytokine release is of great interest. EGF receptor (EGFR) and its linked signaling cascades are not only a key promoter of cell proliferation and migration but also a critical mediator of various pathophysiological events.[17] EGFR activation has been identified in response to UV light, osmotic stress, membrane depolarization, cytokines, chemokines, and cell adhesion elements. In the corneal epithelium, EGFR transactivation is elicited by lysophosphatidic acid (LPA), adenosine triphosphate (ATP), wounding, and flagellin.[18] These findings prompted us to determine whether hyperosmotic stimuli–induced increases in proinflammatory cytokine re-

lease are dependent on EGFR transactivation and the role of TRPV1 in such processes.

MAPK family activation, a downstream event of EGFR stimulation, can also be triggered by osmotic shock. Both hypertonic and hypotonic exposures can activate MAPK.[16,19]Exposure of the mouse corneal surface to hypertonic stress stimulated ERK, p38, and Jun NH$_2$-terminal kinase (JNK) MAPK signaling, which led to increases in IL-1β, TNFα, and metalloproteinase (MMP)-9 expression levels.[20,21]Both the duration and the magnitude of MAPK phosphorylation are determinants of types of responses induced by their activation.[22]In HCECs, the duration and magnitude of ERK and p38 phosphorylation determined EGF-induced proliferation and migration. Prolonged p38 phosphorylation by suppression of ERK signaling pathway promotes EGF-induced migration. On the other hand, proliferation was enhanced when ERK phosphorylation was prolonged by eliminating glycogen synthase kinase (GSK-3)–induced dephosphorylation of ERK.[23,24] Such modulation of MAPK-induced signaling by EGF and neural growth factor (NGF) occurs in PC12 cells, a neural precursor cell line. With EGF, ERK MAPK activation peaked at 5 minutes and then rapidly declined. This pattern of ERK activation promoted cell proliferation. In contrast, with NGF, ERK activation remained high for hours, and the cells stopped proliferating and instead differentiated into neurons.[25]As different responses induced by TRPV1 and EGF activation are both dependent on MAPK signaling, it is convincible that each of the responses is associated with a unique pattern of MAPK stimulation.

Another mediator in the process of hypertonicity-induced inflammation is nuclear factor (NF)-κB protein. NF-κB is a latent transcription factor that lies at the center of many inflammatory responses induced by infection and injury.[26–28] NF-κB is implicated in mediating dry eye–induced ocular surface inflammation because the inhibition of NF-κB reduces the inflammatory response.[1] However, given the complex etiology of dry eye inflammation, including cytokines, chemokines, and MMPs, the importance of NF-κB responsiveness to hypertonic stress is unclear in HCECs. Furthermore, the interaction between MAPK and NF-κB in mediating inflammation depends on types of stimuli and cells.[29–32]Therefore, investigation is warranted to probe for the role of MAPK and NF-κB in hypertonicity-induced inflammation in corneal epithelial cells.

In the present study, we identified that exposure to hyperosmotic stimuli activated the TRPV1 channel. This resulted in EGFR transactivation through metalloproteinase-dependent HB-EGF shedding. TRPV1-EGFR signaling cascades contributed to the phosphorylation of ERK and p38 MAPK and to subsequent activation of NF-κB, leading to increases in IL-6 and IL-8 release.

MATERIALS AND METHODS

Materials

TRPV1 inhibitor capsazepine, EGFR antagonist AG 1478, PGE2, MMP-1 inhibitor TIMP1, broad-spectrum MMP inhibitor GM 6001, HB-EGF inhibitor CRM 197, ERK inhibitor PD 98059, p38 inhibitor SB 203580, and NF-κB inhibitor pyrrolidinedithiocarbamate (PDTC) were purchased from Sigma-Aldrich (St. Louis, MO). The TRPV1 inhibitor JYL 1421 was a generous gift from Jeewoo Lee (College of Pharmacy, Seoul National University, Seoul, South Korea). Antibodies of phospho-EGFR, total-EGFR, phospho-ERK, total-ERK, total-p38, and β-actin were from Santa Cruz Biotechnology (Santa Cruz, CA). Anti–phospho-p38 and phospho-IκB-α were from Cell Signaling Technology (Danvers, MA). IL-6 and IL-8 ELISA kits were from R&D Systems (Minneapolis, MN).

Cell Culture

SV40 adenovirus–immortalized HCECs a generous gift from Araki-Sasaki, (Kagoshima Miyata Eye Clinic, Kagoshima, Japan), were cultured in supplemented Dulbecco's modified Eagle's medium (DMED/F12). After reaching 80% to 90% confluence, cells were detached with 0.5% trypsin-EDTA and were subcultured in DMEM/F12 medium supplemented with 10% fetal bovine serum (FBS), 5 ng/mL EGF, 5 μg/mL insulin, and 40 μg/mL gentamicin in a humidified incubator with 5% CO$_2$, 95% atmosphere air at 37°C.

Intracellular Calcium Fluorescence Imaging

Relative changes in intracellular Ca^{2+} concentration were measured with ISEE 5.5.9 analytical imaging software in conjunction with a single-cell fluorescence imaging system (Inovision Corp., Raleigh, NC). HCECs grown on circular 22-mm coverslips were loaded with 3 μM fura 2-AM (Invitrogen-Molecular Probes, Carlsbad, CA) at 37°C for 50 minutes with or without test compounds. Cells were then washed with prewarmed (37°C) NaCl Ringer's solution (138 mM NaCl, 5 mM KCl, 1 mM CaCl$_2$, 1 mM KH$_2$PO$_4$, 1 mM MgCl$_2$, 10 mM glucose, and 10 mM HEPES, pH 7.4, 300 mOsm). Hyperosmotic solutions were created by supplementing sucrose in the isotonic Ringer's solution. Sucrose increases hyperosmotic stress without changing transmembrane ionic strength.[33]Osmolarities of 375 mOsm, 450 mOsm, 500 mOsm, and 600 mOsm were produced by adding 75 mM, 150 mM, 200 mM, and 300 mM sucrose, respectively, to the Ringer's solution. Osmolarity was verified based on measurements of freezing-point depression (Micro-Osmette Osmometer; Precision System, Natick, MA). Ca^{2+}-free solution was formulated by eliminating CaCl$_2$ and adding 2 mM EGTA in the Ringer's solution. Coverslips were placed on the stage of an inverted microscope (Diaphot 200; Nikon, Tokyo, Japan), on which cells were alternately illuminated every 5 seconds at 340 and 380 nm; signal emission was monitored at 510 nm using a charge-coupled device camera (Roper Scientific; Photometrics, Tucson, AZ). Microscopic fields containing five to 10 cells were examined; at least three coverslips were used for each condition. Results were plotted as mean of ratio of F340/F380 nm $\pm$ SEM from at least three independent experiments.

Western Blot Analysis

HCECs cultured on 33-mm culture dishes were lysed using lysis buffer containing 20 mM Tris, 150 mM NaCl, 1 mM EDTA, 1 mM EGTA, 1% Triton X-100, 2.5 mM sodium pyrophosphate, 1 mM β-glycerol phosphate, and 1 mM Na$_3$VO$_4$, pH 7.5, with a protease inhibitor mixture (1 mM PMSF, 1 mM benzamidine, 10 μg/mL leupeptin, and 10 μg/mL aprotinin) for at least 10 minutes Cells were scraped with a rubber policeman, followed by sonication (4 seconds by 4 cycles at 50 mV) and centrifugation (13,000 rpm for 15 minutes at 5°C). Supernatants were harvested and stored at −80°C until analysis. The protein concentration of each lysate was determined by bicinchoninic acid assay (micro BCA protein assay kit; Pierce Biotechnology, Rockford, IL). After boiling samples for 5 minutes, equal amounts of protein were fractionated onto 10% SDS-polyacrylamide gels, followed by electrophoresis and blotting onto polyvinylidene difluoride membranes (Bio-Rad, Hercules, CA). Membranes were blocked with blocking buffer, 5% fat-free milk in 0.1% Tris-buffered solution/Tween-20, for 1 hour at room temperature and then probed overnight at 5°C with antibodies of interest (1:1000). Membranes were incubated with goat anti-rabbit or mouse IgG for 1 hour at room temperature (1:2000). Immunobound antibody was visualized using an enhanced chemiluminescence detection system (ECL Plus; GE Healthcare, Piscataway, NJ). Images were analyzed by densitometry (SigmaScan Pro; Sigma). All experiments were repeated at least three times unless otherwise mentioned.

ELISA

ELISA (R&D Systems) for IL-6 and IL-8 was performed according to the manufacturer's instructions. The amount of IL-6 or IL-8 in the culture medium was normalized according to the total amount of cellular protein lysed with 5% SDS and 0.5 N NaOH. Results are expressed as mean of picograms of IL-6 or IL-8 per milligrams of cell lysate $\pm$ SEM ($n = 3$).

RESULTS

Hyperosmotic Stress Activates TRPV1 Channel

We determined whether a hyperosmotic challenge could elicit the same response in HCECs by evaluating Ca^{2+}-sensitive fluorescence intensity after a 450 mOsm hyperosmotic medium was carefully introduced. The 450 mOsm (150 mM sucrose) was chosen because it stimulated significant Ca^{2+} transients without causing HCEC detachment. Figure 1A shows a typical
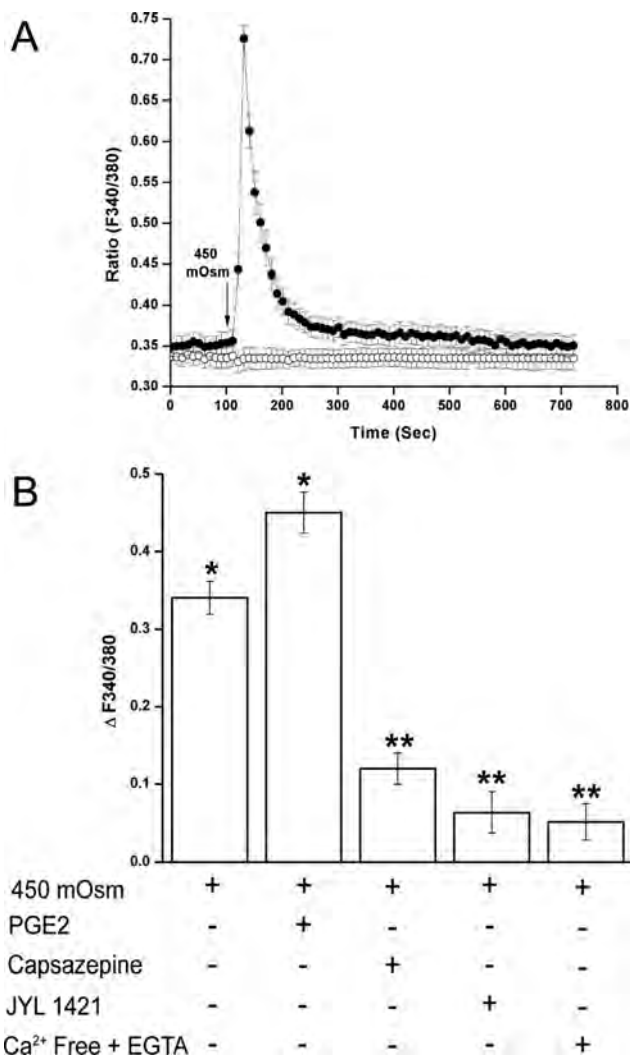
FIGURE 1. Hypertonicity-induced TRPV1 activation in HCECs. (**A**) Fluorescence intensity output at 510 nm was monitored, resulting from alternate excitation of wavelengths 340 and 380 nm. Their ratios were indicative of relative changes in intracellular Ca^{2+} concentration. The basal fluorescence level was measured for 2 minutes, followed by a 10-minute recording in 450 mOsm sucrose-enhanced medium (*filled circle*). Control fluorescence trace (*open circle*) was obtained in the 300 mOsm iso-osmotic medium. A sham substitution was performed after 2 minutes that did not change the fluorescence ratio. The *arrow* under fluorescence traces indicate the presence of 450 mOsm or sham (300 mOsm) medium. (**B**) Cells were pretreated with PGE2 (1 μM), TRPV1 inhibitor capsazepine (10 μM) or JYL 1421 (1 μM), or exposure to Ca^{2+}-free medium added with 2 mM EGTA for 30 minutes before 450 mOsm medium was introduced. Changes in fluorescence intensity are summarized and expressed as mean ± SEM ($n = 3$). Each of the indicated conditions was performed in triplicate, and 5 to 10 cells per condition were monitored. *$P < 0.01$ vs. untreated control. **$P < 0.01$ vs. treated with 450 mOsm medium alone.

time-dependent effect of substitution of an isotonic medium with a 450 mOsm medium on fura2-loaded cells. A 2-minute basal fluorescence level was recorded. Within 20 seconds, exposure to the 450 mOsm medium (indicated by arrow) doubled ($n = 3$) the increases in Ca^{2+} transients: the ratio increased from 0.35 ± 0.01 to a maximal value 0.73 ± 0.02. This was followed by a nearly complete recovery to the basal level within the next 400 seconds (filled line). Sham substitution with an isotonic solution failed to elicit any change of Ca^{2+} level (empty line). Recent studies show that in rat pulmonary sensory neurons, PGE2 enhanced capsaicin-induced increases in the whole cell currents density and action potential frequency.[34] We then examined in HCECs whether PGE2 can enhance TRPV1 channel-induced Ca^{2+} influx. Figure 1B shows that pretreatment with PGE2 (1 μM) increased hypertonicity-induced Ca^{2+} transients by 32.4% ± 3%. JYL 1421 is a more potent TRPV1 antagonist than capsazepine.[35] Exposure to capsazepine (10 μM) or JYL 1421 (1 μM) suppressed Ca^{2+} transients by 65% ± 2% and 81% ± 3%, respectively. Similarly Ca^{2+}-free extracellular medium supplemented with EGTA (2 mM) suppressed Ca^{2+} transients by 89% ± 2%. Thus, hypertonicity stimulated TRPV1 channel-mediated Ca^{2+} influx.
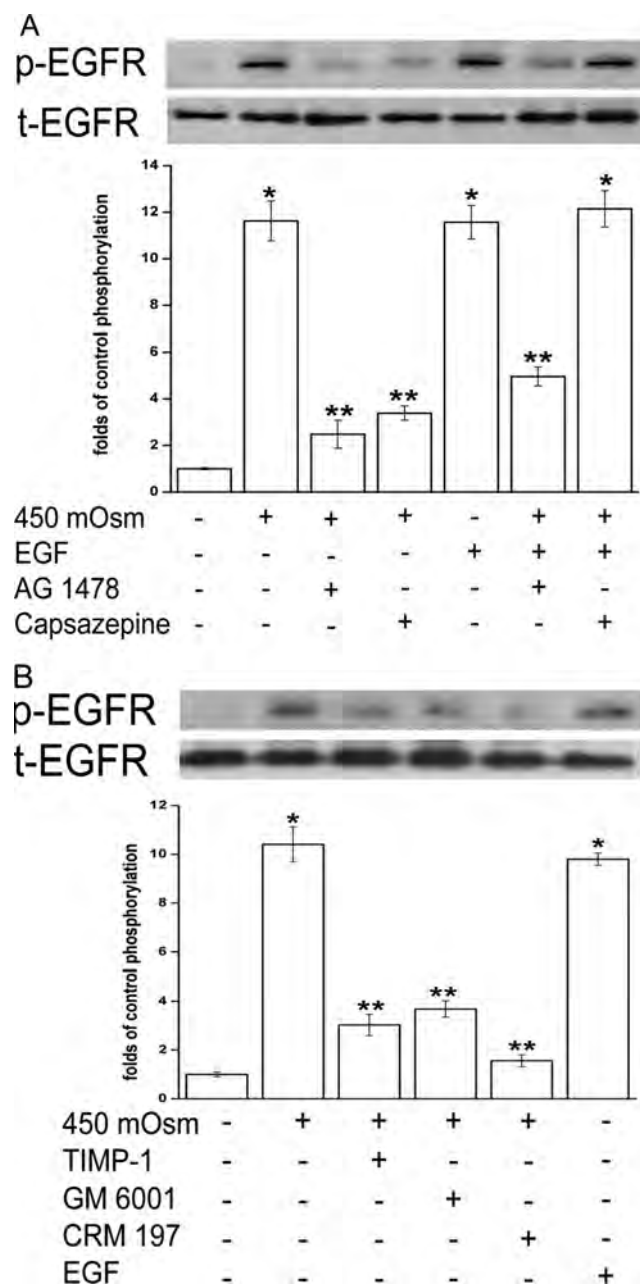
Hypertonicity-Stimulated TRPV1 Transactivates EGFR

Because various mediators elicit responses through the transactivation of EGFR, we examined whether TRPV1 stimulation is required for hypertonicity-induced EGFR transactivation and the underlying mechanism of such transactivation. In Figure 2A, both 450 mOsm medium and EGF (5 ng/mL) stimulated EGFR phosphorylation (p-EGFR) by 10.6-fold (lanes 2 and 5). Such increases in p-EGFR formation were suppressed with either pretreatment with an EGFR antagonist AG 1478 (10 μM, lane 3) by 86% or capsazepine (10 μM, lane 4) by 77.5%. Concurrent exposure to EGF and the hyperosmotic medium prevented the inhibitory effect of capsazepine on p-EGFR formation (lane 3 vs. lane 7). On the other hand, EGF and hyperosmotic dual stimuli only slightly alleviated AG 1478 inhibition of p-EGFR (lane 3 vs. lane 6). These results indicate that EGF can phosphorylate EGFR regardless of TRPV1 activity, whereas TRPV1 activation–induced phosphorylation of EGFR occurred only when EGFR was not inhibited. Therefore, hypertonicity induces EGFR transactivation by stimulating TRPV1 channels.

The MMP-dependent HB-EGF shedding process mediates EGFR transactivation by injury, ATP, and LPA.[21,36,37] We explored whether similar signaling cascades are required for hypertonicity-induced EGFR transactivation by TRPV1. In Figure 2B, TIMP-1 (100 ng/mL), an MMP-1–specific inhibitor, GM 6001 (50 μM), a broad-spectrum MMP inhibitor, or CRM 197 (10 μg/mL), an HB-EGF inhibitor, suppressed 450 mOsm challenge-induced p-EGFR formation by 71%, 65%, and 85%, respectively. Thus, hyperosmotic challenge-elicited p-EGFR formation was suppressed by blocking TRPV1, MMP, or HB-EGF, indicating TRPV1-mediated MMP-dependent HB-EGF shedding underlies hypertonicity-induced EGFR transactivation.

MAPK Is Activated after TRPV1 Transactivation of EGFR

We have previously reported that p38 MAPK activates Na-K-2 Cl cotransporter 1, which is critical for hypertonicity-induced regulatory volume increases and cell survival.[16,19] In addition, p38 and JNK activation mediates hypertonicity-induced increases in IL-1β secretion in HCECs.[38] Other studies indicate that a global activation of MAPK signaling occurs when corneal epithelial cells are exposed to hyperosmolar stress.[1] We exam-

A

FIGURE 2. Dependence of hypertonicity-induced EGFR transactivation on TRPV1 stimulation. (A) Cells were pretreated for 30 minutes with a TRPV1 antagonist capsazepine (10 μM) or an EGFR inhibitor AG 1478 (10 μM) before 450 mOsm medium or EGF (5 ng/mL) was introduced. (B) Cells were pretreated for 30 minutes with an MMP-1 inhibitor TIMP-1 (100 ng/mL), a broad-spectrum MMP inhibitor GM 6001 (50 μM), or an HB-EGF inhibitor CRM 197 (10 μg/mL), followed by exposure to 450 mOsm medium for 5 minutes. Exposure to EGF alone served as a positive control. Cell extracts were probed for phosphorylated EGFR (p-EGFR) using anti–p-EGFR antibody by Western blot analysis. Membranes were then stripped and reprobed for total EGFR (t-EGFR) using anti–t-EGFR antibody. Amounts of t-EGFR served as loading controls. Results of a representative experiment are given. Results are summarized in a bar graph below and expressed as mean $\pm$ SEM ($n = 3$). *$P < 0.01$ vs. untreated control. ** $P < 0.01$ vs. treated with 450 mOsm medium alone.

ined ERK and p38 MAPK activities after hypertonicity-stimulated TRPV1-EGFR signaling.

Hyperosmotic stimuli induced ERK and p38 phosphorylation in ways that were tonicity and time dependent. Increases in tonicities from 300 to 600 mOsm elicited biphasic changes in the amounts of p-ERK and p-p38 (Fig. 3A), with maximal p-ERK and p-p38 formations at 500 mOsm and 450 mOsm, respectively. Figure 3B shows that on exposure to 450 mOsm, p-ERK and p-p38 formation was elevated until 60 minutes, followed by partial return to basal levels at 120 minutes

To determine the roles of TRPV1 and EGFR in mediating MAPK responses to a hyperosmotic challenge, the effect of either TRPV1 or EGFR suppression on ERK and p38 phosphorylation was studied. In Figure 4A, capsazepine (10 μM, lane 3) and AG 1478 (10 μM, lane 4) suppressed ERK phosphorylation (p-ERK) during exposure to 450 mOsm by 66% and 51%, respectively. In addition, ERK phosphorylation was abolished by its inhibitor, PD 98059 (10 μM, lane 7). EGF rescued capsazepine-suppressed p-EGFR but did not alter AG 1478 inhibition of p-EGFR in the presence of the hyperosmotic medium (Fig. 2A). We evaluated whether EGF had the same effect on p-ERK as it had on p-EGFR formation when either TRPV1 or EGFR was inhibited. Accordingly, cells were exposed to 450 mOsm medium supplemented with 5 ng/mL EGF after pretreatment with either capsazepine (10 μM) or AG 1478 (10 μM). The combination of EGF and hyperosmotic stimuli resulted in complete recovery of p-ERK formation from capsazepine suppression (Fig. 4A, lane 3 vs. lane 5). The amount of p-ERK returned to the same level as that induced by 450 mOsm medium or EGF alone (lanes 2 and 8). However, this double-stimuli strategy did not overcome AG 1478 inhibition of p-ERK (lane 6). In other words, EGF prevented capsazepine from suppressing hypertonicity-induced ERK phosphorylation. This occurred because EGF can directly activate EGFR-linked MAPK signaling. Therefore, hypertonicity-induced ERK activation is dependent on EGFR transactivation by TRPV1.

Similarly, the hypertonicity-stimulated p38 response to either TRPV1 or EGFR inhibition mirrors the ERK response. In Figure 4B, either capsazepine(10 μM, lane 3), AG 1478 (10 μM, lane 4), or a p38 antagonist, SB 203580 (10 μM, lane 7),

A

B
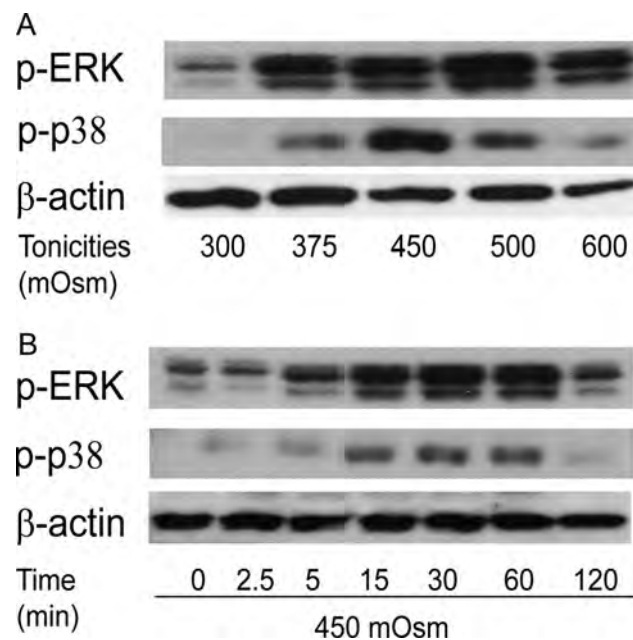
FIGURE 3. Hypertonicity activation of ERK and p38 MAPK in a tonicity- and a time-dependent manner. (A) Cells were exposed to 300, 375, 450, 500, and 600 mOsm media for 15 minutes. (B) Cells were exposed to 450 mOsm medium for 0, 2.5, 5, 15, 30, 60, and 120 minutes. Western blot analysis was used to detect phosphorylated ERK (p-ERK) and phosphorylated p38 (p-p38). Membranes were then stripped and reprobed for β-actin to validate the loading equivalence.

A

B
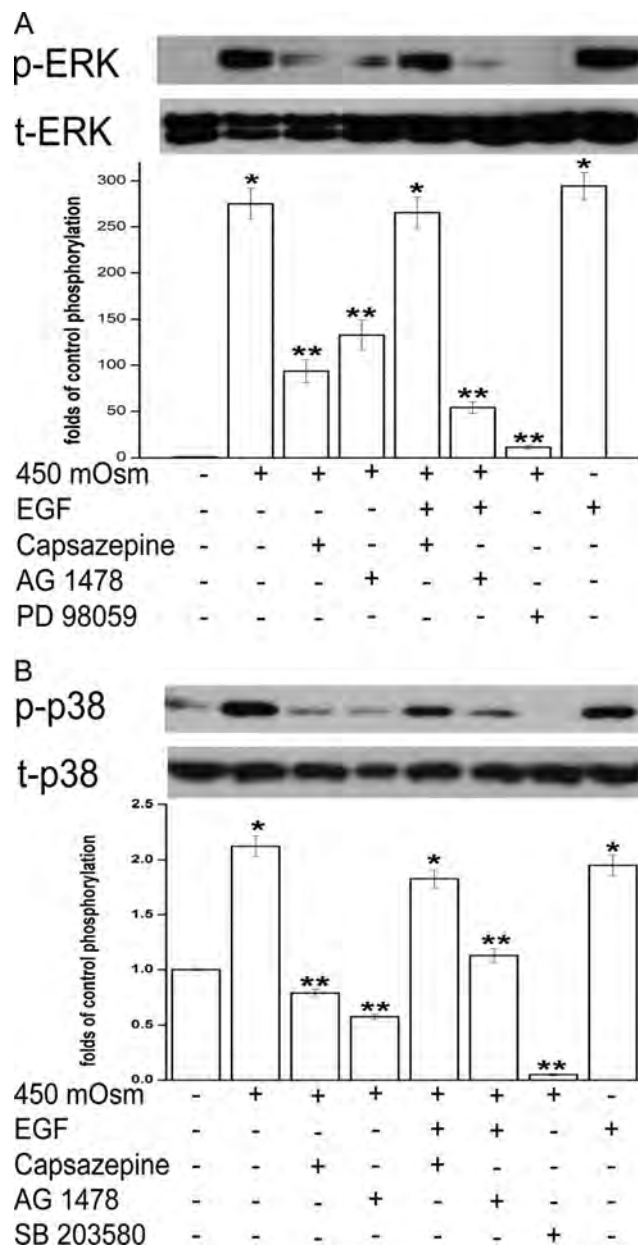
FIGURE 4. Effects of TRPV1 and EGFR modulation on hypertonicity-induced ERK and p38 MAPK activation. (**A**) Cells were pretreated for 30 minutes with capsazepine (10 μM), AG 1478 (10 μM), or an ERK inhibitor PD 98059 (10 μM) before exposure to 450 mOsm medium or EGF (5 ng/mL). Cell extracts were subjected to Western blot analysis with anti–p-ERK. Membranes were then stripped and reprobed for total ERK (t-ERK) using anti–t-ERK antibody. (**B**) Cells were pretreated for 30 minutes with either capsazepine (10 μM), AG 1478 (10 μM), or p38 inhibitor SB 203580 (10 μM) before exposure to 450 mOsm medium or EGF (5 ng/mL). Cell extracts were subjected to Western blot analysis with anti–p-p38. Membranes were then stripped and reprobed for total p38 (t-p38) using anti–t-p38 antibody. Results are summarized in bar graphs and expressed in mean $\pm$ SEM ($n = 3$). *$P <$ 0.01 vs. untreated control. **$P < 0.01$ vs. treated with 450 mOsm medium alone.

suppressed hypertonicity-stimulating phosphorylated p38 to levels lower than their control (lanes 3, 4, 7). Exposure to a combination of EGF (5 ng/mL) and the 450 mOsm medium restored p-p38 formation despite the presence of capsazepine; phosphorylation of p38 reached 1.3-fold the level of p38 formation induced by 450 mOsm medium alone (lane 3 vs. lane 5). In

the presence of EGF, AG 1478 suppressed p-p38 formation near the control level (lane 6). Therefore, hypertonicity activated ERK and p38 MAPK through TRPV1-mediated EGFR transactivation.

## NF-κB Is Activated after TRPV1 Transactivation of EGFR

NF-κB activation mediates a host of physiological responses that include increases in proinflammatory cytokine release.[26–28] We determined the impact of hyperosmotic stress on NF-κB in the presence of an inhibitor of TRPV1, EGFR, ERK, or p38. To make this assessment, NF-κB activation was evaluated based on changes in phosphorylation status of the NF-κB inhibitory component, IκB-α, in response to 450 mOsm medium. Such a readout evaluates NF-κB activation because NF-κB stimulation occurs only when IκB-α is phosphorylated, which enables IκB-α to detach from its complexation with NF-κB and allows active components of NF-κB, RelA, and p50 to translocate to the nucleus and initiate gene transcription and expression.

Figure 5A shows that increases in IκB-α phosphorylation (p-IκB-α) occurred in a tonicity-dependent manner after 1-hour exposure to either 300 (isosmotic), 375, or 450 mOsm medium. The selectivity of these effects was validated by showing that with the NF-κB inhibitor PDTC (50 μM, lane 4), IκB-α phosphorylation was completely suppressed. Figure 5B shows that with 450 mOsm medium, p-IκB-α formation increased to reach a maximal level after 1 hour, which was followed by a partial decline during the next hour.

To document how 450 mOsm stress induced p-IκB-α formation, we compared the effects of TRPV1, EGFR, ERK, or p38 inhibition on this response. Figure 6 shows that at 1 hour p-IκBα formation increased by more than 8-fold. Ten μM capsazepine suppressed p-IκB-α by approximately 90% (lane 3). AG 1478 (10 μM), PD 98059, and SB 203580 suppressed p-IκB-α formation by 77%, 56%, and 69%, respectively (lanes 5–7). With capsazepine (10 μM) in the 450 mOsm medium, EGF (5 ng/mL) supplementation induced an approximately

A

B
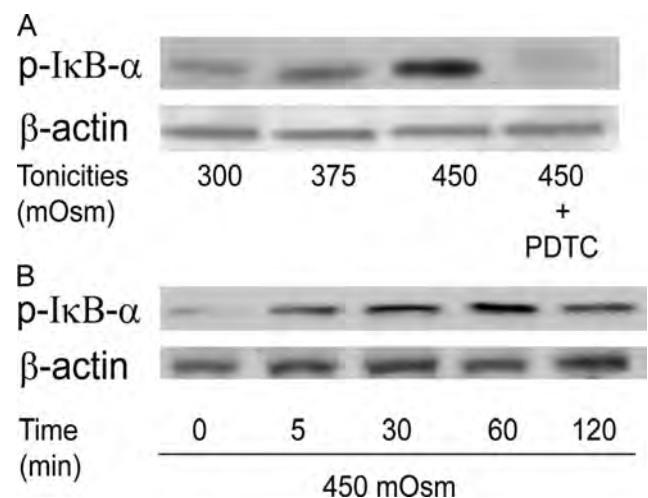
FIGURE 5. Hypertonicity stimulation of IκB-α phosphorylation in tonicity and in a time-dependent manner. (**A**) Cells were exposed to 300, 375, and 450 mOsm media for 1 hour. Specificity of IκB-α phosphorylation was validated with pretreatment of NF-κB inhibitor PDTC (50 μM) before exposure to 450 mOsm medium. (**B**) Cells were exposed to 450 mOsm medium for 0, 5, 30, 60, and 120 minutes. Cell extracts were subjected to Western blot analysis for phosphorylated IκB-α (p-IκB-α) with anti–p-IκB-α antibody. Membranes were then stripped and reprobed for β-actin using anti–β-actin antibody to validate load equivalence.
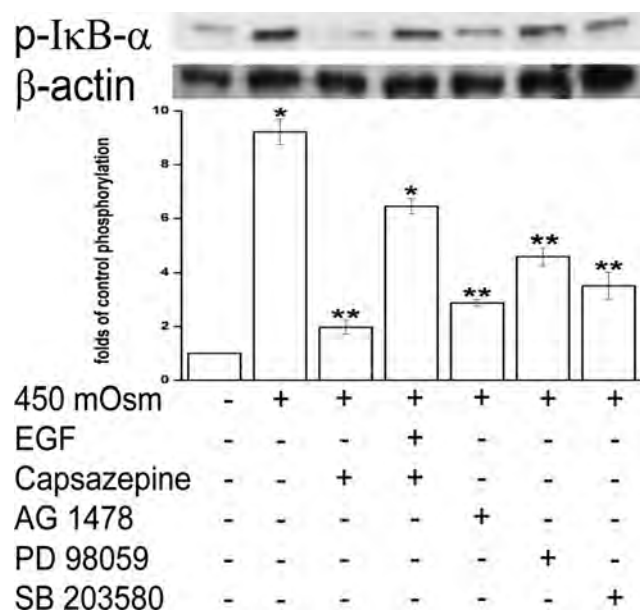
FIGURE 6. Effects of modulation of TRPV1, EGFR, ERK, and p38 on hypertonicity-induced IκB-α phosphorylation. Cells were pretreated for 30 minutes with capsazepine (10 μM), AG 1478 (10 μM), PD 98059 (10 μM), or SB 203580 (10 μM) before exposure to 450 mOsm medium or EGF (5 ng/mL). Cell extracts were probed for p-IκB-α by Western blot analysis. Membranes were then stripped and reprobed for β-actin using anti–β-actin antibody. Results were summarized in bar graphs and expressed as mean ± SEM ($n = 3$). *$P < 0.01$ vs. untreated control. **$P < 0.01$ vs. treated with 450 mOsm medium alone.

4.6-fold increase in p-IκB-α formation above that obtained in the absence of EGF (lane 3 vs. lane 4). Declines of p-IκB-α formation elicited by the suppression of EGFR, ERK, and p38 MAPK confirm that EGFR and its linked MAPK signaling contribute to NF-κB activation. However, these individual declines did not reach the baseline level, suggesting potential signaling pathways in addition to those linked with EGFR affect NF-κB activity.

Hypertonicity Induces Increases in IL-6 and IL-8 Release through TRPV1 Activation and EGFR Pathway Transactivation

TRPV1 channel activation by capsaicin in HCECs induces increases in IL-6 and IL-8 release through transient increases in plasma membrane Ca^{2+} and global MAPK stimulation.[16] We determined whether exposure to 450 mOsm induced a similar response through the same pathways activated by capsaicin. In 450 mOsm hyperosmotic medium, IL-6 (Fig. 7A) and IL-8 (Fig. 7B) release increased by 2.8- and 2.6-fold (lane 2), respectively, whereas capsazepine (10 μM) abolished such increases (lane 3). Therefore, hypertonicity-induced increases in IL-6 and IL-8 release are largely elicited through TRPV1 activation by this challenge.

The role of EGFR and its linked MAPK and NF-κB pathway in the stimulation of IL-6 and IL-8 release was studied by blocking EGFR, ERK, p38, or NF-κB phosphorylation. In Figures 7A and 7B, inhibition of EGFR activation by AG 1478 (lane 4) resulted in decreases of IL-6 and IL-8 release by 77% and 86%, ERK inhibitor PD 98059 (10 μM, lane 5) by 52% and 84%, and p38 inhibitor SB 203580 (10 μM, lane 6) by 71% and 84%, respectively. PDTC (50 μM, lane 7) abrogated these increases in IL-6 and IL-8 release. Thus, blockage of any aforementioned component activated by hypertonicity resulted in declines in IL-6 and IL-8 release. Inhibition of TRPV1 or NF-κB completely

suppressed IL-6 and IL-8, whereas blockage of EGFR or MAPK (ERK and p38) partially suppressed these cytokines. This result is consistent with the finding that only a fraction of hypertonicity-induced NF-κB phosphorylation is attributable to EGFR and MAPK signaling pathways (Fig. 6).
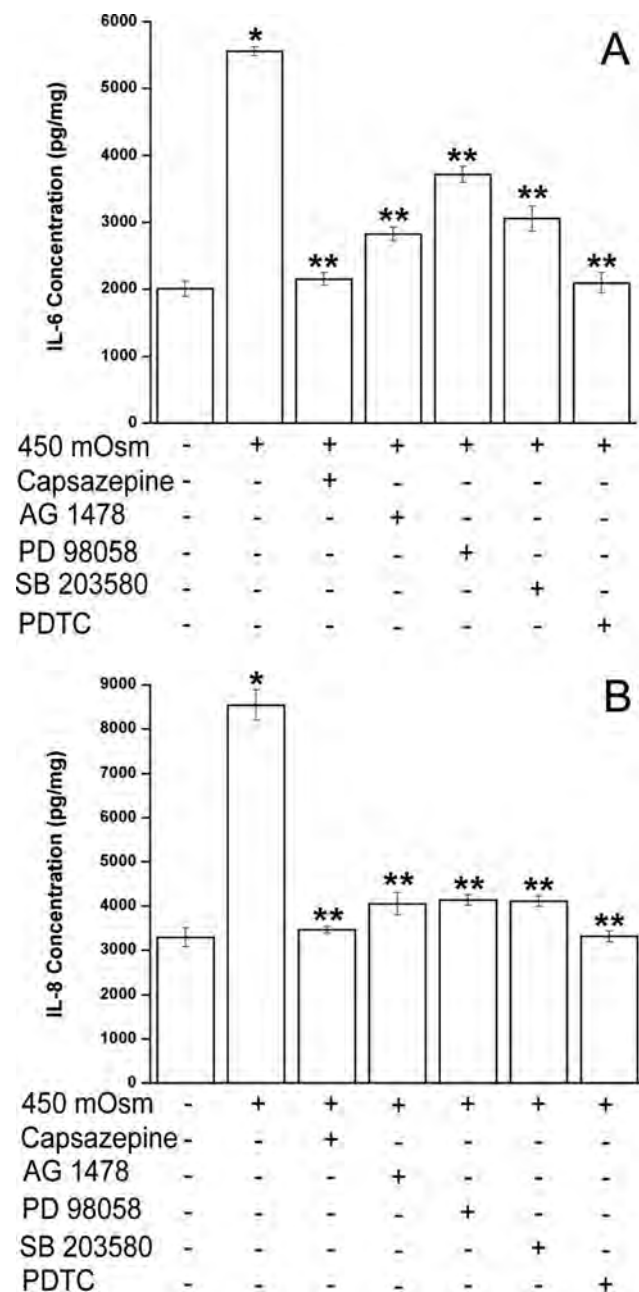
FIGURE 7. Effects of TRPV1, EGFR, ERK, p38, and NF-κB inhibition on hypertonicity-induced increases in IL-6 and IL-8 release. Cells were pretreated for 30 minutes with capsazepine (10 μM), AG 1478 (10 μM), PD 98059 (10 μM), SB 203580 (10 μM), or NF-κB inhibitor PDTC (50 μM) before exposure to 450 mOsm medium. After 24 hours' incubation, supernatants were collected and analyzed for IL-6 (**A**) and IL-8 (**B**) using ELISA. Results were normalized to sample protein concentrations (picogram per milligram protein lysates) and summarized in bar graphs expressed as mean ± SEM ($n = 3$). *$P < 0.05$ vs. untreated control. **$P < 0.05$ vs. treated control with 450 mOsm medium alone.

DISCUSSION

In HCECs, capsaicin induced TRPV1 channel activation followed by increases in plasma membrane Ca^{2+} influx leading to global MAPK stimulation and increases in IL-6 and IL-8 release.[16] Some studies show that TRPV1 is required for osmosensing hypertonic stimulus in various tissues.[11,14] We sought to determine whether hyperosmotic stress can also induce TRPV1 activation and increased IL-6 and IL-8 release in HCECs given that increased tear film osmolarity is associated with tissue inflammation in dry eye disease. Indeed, we found that hyperosmotic stress induced TRPV1 activation, leading to increases in IL-6 and IL-8 release. This occurred through EGFR transactivation and its linked MAPK and NF-κB signaling pathway stimulation.

Exposure to a 450 mOsm medium induced a transient increase in plasma membrane Ca^{2+} influx (Fig. 1A). TRPV1 activation accounted for this response because capsazepine or JYL 1421 reduced such influx, whereas PGE2 enhanced hypertonicity-mediated TRPV1 Ca^{2+} influx (Fig. 1B). This effect of PGE2 may be attributable to TRPV1 sensitization because PGE2 in rabbit corneal epithelial cells stimulates adenylate cyclase leading to elevated cAMP levels and protein kinase A (PKA) activation.[39] In some other tissues, it was shown that there are consensus phosphorylation sites on TRPV1 for PKA-mediated sensitization of this channel.[7,34] However, hypertonicity-induced Ca^{2+} transients through plasma membrane TRPV1 activation do not entirely account for these responses. This is indicated because the suppression of TRPV1 did not completely suppress Ca^{2+} transients (Fig. 1B). Similar results are found in dorsal root ganglion neurons in which heat-induced TRPV1 activation accounts for only 47% of the increases in intracellular Ca^{2+}, whereas total extracellular Ca^{2+} influx accounts for 76%.[40] A possible source for the remaining intracellular Ca^{2+} increases may be release from intracellular stores. Several possible pathways—IP3- and ryanodine-sensitive Ca^{2+} pathways, which were identified in corneal epithelial cells and in some other tissues—can mediate such release.[40–42] Therefore, hypertonicity-induced Ca^{2+} transients may arise from both TRPV1-mediated trans-plasma membrane influx and release from intracellular store, though TRPV1 stimulation accounts for most of the increases in intracellular Ca^{2+} influx.

EGFR and its linked signaling pathways serve as a hub for various extracellular stimuli to elicit cell inflammation, proliferation, migration, and differentiation. These stimuli include G-protein–coupled receptor ligands (phenylephrine, carbachol, thrombin, endothelin-1), physical/chemical stress (Ca^{2+} or K^+ influx, wound, UV-B, oxidative stress, anisosmotic conditions), and growth factors and cytokines (EGF, insulin-like growth factor, basic fibroblast growth factor, IL-1β, IL-8).[43,44] With hypertonic stress, EGFR transactivation occurs to induce increases in inflammatory mediator PGE2 and cyclooxygenases-2 (COX-2) stimulation in renal medullary epithelial cells.[45] EGFR transactivation in corneal epithelial cells occurred through TRPV1 activation by hypertonic stress, leading to MAPK/NF-κB signaling pathway stimulation. Such activation, in turn, induced increases in IL-6 and IL-8 release. Our finding that TRPV1 activation by hypertonic stress induced increases in IL-6 and IL-8 release broadens the diversity of responses in HCECs that can be induced by EGFR transactivation.

The fact that EGF relieved capsazepine inhibition of EGFR phosphorylation (Fig. 2A), ERK and p38 MAPK activation (Figs. 4A, 4B) and IκB-α stimulation (Fig. 6) validates that hypertonicity-stimulated TRPV1 transactivates EGFR. We found, as reported in a number of previous studies,[21] that EGFR transactivation is dependent on MMP-1 activation, leading to EGF release from its binding to heparin by sheddase (Fig. 2B). This is evident because hypertonicity-induced EGFR transactivation was blocked by preinhibiting MMPs with TIMP-1 or GM6001 and HB-EGF sheddase with CRM 197. Yin and Yu[46] documented that early (up to 10 minutes) ERK activation by ATP, LPA, or wounding contributes to a disintegrin and metalloprotease (ADAM) activation and shedding of EGF from heparin EGF in HCECs, whereas ERK activation after 10 minutes is dependent on EGFR stimulation. Such early ERK activation was instead controlled by calcium influx, Src kinase and PKC activation.[46] We found that hypertonic challenge–induced MAPK stimulation (Fig. 4) was obtained at 15 minutes. Presumably by this time both EGFR-independent and -dependent ERK activation occurred. This consideration might explain why hypertonicity-activated ERK was only partially blocked by the EGFR inhibitor AG 1478 (Fig. 4A), whereas at the same time p38 activation was completely reduced to the control level by the same compound (Fig. 4B). AG1478 only blocked the portion of phosphorylated ERK that was dependent on EGFR. Our finding that hypertonic-induced TRPV1 activation led to EGFR transactivation suggested that increases in Ca^{2+} influx may be prerequisite for EGFR transactivation. This suggestion is supported by two studies in which ionomycin-dependent Ca^{2+} influx activated EGFR by stimulating metalloproteinase cleavage of HB-EGF.[47,48]

Hypertonic stress–increased IL-6 and IL-8 release was largely but incompletely suppressed by the EGFR inhibitor AG1478 (Fig. 7). Similarly, the suppression of EGFR did not abolish ERK, p38 (Figs. 4A, 4B), or NF-κB (Fig. 6). One explanation for this partial rather than complete inhibitory effect of AG1478 is that TRPV1 activation results in the stimulation of additional signaling pathways parallel to EGFR transactivation. Such a parallel cascade complements canonical EGFR-dependent signaling either by enhancing the magnitude of NF-κB or by modulating the duration or magnitude of MAPK activation.

Transforming growth factor β–activated kinase 1 (TAK1) is indicated in mediating LPS-induced expression of inflammatory mediators through NF-κB and p38 MAPK activation.[49] Our data (unpublished, 2009) also show a role for TAK1 in TRPV1 signaling because only capsaicin, but not EGF, caused the phosphorylation of TAK1, which was suppressed by TAK1 inhibitor 5Z-7-oxozeaenol. Should TAK-1 mediate EGFR-independent NF-κB and MAPK activation after TRPV1 stimulation, TRPV1 activation–elicited inflammatory responses can be the result of combined contributions by EGFR-dependent and TAK-dependent (EGFR-independent) NF-κB signaling pathways.

Alternatively, control of the duration and magnitude of MAPK activation may contribute to different outcomes by capsaicin and EGF. Compared with EGF or hypotonicity, hypertonicity-induced ERK and p38 MAPK activation was slower.[22,50] When exposed to the 450 mOsm solution, phospho-Erk1/2 and phospho-p38 lasted more than 2 hours with the peak at 1 hour (Fig. 3A), whereas with EGF or hypotonic stress, activation occurred within 2 hours with the peak within 15 minutes.[23,51] Such a difference in duration and magnitude of MAPK activation may be modulated through mediated negative feedback control of mitogen kinase protein phosphatases (MKP/DUSP).[24] Glycogen synthase kinase (GSK)-3 further regulates MPK/DUSP activity. Active GSK-3, trademarked by its dephosphorylated form, phosphorylates and stabilizes DUSP1, which enables DUSP1 to dephosphorylate and suppress ERK and p38 signaling. However, once GSK-3 is inactivated by EGF-induced phosphorylation, its control of MAPK signaling through DUSP1 is lost. Our recent study (unpublished data, 2010) shows that TRPV1 activation of JNK MAPK was also regulated by the same mechanism. In DUSP1 knockdown cells, capsaicin induced longer JNK phosphorylation and larger increases in IL-6 and IL-8 than in occurred in wild-type cells. On the other hand, in macrophages and other epithelial cells,
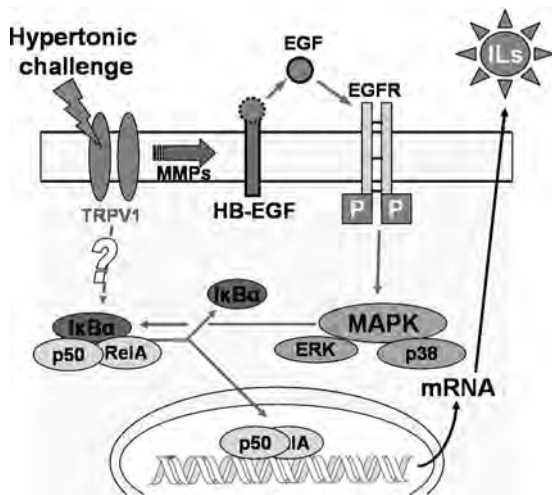
FIGURE 8. Signaling pathways mediating hypertonicity stimulated increases in IL-6 and IL-8. Hypertonic stress activated the TRPV1 channel. TRPV1 stimulation leads to the transactivation of EGFR through MMP-dependent HB-EGF shedding, followed by MAPK and NF-κB activation and to EGFR-independent NF-κB stimulation. Activated NF-κB translocates to nucleus and promotes the production of IL-6 and IL-8.

overexpression of DUSP1 shortened ERK, p38, and JNK activation, leading to the suppression of proinflammatory cytokine expression.[52–55] These results suggest that TRPV1 activation may elicit, through EGFR-linked signaling, increases in IL-6 and IL-8 release by causing more rapid GSK-3 inhibition/phosphorylation than that induced by EGF. As a result, DUSP1 degradation occurs so promptly that MAPK signaling activation gradually increases, leading to increases in IL-6 and IL-8 release. Efforts are warranted to address the effect of hyperosmotic stimuli on DUSP phosphorylation and stabilization.

In summary, our results show that hyperosmotic stress–induced increases in IL-6 and IL-8 release are dependent on TRPV1 activation. Such stimulation transactivates EGFR through MMP-mediated HB-EGF ectoderm shedding, consequently activating ERK and p38 MAPK and NF-κB signaling pathways. In addition, TRPV1 may activate a parallel EGFR-independent signaling cascade, which enhances NF-κB activation magnitude and inflammatory cytokine expression (Fig. 8). The identity of such a parallel pathway and its interaction with the TRPV1/EGFR/MAPK/NF-κB pathway is promised for future investigation.

References

1. Luo L, Li DQ, Corrales RM, Pflugfelder SC. Hyperosmolar saline is a proinflammatory stress on the mouse ocular surface. *Eye Contact Lens.* 2005;31:186–193.

2. Tomlinson A, Khanal S, Ramaesh K, Diaper C, McFadyen A. Tear film osmolarity: determination of a referent for dry eye diagnosis. *Invest Ophthalmol Vis Sci.* 2006;47:4309–4315.

3. Gilbard JP, Kenyon KR. Tear diluents in the treatment of keratoconjunctivitis sicca. *Ophthalmology.* 1985;92:646–650.

4. Papa V, Aragona P, Russo S, Di Bella A, Russo P, Milazzo G. Comparison of hypotonic and isotonic solutions containing sodium hyaluronate on the symptomatic treatment of dry eye patients. *Ophthalmologica.* 2001;215:124–127.

5. Alessandri-Haber N, Yeh JJ, Boyd AE, et al. Hypotonicity induces TRPV4-mediated nociception in rat. *Neuron.* 2003;39:497–511.

6. Becker D, Blase C, Bereiter-Hahn J, Jendrach M. TRPV4 exhibits a functional role in cell-volume regulation. *J Cell Sci.* 2005;118:2435–2440.

7. Amadesi S, Cottrell GS, Divino L, et al. Protease-activated receptor 2 sensitizes TRPV1 by protein kinase C epsilon- and A-dependent mechanisms in rats and mice. *J Physiol.* 2006;575:555–571.

8. Liedtke W, Choe Y, Marti-Renom MA, et al. Vanilloid receptor-related osmotically activated channel (VR-OAC), a candidate vertebrate osmoreceptor. *Cell.* 2000;103:525–535.

9. Strotmann R, Harteneck C, Nunnenmacher K, Schultz G, Plant TD. OTRPC4, a nonselective cation channel that confers sensitivity to extracellular osmolarity. *Nat Cell Biol.* 2000;2:695–702.

10. Sidhaye VK, Guler AD, Schweitzer KS, D'Alessio F, Caterina MJ, King LS. Transient receptor potential vanilloid 4 regulates aquaporin-5 abundance under hypotonic conditions. *Proc Natl Acad Sci U S A.* 2006;103:4747–4752.

11. Liu L, Chen L, Liedtke W, Simon SA. Changes in osmolality sensitize the response to capsaicin in trigeminal sensory neurons. *J Neurophysiol.* 2007;97:2001–2015.

12. Sharif Naeini R, Witty MF, Seguela P, Bourque CW. An N-terminal variant of Trpv1 channel is required for osmosensory transduction. *Nat Neurosci.* 2006;9:93–98.

13. Yokoyama T, Saito T, Ohbuchi T, et al. TRPV1 gene deficiency attenuates miniature EPSC potentiation induced by mannitol and angiotensin II in supraoptic magnocellular neurons. *J Neurosci.* 2010;30:876–884.

14. Ciura S, Bourque CW. Transient receptor potential vanilloid 1 is required for intrinsic osmoreception in organum vasculosum lamina terminalis neurons and for normal thirst responses to systemic hyperosmolality. *J Neurosci.* 2006;26:9069–9075.

15. Taylor AC, McCarthy JJ, Stocker SD. Mice lacking the transient receptor vanilloid potential 1 channel display normal thirst responses and central Fos activation to hypernatremia. *Am J Physiol Regul Integr Comp Physiol.* 2008;294:R1285–R1293.

16. Zhang F, Yang H, Wang Z, et al. Transient receptor potential vanilloid 1 activation induces inflammatory cytokine release in corneal epithelium through MAPK signaling. *J Cell Physiol.* 2007;213:730–739.

17. Gschwind A, Zwick E, Prenzel N, Leserer M, Ullrich A. Cell communication networks: epidermal growth factor receptor transactivation as the paradigm for interreceptor signal transmission. *Oncogene.* 2001;20:1594–1600.

18. Gao N, Kumar A, Jyot J, Yu FS. Flagellin-induced corneal antimicrobial peptide production and wound repair involve a novel NF-kappaB-independent and EGFR-dependent pathway. *PLoS One.* 2010;5:e9351.

19. Bildin VN, Wang Z, Iserovich P, Reinach PS. Hypertonicity-induced p38MAPK activation elicits recovery of corneal epithelial cell volume and layer integrity. *J Membr Biol.* 2003;193:1–13.

20. Luo L, Li DQ, Doshi A, Farley W, Corrales RM, Pflugfelder SC. Experimental dry eye stimulates production of inflammatory cytokines and MMP-9 and activates MAPK signaling pathways on the ocular surface. *Invest Ophthalmol Vis Sci.* 2004;45:4293–4301.

21. Xu KP, Ding Y, Ling J, Dong Z, Yu FS. Wound-induced HB-EGF ectodomain shedding and EGFR activation in corneal epithelial cells. *Invest Ophthalmol Vis Sci.* 2004;45:813–820.

22. Ebisuya M, Kondoh K, Nishida E. The duration, magnitude and compartmentalization of ERK MAP kinase activity: mechanisms for providing signaling specificity. *J Cell Sci.* 2005;118:2997–3002.

23. Wang Z, Yang H, Tachado SD, et al. Phosphatase-mediated crosstalk control of ERK and p38 MAPK signaling in corneal epithelial cells. *Invest Ophthalmol Vis Sci.* 2006;47:5267–5275.

24. Wang Z, Yang H, Zhang F, Pan Z, Capo-Aponte J, Reinach PS. Dependence of EGF-induced increases in corneal epithelial proliferation and migration on GSK-3 inactivation. *Invest Ophthalmol Vis Sci.* 2009;50:4828–4835.

25. Brightman FA, Fell DA. Differential feedback regulation of the MAPK cascade underlies the quantitative differences in EGF and NGF signalling in PC12 cells. *FEBS Lett.* 2000;482:169–174.

26. Denk A, Goebeler M, Schmid S, et al. Activation of NF-kappa B via the Ikappa B kinase complex is both essential and sufficient for proinflammatory gene expression in primary endothelial cells. *J Biol Chem.* 2001;276:28451–28458.

27. Fritz EA, Jacobs JJ, Glant TT, Roebuck KA. Chemokine IL-8 induction by particulate wear debris in osteoblasts is mediated by NF-kappaB. *J Orthop Res.* 2005;23:1249–1257.

28. Craig R, Larkin A, Mingo AM, et al. p38 MAPK and NF-kappa B collaborate to induce interleukin-6 gene expression and release: evidence for a cytoprotective autocrine signaling pathway in a

cardiac myocyte model system. *J Biol Chem.* 2000;275:23814–23824.

29. Schwenger P, Alpert D, Skolnik EY, Vilcek J. Activation of p38 mitogen-activated protein kinase by sodium salicylate leads to inhibition of tumor necrosis factor-induced IkappaB alpha phosphorylation and degradation. *Mol Cell Biol.* 1998;18:78–84.

30. Kalari S, Zhao Y, Spannhake EW, Berdyshev EV, Natarajan V. Role of acylglycerol kinase in LPA-induced IL-8 secretion and transactivation of epidermal growth factor-receptor in human bronchial epithelial cells. *Am J Physiol Lung Cell Mol Physiol.* 2009;296:L328–L336.

31. Bhattacharyya A, Pathak S, Datta S, Chattopadhyay S, Basu J, Kundu M. Mitogen-activated protein kinases and nuclear factor-kappaB regulate *Helicobacter pylori*-mediated interleukin-8 release from macrophages. *Biochem J.* 2002;368:121–129.

32. Aga M, Watters JJ, Pfeiffer ZA, Wiepz GJ, Sommer JA, Bertics PJ. Evidence for nucleotide receptor modulation of cross talk between MAP kinase and NF-kappa B signaling pathways in murine RAW 264.7 macrophages. *Am J Physiol Cell Physiol.* 2004;286:C923–C930.

33. Wang KN, Wondergem R. Effects of hyperosmotic medium on hepatocyte volume, transmembrane potential and intracellular K+ activity. *Biochim Biophys Acta.* 1991;1069:187–196.

34. Schnizler K, Shutov LP, Van Kanegan MJ, et al. Protein kinase A anchoring via AKAP150 is essential for TRPV1 modulation by forskolin and prostaglandin E2 in mouse sensory neurons. *J Neurosci.* 2008;28:4904–4917.

35. Wang Y, Szabo T, Welter JD, et al. High affinity antagonists of the vanilloid receptor. *Mol Pharmacol.* 2002;62:947–956.

36. Boucher I, Yang L, Mayo C, Klepeis V, Trinkaus-Randall V. Injury and nucleotides induce phosphorylation of epidermal growth factor receptor: MMP and HB-EGF dependent pathway. *Exp Eye Res.* 2007;85:130–141.

37. Prenzel N, Zwick E, Daub H, et al. EGF receptor transactivation by G-protein-coupled receptors requires metalloproteinase cleavage of proHB-EGF. *Nature.* 1999;402:884–888.

38. Chen M, Hu DN, Pan Z, Lu CW, Xue CY, Aass I. Curcumin protects against hyperosmoticity-induced IL-1beta elevation in human corneal epithelial cell via MAPK pathways. *Exp Eye Res.* 2010;90:437–443.

39. Kang SS, Li T, Xu D, Reinach PS, Lu L. Inhibitory effect of PGE2 on EGF-induced MAP kinase activity and rabbit corneal epithelial proliferation. *Invest Ophthalmol Vis Sci.* 2000;41:2164–2169.

40. Greffrath W, Kirschstein T, Nawrath H, Treede R. Changes in cytosolic calcium in response to noxious heat and their relationship to vanilloid receptors in rat dorsal root ganglion neurons. *Neuroscience.* 2001;104:539–550.

41. Wu X, Yang H, Iserovich P, Fischbarg J, Reinach PS. Regulatory volume decrease by SV40-transformed rabbit corneal epithelial cells requires ryanodine-sensitive Ca2+-induced Ca2+ release. *J Membr Biol.* 1997;158:127–136.

42. Tao W, Wu X, Liou GI, Abney TO, Reinach PS. Endothelin receptor-mediated Ca2+ signaling and isoform expression in bovine corneal epithelial cells. *Invest Ophthalmol Vis Sci.* 1997;38:130–141.

43. Higashiyama S, Iwabuki H, Morimoto C, Hieda M, Inoue H, Matsushita N. Membrane-anchored growth factors, the epidermal growth factor family: beyond receptor ligands. *Cancer Sci.* 2008;99:214–220.

44. Cheng H, Kartenbeck J, Kabsch K, Mao X, Marques M, Alonso A. Stress kinase p38 mediates EGFR transactivation by hyperosmolar concentrations of sorbitol. *J Cell Physiol.* 2002;192:234–243.

45. Zhao H, Tian W, Tai C, Cohen DM. Hypertonic induction of COX-2 expression in renal medullary epithelial cells requires transactivation of the EGFR. *Am J Physiol Renal Physiol.* 2003;285:F281–F288.

46. Yin J, Yu FS. LL-37 via EGFR transactivation to promote high glucose-attenuated epithelial wound healing in organ-cultured corneas. *Invest Ophthalmol Vis Sci.* 2010;51:1891–1897.

47. Dethlefsen SM, Raab G, Moses MA, Adam RM, Klagsbrun M, Freeman MR. Extracellular calcium influx stimulates metalloproteinase cleavage and secretion of heparin-binding EGF-like growth factor independently of protein kinase C. *J Cell Biochem.* 1998;69:143–153.

48. Horiuchi K, Le Gall S, Schulte M, et al. Substrate selectivity of epidermal growth factor-receptor ligand sheddases and their regulation by phorbol esters and calcium influx. *Mol Biol Cell.* 2007;18:176–188.

49. Pang HY, Liu G, Liu GT. Compound FLZ inhibits lipopolysaccharide-induced inflammatory effects via down-regulation of the TAK-IKK and TAK-JNK/p38MAPK pathways in RAW264.7 macrophages. *Acta Pharmacol Sin.* 2009;30:209–218.

50. Shaul YD, Seger R. The MEK/ERK cascade: from signaling specificity to diverse functions. *Biochim Biophys Acta.* 2007;1773:1213–1226.

51. Pan Z, Capo-Aponte JE, Zhang F, Wang Z, Pokorny KS, Reinach PS. Differential dependence of regulatory volume decrease behavior in rabbit corneal epithelial cells on MAPK superfamily activation. *Exp Eye Res.* 2007;84:978–990.

52. Lang R, Hammer M, Mages J. DUSP meet immunology: dual specificity MAPK phosphatases in control of the inflammatory response. *J Immunol.* 2006;177:7497–7504.

53. Sakai A, Han J, Cato AC, Akira S, Li JD. Glucocorticoids synergize with IL-1beta to induce TLR2 expression via MAP kinase phosphatase-1-dependent dual inhibition of MAPK JNK and p38 in epithelial cells. *BMC Mol Biol.* 2004;5:2.

54. Chen P, Li J, Barnes J, Kokkonen GC, Lee JC, Liu Y. Restraint of proinflammatory cytokine biosynthesis by mitogen-activated protein kinase phosphatase-1 in lipopolysaccharide-stimulated macrophages. *J Immunol.* 2002;169:6408–6416.

55. Zhao Q, Shepherd EG, Manson ME, Nelin LD, Sorokin A, Liu Y. The role of mitogen-activated protein kinase phosphatase-1 in the response of alveolar macrophages to lipopolysaccharide: attenuation of proinflammatory cytokine biosynthesis via feedback control of p38. *J Biol Chem.* 2005;280:8101–8108.

Appendix B

Dependence of Corneal Epithelial Cell Proliferation on Modulation of Interactions Between ERK1/2 and NKCC1

Zheng Wang[1], Victor N. Bildin[1], Hua Yang[1], José E. Capó-Aponte[1,2], Yuanquan Yang[1] and Peter S. Reinach[1]

[1]Department of Biological Sciences, State University of New York, State College of Optometry, New York,
[2]Visual Sciences Branch, U.S. Army Aeromedical Research Laboratory, Fort Rucker

Abstract
Epidermal growth factor (EGF) receptor stimulation or protein kinase C (PKC) activation enhances corneal epithelial cell proliferation. This response is needed to maintain corneal transparency and vision. We clarify here in human corneal epithelial cells (HCEC) the cause and effect relationships between ERK1/2 and NKCC1 phosphorylation induced by EGF receptor or PKC activation. Furthermore, the roles are evaluated of NF-κB and ERK1/2 in mediating negative feedback control of ERK1/2 and NKCC1 phosphorylation through modulating DUSP1 and DUSP6 expression levels. Intracellular Ca^{2+} rises induced by EGF elicited NKCC1 phosphorylation through ERK1/2 activation. Bumetanide suppressed EGF-induced NKCC1 phosphorylation, transient cell swelling and cell proliferation. This cause and effect relationship is similar to that induced by PKC stimulation. NKCC1 activation occurred through time-dependent increases in protein-protein interaction between ERK1/2 and NKCC1, which were proportional to EGF concentration. DUSP6 upregulation obviated EGF and PKC-induced NKCC1 phosphorylation. NF-κB inhibition by PDTC prolonged ERK1/2 activation through GSK-3 inactivation leading to declines in DUSP1 expression levels. These results show that EGF receptor and PKC activation induce increases in HCEC proliferation through ERK1/2 interaction with NKCC1. This response is modulated by changes in DUSP1- and DUSP6-mediated negative feedback control of ERK1/2-induced NKCC1 phosphorylation.

Copyright © 2011 S. Karger AG, Basel

Introduction

Corneal epithelial cell renewal is essential for the maintenance of tissue transparency and visual acuity since tight junctional barrier function is preserved through this process. This function is required for suppressing pathogenic infiltration into the underlying stroma as well as maintaining the smooth corneal optical properties. This process is under autocrine and paracrine control by a host of cytokines. They interact with their cognate receptors in the basal proliferating layer to modulate and synchronize the events associated with epithelial turnover

[1, 2]. Receptor activation elicits through a myriad of interacting cell signaling pathways all of the responses that underlie epithelial renewal.

Epidermal growth factor (EGF) is a very efficacious promoter of cell proliferation and migration. Accordingly, much effort has been directed towards delineating the cell signaling pathways and transcription factors mediating EGF receptor (EGFR) control of these responses [3]. A number of studies indicate that EGFR activation elicits control of these responses through transient stimulation of a myriad of interacting cell signaling kinase pathways [4-6]. One aspect of this signaling process entails EGF stimulation of KCl cotransporters (KCC), K$^+$ channels and Na:K:2Cl cotransporter 1 (NKCC1) activity [7-9]. However, it is uncertain if ion transport stimulation leads to cell volume swelling and if NKCC1 phosphorylation is reflective of its activation by EGF. Furthermore, it is unclear how changes in the expression levels of dual specific protein phosphatases (DUSPs) that dephosphorylate ERK1/2 are modulated to control the mitogenic response to either EGFR or protein kinase C (PKC) stimulation.

EGF stimulates cell proliferation and migration through transient phosphorylation of the extracellular regulated kinase (ERK), p38 and JNK mitogen activated protein kinase (MAPK) pathways [6, 10]. In addition, the PI3-K/Akt/GSK pathway is activated, which has a negative feedback effect on the duration and magnitude of MAPK pathway activation. The extent of MAPK suppression is dependent on ERK, p38 MAPK and glycogen synthase kinase (GSK)-3α/β-mediated phosphorylation of different DUSPs that have variable MAPK substrate selectivity [11]. Gene microarray analysis of human corneal epithelial cells (HCEC) indicated that only DUSPs 1, 4, 5, and 6 are expressed at significant levels by these cells. DUSP6 is localized to the cytoplasm and is selective for ERK1/2 whereas DUSP5 is nuclear delimited and also selectively interacts with ERK1/2. On the other hand, DUSP1 and DUSP4 are more nonselective and modulate the patterns of activation of the terminal kinases in the ERK, p38 and JNK pathways. We validated DUSP5 and DUSP6 selectivity by showing in HCEC that DUSP5 knockdown with the appropriate short hairpin RNA (shRNA) augmented the mitogenic response to EGF as a consequence of sustained ERK1/2 phosphorylation. On the other hand, in a subline overexpressing DUSP6, this response was suppressed through inhibition of ERK1/2 phosphorylation status [4]. Subsequent to ERK1/2 activation by phosphorylation, NF-κB undergoes activation and nuclear translocation. In addition to ERK1/2 and p38 mediating in HCEC control of DUSP phosphorylation status, in enterocytes MKP-1 (i.e., DUSP1) expression is elicited by NF-κB [12]. However, such a feedback role for NF-κB has not been described in HCEC. Clarification of this question will provide additional insight into how to control the increases in cell proliferation and migration induced by EGFR or PKC stimulation.

Cell cycle progression and proliferation are dependent on specific changes in cell volume during different phases of the cell cycle [13, 14]. Swelling is needed to accommodate the increases in chromatin content for preserving its equivalence between the parental and daughter cells. In the corneal epithelium, the aforementioned increases in K$^+$ channel, KCC and NKCC1 activity occurring during cell cycle progression can also be induced during exposure to an anisoosmotic challenge resulting in activation of regulatory volume behavior by HCEC and rabbit corneal epithelial cells [7, 15-19]. Exposure to a hypertonic challenge initially induces shrinkage followed by restoration of isotonic volume due to stimulation of NKCC1 activity. Alternatively, swelling induced by exposure to a hypotonic challenge elicits shrinkage through increases in KCl efflux. Even though EGF stimulates NKCC1 activity in HCEC, it is unclear if its activation is sufficient to induce swelling subsequent to a regulatory volume decrease resulting from K$^+$ channel and KCC cotransporter activation.

The dependence of a mitogenic response on NKCC1 activation has been established in a number of tissues based on kinase-mediated increases in its phosphorylation status. Some of the kinases directly activating NKCC1 in dorsal root ganglion neurons are the sterile-20-like kinases (SPAK) and oxidative stress response-1 (OSR1) kinase. Upon their activation through phosphorylation by upstream kinases, SPAK and OSR1 bind and phosphorylate specific peptides on NKCC1 and stimulate its activity. Upstream from these kinases are the with-no-lysine (WNK1) kinase osmosensor. Independent of these kinases, there may be others that also activate the NKCC1. Some indication that other kinases may be involved is that the residues on the NKCC1 following protein kinase A (PKA) activation by forskolin are different than the targets of SPAK phosphorylation. Similarly, some of the WNK kinases may not be participants in mediating NKCC1 phosphorylation since expression of a WNK isoform mutant did not block hypertonic-induced PKCα-mediated NKCC1 phosphorylation (i.e., activation) [20]. More recently, it

was shown in human airway epithelial cells that PKCδ acted upstream of SPAK in the phosphorylation of the NKCC1 by hyperosmotic stress [21]. However, growth factors do not activate the endogenous WNK1 osmosensor. Therefore, the identity of the kinase mediating NKCC1 activation by growth factors remains elusive [22].

ERK pathway-dependent phosphorylation of this cotransporter has also been identified in rat heart and cardiomyocytes [23]. In HCEC, neither the extent of ERK1/2 interaction with NKCC1 induced by PKC or EGFR activation nor their cause and effect relationship has been described. Another question is whether or not EGF-induced intracellular calcium ($[Ca^{2+}]_i$) signaling is requisite for ERK pathway activation. Such a possibility exists since in HCEC EGF-induced increases in $[Ca^{2+}]_i$ influx through transient receptor potential canonical 4 (TRPC4) channels are required for the mitogenic response [24].

We show here in HCEC that both EGF and PKC-induced increases in cell proliferation are dependent on NKCC1-induced cell swelling that occur as result of ERK pathway-mediated phosphorylation of this cotransporter. This effect occurs through protein-protein interaction between ERK1/2 and NKCC1. As shown previously for EGF, the mitogenic response to PKC is also negatively regulated by cytoplasmic localized DUSP6 with high specificity for phospho-ERK1/2 (i.e., activated). These results show that control of DUSP6 stabilization through phosphorylation permits regulation of the magnitude of a cytokine-induced increase in cell proliferation. Another negative feedback mediator is NF-κB whose activation by EGF also modulates ERK1/2 activation through control of DUSP1 expression levels.

Materials and Methods

Materials

The R5 antibody to detect NKCC1 phosphorylation is a generous gift from B. Forbush (Yale University). The following antibodies were purchased from Cell Signaling Technology, Inc. (Beverly, MA): phospho-p38, phospho-SAPK/JNK, phospho-Ser 21/9 GSK-3α/β and rabbit polyclonal IgG. Anti-ERK1, phospho-ERK1/2, goat anti-mouse IgG-HRP, goat anti-rabbit IgG-HRP antibody, and anti-(H196) actin, anti-ERK1/2, anti-p38, and β-actin antibodies were purchased from Santa Cruz Biotechnology (Santa Cruz, CA). Calcein-AM was obtained from Invitrogen (Carlsbad, CA). Bumetanide, AG178, phorbol dibutyrate (PDBu), (1,2-Bis(2-aminophenoxy)ethane-N,N,N',N'-tetraacetic acid acetoxymethyl ester (BAPTA/AM), PDTC (pyrroline dithiocarbamate), U0126, EGF, bovine insulin,

gentamicin, and 0.05% trypsin-EDTA solution were purchased from Sigma RBI (St. Louis, MO). Dulbecco's modified Eagle's medium (DMEM)/F12 medium and fetal bovine serum (FBS) were purchased from Gibco-Invitrogen (Carlsbad, CA).

Relative Cell Volume

Fluorescence was measured in HCEC after loading with 1 µM calcein-AM for 15 min at 23°C. Calcein-AM is a cell-permeable calcein derivative that is cleaved and trapped in the cytoplasm. Fluorescence was continuously measured with a 40x objective lens [oil immersion, numerical aperture (NA) 1.3] using a Nikon Diaphot inverted epifluorescence microscope equipped with halogen light source, calcein filter set (480-nm excitation, 490-nm dichroic mirror, 535-nm emission), photomultiplier detector, and 14-bit analog-to-digital converter. HCEC cultured on glass coverslips were secured in a perfusion chamber configured for rapid superfusion of a NaCl Ringers (306 mOsm) solution. It contained (mM): NaCl 147.8, KCl 4.7, MgCl$_2$ 0.4, glucose 5.5, CaCl$_2$ 1.8, and HEPES 5.3; pH adjusted to 7.4. Increases in fluorescence intensity were proportional to decline in osmolarity up to a 50% dilution with distilled water.

Western Blot analysis

Western blot experiments were performed as described [5]. In brief, the HCEC were gently washed twice in cold phosphate-buffered saline (PBS) and harvested in 0.5 ml cell lysis buffer. Cell lysates were centrifuged at 13,000 rpm for 15 min and supernates were collected. Protein content was measured with a bicinchoninic acid assay (BCA) protein assay kit (Pierce Biotechnology, Chicago, IL), and 200 µg protein was diluted with an equal volume of 2X Laemmli buffer. From 20 to 50 µg of denatured protein was electrophoresed on 10% polyacrylamide sodium dodecylsulfate (SDS) minigels and blocking polyvinylidene difluoride (PVDF) membranes with nonfat dry milk. The blots were exposed to the appropriate primary antibody overnight at 4°C. Then they were exposed to a 1:2000 dilution of a secondary antibody with anti-rabbit, anti-goat, or anti-mouse HRP labeled IgG for 1 h at room temperature. The immunoreactive bands were detected with a Western blot analysis kit (Amersham ECL Plus; GE Healthcare Lifesciences, Piscataway, NJ). Films were scanned and band density was quantified using image-conversion software (SigmaScan Pro 5.0; Systat Software, Inc., Mountain View, CA). The monoclonal anti-ERK1/2 and β-actin antibodies were used to test for protein loading equivalence.

Coimmunoprecipitation

Cells were lysed with lysis buffer and spun at 13,000 rpm for 10 min. An aliquot of supernatant containing 500 µg protein was exposed to either an antibody to detect total NKCC1 (i.e., T4), phosphorylated NKCC1 (i.e., R5) or total ERK1/2 antibody and gently agitated overnight at 4°C. The mouse monoclonal anti-NKCC ~T4 was purchased from DSHB (Developmental Studies Hybridoma Bank at the University of Iowa, Iowa City, IA). The T4 antibody binds the carboxy-110 terminus portion ~MET-902 to SER-1212 of human NKCC1 protein. Subsequently, protein A beads were added and cell lysates were exposed for another 2 h at 4°C with gentle agitation. Beads

were washed a few times with PBS and cell lysis buffer. The pellets obtained were resuspended in 50 µl cell lysis buffer, to which was added the same volume of 2X Laemmli buffer. The mixture was boiled for 5 min and then subjected to Western blot analysis with the appropriate antibody.

DUSP6 overexpression subline

This subline was previously established to determine the negative feedback effect of DUSP6 on EGF-induced increases in cytosolic ERK1/2 phosphorylation expression [4]. Stable overexpression of DUSP6 open reading frames (ORF) was accomplished using lentivectors based on the pLEX plasmid (Open Biosystems). The pLEX cassette drives expression of a MYC tagged ORF and the puror gene.

Cell Proliferation

[³H]-thymidine incorporation was performed as described [25]. After 24 h of serum starvation in medium supplemented with 0.5% bovine serum albumin, cells were incubated at 37°C for 1 h with 1 µCi/mL [³H]-thymidine (3.3-4.8 TBq/mmol) and then washed three times with ice-cold 5% trichloroacetic acid and twice with cold 90% ethanol. Cell lysates were solubilized with 0.2 N NaOH and 2% SDS. Radioactivity was monitored using a liquid scintillation counter and the data were normalized to cellular protein content using a modified Lowry assay.

Data Analysis

Data were analyzed using independent Student's two-tailed t-test. The data was considered significant if $p<0.05$. Results are reported as mean ± SEM for at least three independent experiments unless otherwise indicated.

Results

Dependence of proliferation on NKCC1 activation

In corneal epithelial cells, the mitogenic response to EGF occurs through stimulation of ion transporters and channel activity [8, 9]. To delineate if stimulation of NKCC1 by either EGF or a PKC activator, PDBu, is sufficient to induce this response, we determined their individual effects on cell proliferation. Figure 1 shows that during exposure to either 10 ng/ml EGF or 1 µM PDBu, proliferation increased about 1.6 or 1.72-fold, respectively whereas 30 min preincubation with 50 µM bumetanide fully inhibited each of these responses indicating that the mitogenic response to EGF is dependent on NKCC1 activation.

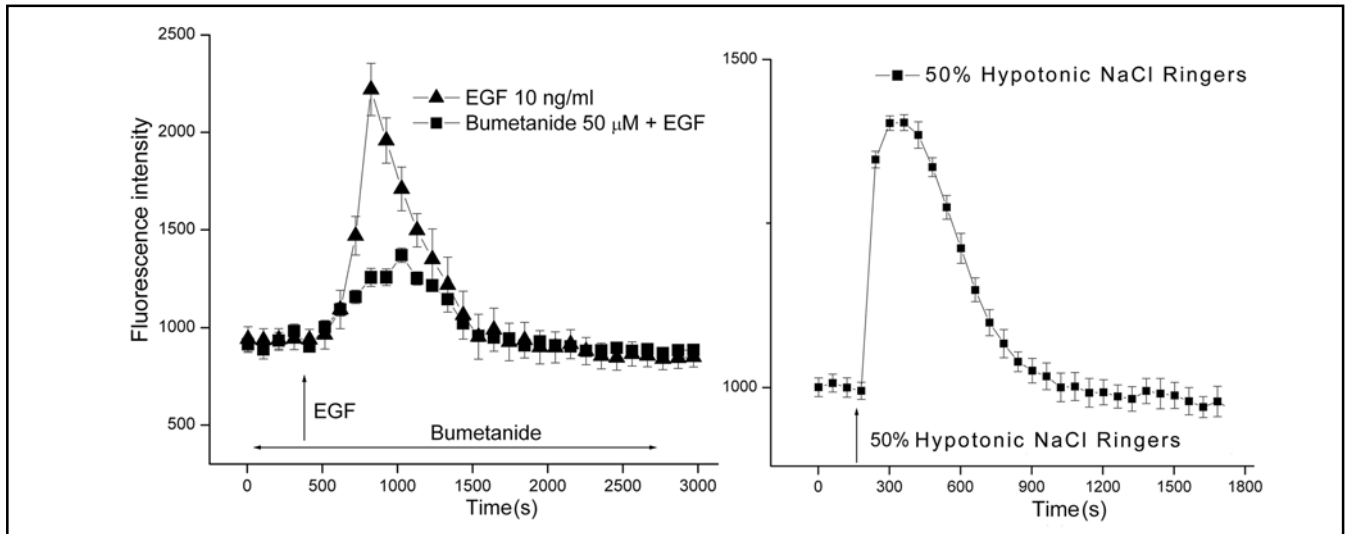### NKCC1 activation induces transient swelling

Even though it is apparent that NKCC1 activation is requisite for EGF and PKC-induced mitogenesis, it was unclear if its increase in activity is associated with cell
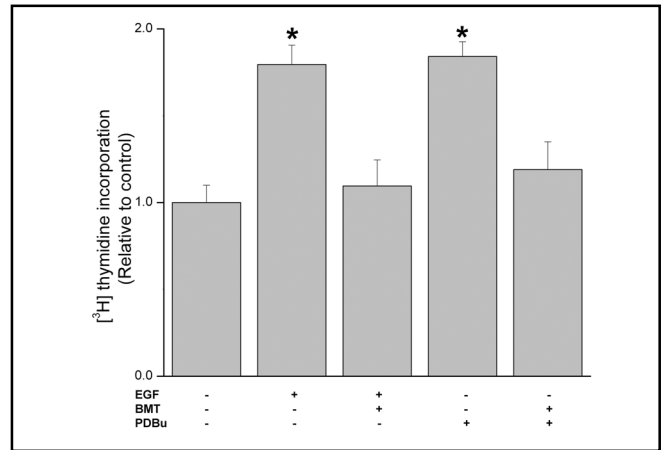
Fig. 1. NKCC1 inhibition suppresses EGF and PDBu-induced increases in cell proliferation. HCEC were pretreated for 30 min with bumetanide (BMT; 50 µM) and in some conditions were then exposed for an additional 20 h to either PDBu (1 µM) or EGF (10 ng/ml). Cells were incubated for 1 h with 1 µCi/mL [³H]-thymidine. Protein content was determined with a BCA protein assay kit. Data are presented as mean ± SEM (n=3). * p < 0.05 versus untreated control.

swelling. To make this assessment, we determined if relative cell volume increased during exposure to 10 ng/ml EGF. Figure 2 (left panel) shows that after about 7 min calcein emitted fluorescence increased more than 2-fold (Mean ± SEM: n=5; p<0.001 versus untreated control) followed by a return to a baseline value after about 12 min. On the other hand, 30 min preexposure to 50 µM bumetanide suppressed this rise by 68% showing that NKCC1 activation contributes to this response. The inability of bumetanide to fully suppress EGF-induced swelling may be indicative of a contribution by an increase in Na:H exchanger activity to this response since EGF-induces swelling in some other epithelia by stimulating Na⁺ influx via this pathway.

We validated that the EGF-induced rise in fluorescence is reflective of swelling by exposing the cells to a 50% hypotonic challenge. Such a stress induces a regulatory volume decrease response leading initially to a decrease in cell volume below the isotonic volume. This decline occurs in HCEC as a consequence of a net loss of KCl mediated by stimulation of K⁺ channel activity and KCC activity [7, 8, 19]. Isotonic volume is eventually restored subsequent to a volume overshoot below the isotonic volume. This occurs through NKCC1 activation [16]. Figure 2 (right panel) shows that the transient increase in fluorescence intensity induced by EGF was mimicked by exposure to a 50% hypotonic challenge. Therefore, this response induced by EGF is reflective of transient cell swelling.

Fig. 2. EGF induces transient HCEC swelling through NKCC1 activation. Calcein loaded HCEC attached to coverslips were placed in a chamber for superfusion of room temperature NaCl Ringers from syringes onto the stage of an epifluorescent microscope. The epifluorescent emission was measured between 503 and 530 nm. Panel A shows that following signal stabilization of about 3 min during control superfusion, the solution was substituted for another containing 10 ng/ml EGF (↑) (Mean ± SEM: n=5 coverslips; p<0.001 versus untreated control). After about 3 min, the corrected signal nearly rapidly doubled followed by gradual decline to reach a baseline level after about 15 more min. Pre-exposure for 30 min to 50 μM bumetanide suppressed the subsequent EGF-induced transient by about 70% (n=5; p<0.001). Panel B shows that substitution of the control 306 mOsm NaCl Ringers with one diluted by 50% induced after about 1 min a transient increase in fluorescence reflective of swelling since calcein is a self-quenching dye (n=4 coverslips; p<0.005 versus isotonic control). The pattern of this transient was very similar to that induced by EGF, but instead is reflective of hypotonic-induced stimulation of KCC and K⁺ channel activity rather than NKCC1 activation by EGF shown in panel A [7, 17].

Time dependent increases in NKCC1 phosphorylation induced by EGF and PDBu

It is well established that NKCC1 phosphorylation by different kinases mediates activation of this cotransporter [21]. Nevertheless, in fibroblasts there is some uncertainty regarding the cause and effect relationship between ERK1/2 and NKCC1 activation since it was reported that growth factor-induced NKCC1 activation precedes ERK1/2 phosphorylation [26]. However, ERK1/2 and PKCδ activation induced NKCC1 phosphorylation in human tracheal epithelial cells [21]. We also used a R5 phospho-specific antibody to determine the time dependence for changes in NKCC1 phosphorylation. R5 was raised to detect phosphorylation of residues Thr212 and Thr217 in human NKCC1 [27]. As the pathways mediating ERK1/2 phosphorylation by EGF and phorbol esters are different from one another [28], the time patterns were also determined of changes in p-ERK1/2 and p-NKCC1 levels induced by 1 μM PDBu. Figure 3A shows that after 5 min exposure to EGF phosphorylation of ERK1/2 increased nearly 4.7-fold, remained essentially stable until 30 min and waned to reach at 90 min a level similar to the baseline value. After 15 min, NKCC1 phosphorylation increased to a

level similar to that reached by ERK1/2 at 5 min. Subsequently, the NKCC1 level waned faster, but stabilized at a value at 90 min that was nearly 2-fold higher than that for ERK1/2. Figure 3B shows that PKC stimulation induced a similar pattern of increases in ERK1/2 and NKCC1 phosphorylation. The level of p-ERK1/2 increased rapidly to reach a maximum value after 5 min followed by declines reaching nearly the baseline level after 90 min. Changes in p-NKCC1 mirrored those for p-ERK1/2. However, the maximum p-NKCC1 level was observed 10 min later than those for ERK1/2. This close association between the time-dependent changes in p-ERK1/2 and p-NKCC1 induced by either EGF or PDBu appears to indicate that ERK1/2 mediates NKCC1 activation.

Dependence of NKCC1 phosphorylation on ERK1/2 activation

Figure 4A documents that the increases in ERK1/2 and NKCC1 phosphorylation were indeed dependent on EGF-induced EGFR and ERK1/2 activation since inhibition for 5 min of EGFR or Mek1/2 activation with either 5 μM AG1478 or 10 μM U0126, respectively blocked EGF-induced increases in both p-ERK1/2 and
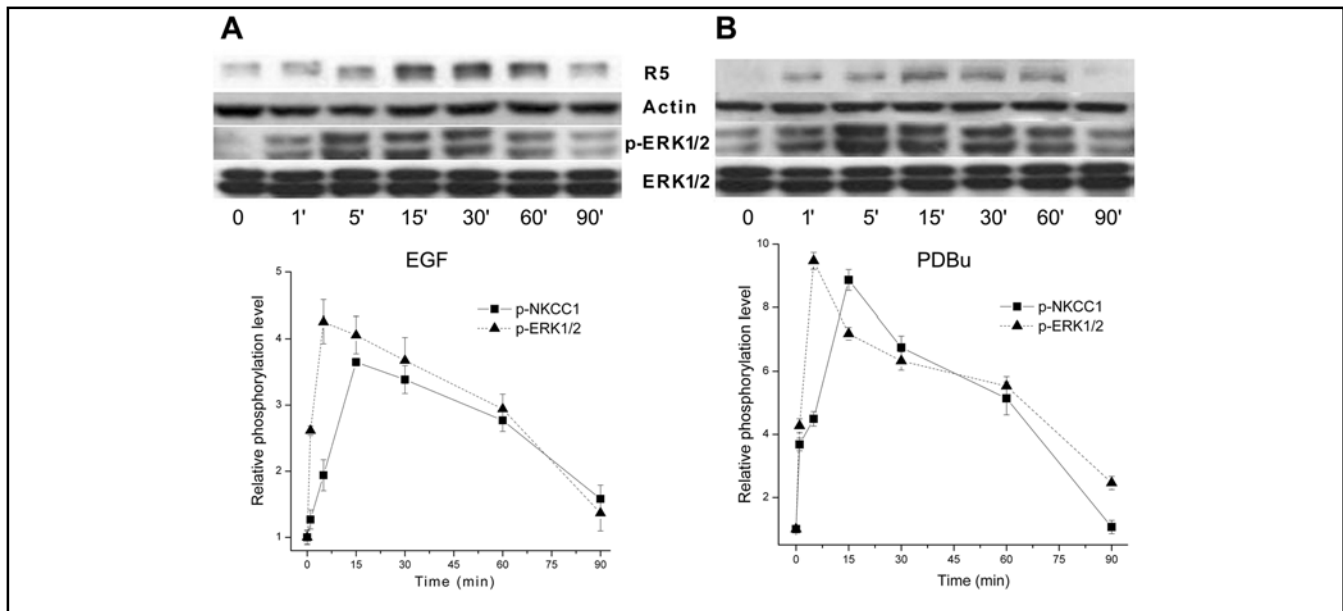
Fig. 3. Time-dependent changes in ERK1/2 and NKCC1 phosphorylation status induced by EGF and PDBu. HCEC were serum starved for 24 h at 80% to 90% confluence. Panel A shows the effects of exposure to 10 ng/ml EGF for up to 90 min with a representative Western blot analysis of anti-phosphor p-NKCC1 (i.e., R5) and p-ERK1/2 antibody binding. Panel B shows cells exposed to 1 µM PDBu and Western blot analysis performed using the same antibodies as those shown in panel A. Equal loading of proteins was confirmed by reprobing the blots with β-actin.

p-NKCC1 formation. In addition, these results indicate that EGF-induced NKCC1 activation is completely ERK pathway-dependent. To clarify whether or not ERK1/2 phosphorylation is a result or a cause of NKCC1 activation, we determined the cause and effect relationship between NKCC1 and ERK1/2 activation by comparing the effects of either 25 or 50 µM bumetanide on EGF-induced NKCC1 and ERK1/2 phosphorylation (Fig. 4B). Preinhibition for 30 min with either 25 or 50 µM bumetanide abolished the EGF-induced increases in NKCC1 phosphorylation status, but had no effect on ERK1/2 activation. Taken together, NKCC1 activation occurred as a consequence of ERK1/2 activation.

PKC mediates NKCC1 phosphorylation through ERK1/2 activation

We determined if the cause and effect relationship between ERK1/2 and NKCC1 activation by PKC is the same as that for EGF. Figure 5 compares the individual effects of 50 µM bumetanide or 10 µM U0126 on PDBu-induced ERK1/2 and NKCC1 phosphorylation. A 30 min preincubation with bumetanide completely blocked a near 6-fold increase in NKCC1 phosphorylation, but had only an insignificant effect on the 7.4-fold increase in ERK1/2 phosphorylation induced by PDBu. On the other hand, preincubation with U0126 completely abolished both PDBu-induced ERK1/2 and NKCC1 activation. This

difference indicates that PKC-induced NKCC1 activation is completely dependent on Mek1/2-mediated ERK1/2 phosphorylation whereas bumetanide failed to block ERK1/2 activation by PKC.

*Dependence of ERK1/2 activation by EGF on Ca^{2+} influx*

EGF-induced increases in HCEC proliferation are dependent on its activation of plasma membrane Ca^{2+} influx through one isotype of the TRP canonical superfamily designated TRPC4 [24]. We determined if EGF-induced ERK1/2 and NKCC1 phosphorylation is dependent on cytosolic $[Ca^{2+}]_i$ content. Figure 6 shows that large increases in the phosphorylation level of both proteins caused by 10 ng/ml EGF at 5 min similarly waned as a function of increases in BAPTA-AM concentration (unstimulated control level not shown). With 120 µM BAPTA-AM, EGF-induced ERK1/2 and NKCC1 phosphorylation was fully attenuated. This result suggests that there is a direct dependence between ERK1/2 and NKCC1 activation on transient rises in $[Ca^{2+}]_i$ levels induced by EGF.

EGF-induces ERK1/2-NKCC1 interaction

To determine if ERK1/2 activation elicits a close association with NKCC1, we probed for time-dependent increases in protein-protein interaction between them.
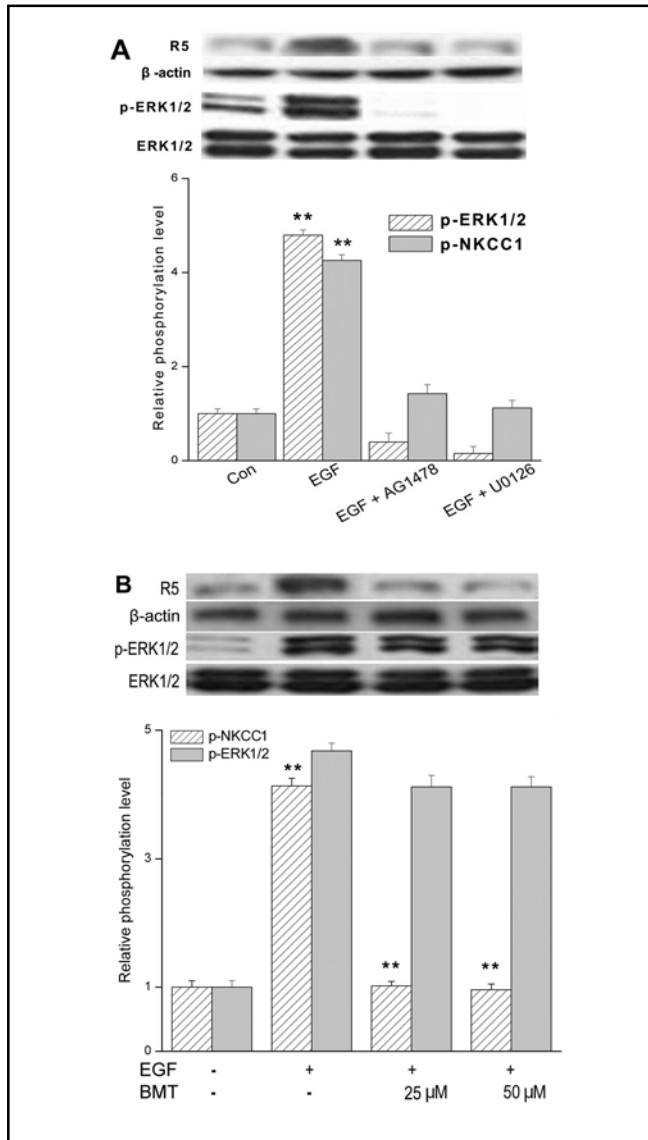
Fig. 4. Dependence of NKCC1 activation on EGFR-linked signaling. HCEC were serum starved for 24 h at 80% to 90% confluence. (A) Representative Western blot analysis comparing the effects of exposure to 10 ng/ml EGF after a 5 min exposure in the presence and absence of either 5 μM AG1478 or 10 μM U0126 on ERK1/2 and NKCC1 phosphorylation (n=3; **p<0.001 versus untreated control). The blots were probed with anti p-NKCC1 (i.e., R5) and p-ERK1/2 antibodies. Equal loading of proteins was confirmed by reprobing the same blot with anti total ERK1/2 antibody. Summary of changes in ERK1/2 and NKCC1 phosphorylation status is shown below the aforementioned blots. (B) Representative experiments of the dose-dependent inhibitory effects of 25 to 50 μM bumetanide (BMT) with 10 ng/ml EGF-induced NKCC1 phosphorylation detected with the anti p-NKCC1 and p-ERK1/2 antibodies (n=3; **p<0.001 versus NKCC1 phosphorylation levels treated with BMT). Equivalent protein loading was confirmed by reprobing the same blot with actin and ERK1/2 antibody, respectively. Data represent the mean ± SEM of three independent experiments.
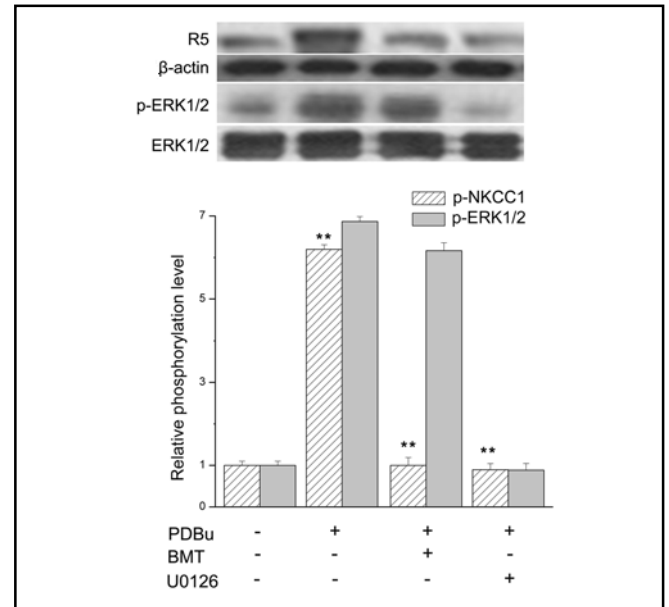
Fig. 5. Inhibition of PDBu-induced PKC activation of NKCC1 and ERK1/2 phosphorylation. HCEC were serum starved for 24 h at 80% to 90% confluence. Representative Western blot analysis comparing the effects of exposure to 1 μM PDBu in the presence and absence of either 50 μM bumetanide (BMT) (**p<0.001 PDBu versus treat with BMT). or 10 μM U0126 (**p<0.001 PDBu versus treat with U0126 on phosphorylation levels in both NKCC1 and ERK1/2). on p-NKCC1 and p-ERK1/2 detected with anti p-NKCC1 (i.e., R5) and p-ERK1/2 antibodies. Equivalent protein loading was confirmed by reprobing the same blot with anti actin and ERK1/2 antibody, respectively. Data represent the mean ± SEM of three independent experiments.

First, we assessed if there are any changes in the amounts of p-ERK1/2 associated with total NKCC1 during EGF exposure. Membrane enriched fractions of EGF stimulated cells were subjected to SDS polyacrylamide gel electrophoresis. A representative image shown in Figure 7 (insert) indicates that EGF caused a time-dependent increase in amounts of both NKCC1 (upper band) and phospho-ERK1/2 (lower band) in the same fraction. The summary plot shows that their content changed with a similar pattern and after 15 min rose about 2.3 or 5-fold for NKCC1 or p-ERK1/2, respectively. This parallelism suggests that during stimulation of the resting cells with EGF an interaction occurred between phosphorylated ERK1/2 and membrane associated NKCC1.
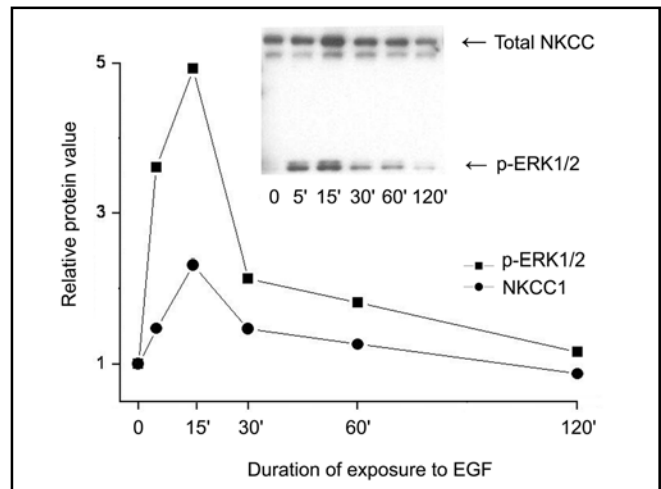
Dose dependent effects of EGF on ERK1/2-NKCC1 interaction

To validate protein-protein interaction between phosphorylated ERK1/2 and total NKCC1, pull down
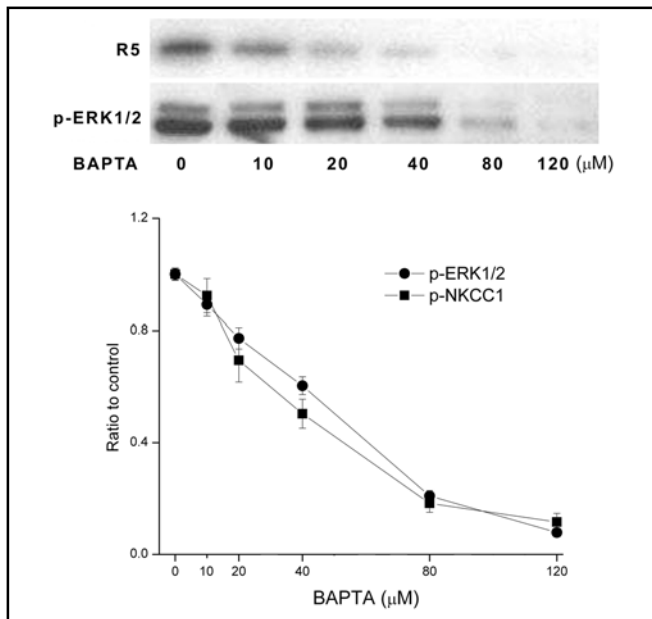
Fig. 6. Dependence of EGF-induced ERK1/2 and NKCC1 phosphorylation on $[Ca^{2+}]_i$. HCEC were serum starved for 24 h at 80% to 90% confluence. Representative Western blot analysis compares the dose dependent inhibitory effects of exposure to BAPTA on 10 ng/ml EGF-induced p-NKCC1 and p-ERK1/2 formation detected with the anti p-NKCC1 (i.e., R5) and p-ERK1/2 antibodies. HCEC were preincubated for 30 min with each of the indicated BAPTA concentrations prior to exposure to EGF for an additional 5 min. Results were normalized to the increase in p-ERK1/2 formation obtained after 5 min in the absence of BAPTA. Data represent the mean ± SEM of three independent experiments (at concentrations over 40 µM BAPTA, p<0.001 versus untreated control).
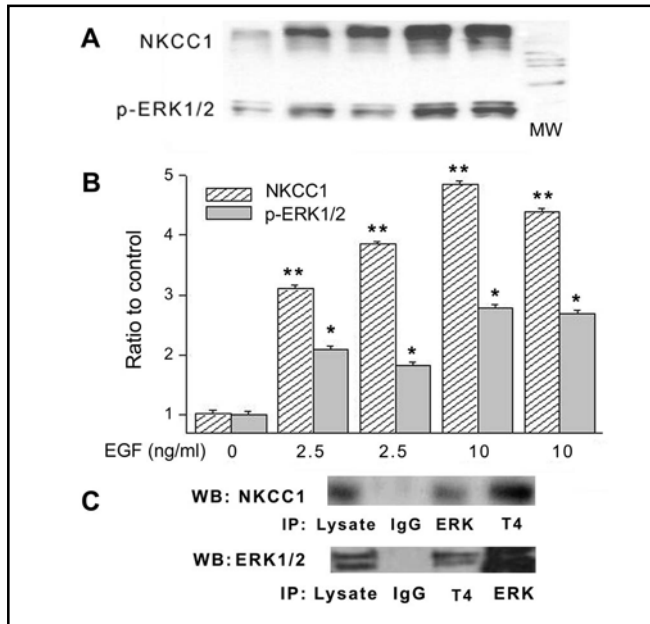

Fig. 7. Time-dependent changes in p-ERK1/2 association with NKCC. HCEC were serum starved for 24 h at 80% to 90% confluence. Cells were exposed to 10 ng/ml EGF for up to 120 min. Membrane-enriched fractions were obtained following centrifugation. Pellets were probed for relative amounts of total NKCC1 with the anti T4 antibody and p-ERK1/2 antibodies at the indicated times following exposure to EGF. Data represent the mean ± SEM of three independent experiments (after 15 min exposure to EGF, p<0.002 total NKCC versus untreated control; or p<0.001 p-ERK1/2 versus untreated control, respectively). The error bars fall within the range of the indicated symbols for p-ERK1/2 and NKCC1.

experiments with a specific p-ERK1/2 antibody were performed. Figure 8A demonstrates that EGF caused concentration-dependent increases in the amounts of association of NKCC1 with p-ERK1/2. Figure 8B provides a summary of the results obtained with duplicate samples each performed in triplicate that were exposed to 2.5 or 10 ng/ml EGF. There is a clear correspondence between increases in p-ERK1/2 and total NKCC1 in cell extracts, which rose with 10 ng/ml EGF up to 4 and 8-fold, respectively. This association between p-ERK1/2 and NKCC1 levels suggests that p-ERK1/2 co-localized with NKCC1 and could be one of the kinases directly involved in EGF-induced NKCC1 activation. To further validate their colocalization, we immunoprecipitated NKCC1 and probed the immune complexes for p-ERK1/2 and vice versa. The results shown in Fig. 8C demonstrate that there was a significant amount of NKCC1 in the immune complexes of ERK1/2 (top panel) and similarly ERK1/2 was found in the NKCC1 complexes (bottom panel). These results also strongly support that protein-

protein interaction occurred between p-ERK1/2 and NKCC1.

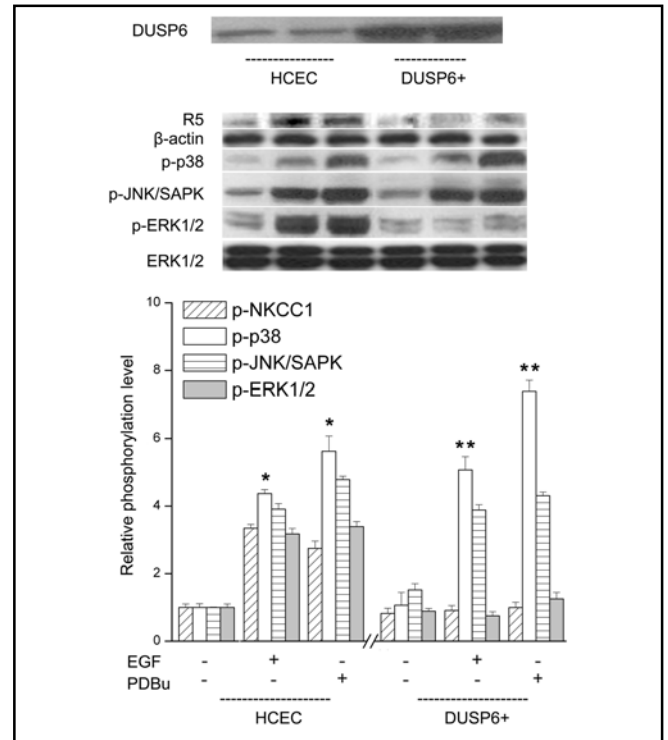*Negative feedback control by DUSP6 of ERK1/2 activation*

The mitogenic responses in HCEC to EGFR and PKC stimulation are dependent on the duration and magnitude of ERK1/2 activation [6]. DUSP6 inactivates p-ERK1/2 through dephosphorylating serine and threonine residues on this terminal kinase. We determined if DUSP6 overexpression in a subline altered the effects of EGFR or PKC activation on NKCC1, p38, JNK1/2 and ERK1/2 phosphorylation status. Figure 9 contrasts in each case the difference between the individual effects of 15 min exposure to either EGF or PDBu on each of the aforementioned entities. In control cells, 15 min exposure to either EGF or PDBu led to increases in phosphorylation status of all kinases whereas in the DUSP6 overexpressing cell line only increases in ERK1/2 and NKCC1 phosphorylation were completely suppressed. Such suppression fully obviated increases in cell proliferation induced by PKC stimulation with 1 µM PDBu (data not shown). These effects indicate that ERK1/2 inactivation blocks NKCC1 phosphorylation.

Fig. 8. Pull-down experiments validate NKCC1-p-ERK1/2 interaction induced by EGF. HCEC were serum starved for 24 h at 80% to 90% confluence. (A) Cells were exposed to either 2.5 or 10 ng/ml EGF for 10 min. Membrane enriched pellets were obtained from different cell lysates and Western blot (WB) probing for either p-ERK1/2 or total NKCC1 association with p-ERK1/2 and T4 antibodies, respectively. (B) Results of experiments performed in duplicate at each concentration normalized to the amounts detected prior to exposure to EGF (Exposure to 2.5 or 10 ng/ml EGF, *p<0.05 p-ERK1/2 versus untreated control; **p<0.001 NKCC1 versus untreated control). (C) Co-localization validation entailed immunoprecipitation (IP) with beads bound to ERK1/2 or NKCC1 followed by probing the precipitate with either anti T4 or ERK1/2 antibodies using Western blot analysis. In the IPs were obtained with either the anti T4 antibody or ERK1/2 antibody, there are increases in the amounts of ERK1/2 and NKCC1, respectively. These results validate that exposure to EGF-induces increases in the amounts of p-ERK1/2 associating with NKCC1. Cells were exposed to 10 ng/ml for 10 min. The results shown were obtained from two different experiments each performed in triplicate.

Fig. 9. Selective inhibition in DUSP6 overexpression HCEC subline (DUSP6+) of EGF and PDBu -induced ERK1/2 and p-NKCC1 phosphorylation. HCEC were serum starved for 24 h at 80% to 90% confluence. Representative Western blot analysis compares p-NKCC1, p-p38, p-JNK1/2/SAPK and p-ERK1/2 formation with the appropriate antibody in cell lysates obtained from wildtype and the DUSP6 overexpressing HCEC subline. Summaries of the individual effects of DUSP6 overexpression are shown below of data (mean ± SEM: n=3; *p<0.05 versus untreated control) obtained from three individual experiments. DUSP6 overexpression selectively blocked EGF and PDBu-induced p-NKCC1 and p-ERK1/2 (n=3; **p<0.001 versus EGF and PDBu-induced p-p38 and p-JNK1/2/SAPK), which is consistent with the notion that NKCC1 phosphorylation is dependent on ERK1/2 activation by either EGF or PDBu.

NF-κB inactivation by PDTC destabilizes DUSP1 expression

The phosphorylation status of DUSPs affects their stability, which in turn modulates through negative feedback the duration and magnitude of ERK1/2 activation and the resulting mitogenic response to a growth factor [29]. As ERK1/2 and GSK-3α/β mediate DUSP1 phosphorylation, changes in DUSP1 expression levels shape the duration and magnitude of both ERK1/2 and p38 phosphorylation [5, 6]. Such shaping has not been shown to be related to changes in DUSP activity, but rather DUSPs stabilization is modulated through changes in their phosphorylation status [30]. It was recently shown

in enterocytes that DUSP1 stabilization is also affected by NF-κB activation, which in turn has a negative feedback effect on p38-induced phosphorylation [12].

We determined if NF-κB inhibition by 50 μM PDTC affects EGF-induced changes in NKCC1, ERK1/2 and GSK-3α/β phosphorylation as well as total DUSP1 expression.

To make such an assessment, HCEC were preincubated with PDTC followed by 15 min exposure to 10 ng/ml EGF. Figure 10 compares the effects of EGF alone at 15 min with those of exposure to EGF for up to 90 min in the presence of PDTC. With EGF alone, the DUSP1 level was much higher than that in the presence

of both EGF and PDTC. Such a difference was associated with higher levels of phosphorylated NKCC1, ERK1/2 and GSK-3α/β than those obtained in the absence of PDTC. It should be recalled that an increase in GSK-3α/β phosphorylation is reflective of inhibition of this kinase. Interestingly, the elevated levels of p-GSK-3α/β were accompanied by a marked decline in DUSP1 expression levels over a 90 min period. This decline in DUSP1 expression is attributable to EGF-induced inactivation of GSK-3α/β through its activation of the PI3-K/Akt/GSK-3 pathway in HCEC [6]. The accompanying stabilization of the increase in EGF-induced ERK1/2 phosphorylation is therefore accountable for by loss of DUSP1 stabilization resulting from PDTC promotion of GSK-3α/β inactivation (i.e., sustained phosphorylation).

Discussion

In HCEC, some of the downstream signaling events induced by EGFR stimulation include transient activation of the MAPK superfamily as well as the PI3-K/Akt signaling cascade, PKC and time-dependent stimulation of K^+ channel, KCC along with increases in NKCC1 activity [7-9, 31-33]. All of these changes are linked to NF-κB activation whose p50/p65 subunits induce promoter activation leading to the expression of genes underlying proliferation [3]. MAPK activation is under the negative feedback control elicited by DUSPs 1, 4, 5 and 6 whose stabilization by kinases is phosphorylation-dependent [4, 30]. The goal of the current study was to: 1) better delineate the interdependence between the aforementioned signaling events in modulation of EGF and PKC-induced mitogenesis; 2) clarify how changes in DUSPs 1 and 6 expression levels elicit negative feedback control of ERK1/2-induced NKCC1 activation.

Even though earlier studies showed that modulation of NKCC1 activity affects mitogen-induced increases in cell proliferation, there was no evidence indicating that swelling is attributable to its stimulation [9, 16]. Here we show (Fig. 2: left panel) that EGF induced transient increases in apparent cell volume, which were associated with ERK1/2-induced NKCC1 phosphorylation. This cause and effect relationship is in agreement with a study using mice astrocytes in which exposure to a high K^+ containing medium induced swelling that is dependent on ERK1/2 activation of NKCC1[34]. The changes induced by PKC activation are also supportive of this cause and effect relationship. This is evident since PDBu, whose
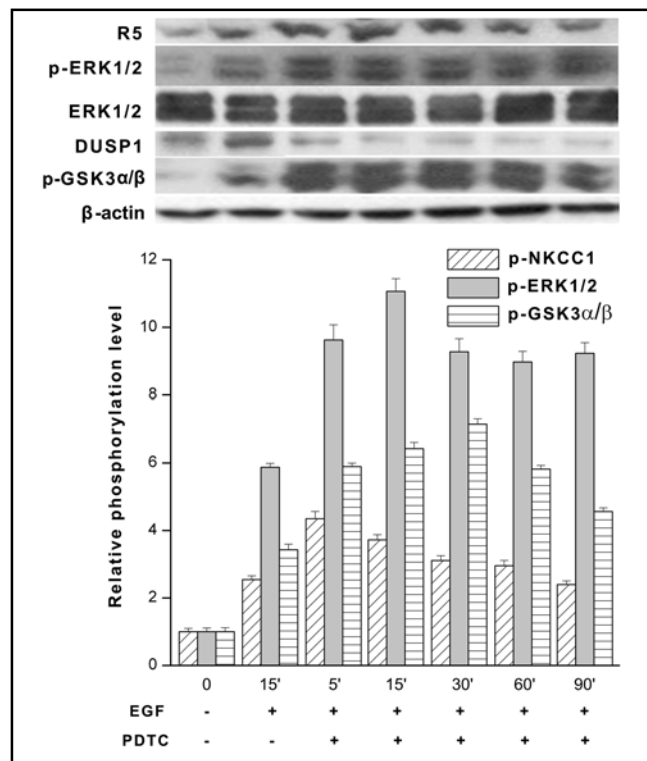
Fig. 10. NF-κB inhibition prolongs EGF-induced ERK1/2 activation through downregulation of DUSP1 expression. HCEC were serum starved for 24 h at 80% to 90% confluence. Cells were exposed to 10 ng/ml EGF either in the presence or absence of 50 μM PDTC and cell lysates were obtained at each of the indicated times up to 90 min. The results obtained with PDTC following 15 min incubation and exposure to EGF for another 15 min are compared to those with EGF for up to 90 min without PDTC. Western blot analysis was performed with p-NKCC1, p-ERK1/2 and equivalent protein loading was confirmed with the anti ERK1/2 antibody. Under the same conditions individual changes in DUSP1 and p-GSK-3α/β expression detected with the appropriate antibody. Data represent the mean ± SEM of three independent experiments. It is notable that PDTC exposure resulted in sustained p-ERK1/2 and p-NKCC1 formation over the 90 min (p<0.001 versus untreated control) period whereas declines in total DUSP1 exposure were accompanied by pronounced and continuous p-GSK3-α/β expression (p<0.05 versus untreated control). PDTC appears to inhibit GSK-3α/β through phosphorylation leading to declines in DUSP1 expression. Such declines account for sustained ERK1/2 phosphorylation due to loss of negative feedback control by DUSP1 of ERK1/2 activation.

effects may not be limited to PKC activation, induced a maximal increase in ERK1/2 phosphorylation after the first 5 min whereas an increase in NKCC1 phosphorylation status reached its peak only after 15 min (Fig. 3). Furthermore, the subsequent decreases in the phospho-NKCC1 levels mirrored those of phospho-ERK1/2.

It should be mentioned that an increase in NKCC1 phosphorylation status detected with the R5 antibody might not necessarily be reflective of a corresponding change in its ion transport activity. Recently, it was shown in HEK-293 cells expressing NKCC1 that increases in its phosphorylation status detected with this antibody were not in all cases accompanied by ion transport activity stimulation. This disconnect led to the conclusion that NKCC1 phosphorylation is necessary, but not sufficient for inducing ion transport stimulation. Nevertheless, the R5 antibody provided meaningful results showing that declines in NKCC1 phosphorylation status were associated with proportional decreases in ion transport activity [35].

In some other tissues, growth factors and hypertonic stress initially induce NKCC1 activation through either PKC phosphorylation or ERK1/2 phosphorylation [20, 21, 23]. In HCEC, ERK pathway inhibition also eliminated increases in ERK1/2 and NKCC1 phosphorylation status induced by PDBu. Both of these events appear to be dependent on EGF-induced rises in $[Ca^{2+}]_i$ since the declines in their activation mirrored one another as a function of increases in BAPTA-AM concentration (Fig. 6). This dependence of MAPK activation on Ca^{2+} influx induced by EGF was described in conjunctival goblet cells and mice astrocytes [36, 34].

Even though we found that EGF induced time- and concentration-dependent increases in the interaction between phospho-ERK1/2 and total NKCC1 in membrane enriched fractions (Figs. 7 and 8), these results do not indicate whether phospho-ERK1/2 directly activates NKCC1. Nevertheless, NKCC1 phosphorylation is dependent on ERK1/2 activation by either EGF or PDBu since DUSP6 overexpression (Fig. 9) only blocked NKCC1 and ERK1/2 phosphorylation. Phosphorylation of NKCC1 by SPAK and OSR1 kinases is downstream from ERK1/2 in other tissues and is critical in NKCC1 activation. These kinases induce NKCC1 activation in response to cell shrinkage, injury and other effectors, but not growth factors [22]. They may not have redundant function, but are individually activated by different upstream signaling pathways. For example, in dorsal root ganglion neurons SPAK and OSR1 both

mediate NKCC1 phosphorylation whereas in different tissues their direct involvement in this process is variable [20]. In any case, the identity remains elusive of the kinases mediating ERK1/2-induced NKCC1 phosphorylation.

The results shown in Fig. 10 indicate that DUSP1 expression is also modulated by changes in NF-κB activity as well as the ERK1/2 and PI3-K/Akt/GSK-3 pathway. This is evident since PDTC caused DUSP1 expression to decline resulting in sustained and prolonged phosphorylation of ERK1/2 and GSK-3α/β as well as larger increases in p-NKCC1 formation. This change in the ERK1/2 phosphorylation pattern suggests that PDTC also inhibits GSK-3α/β since its inhibition by a GSK-3α/β inhibitor, SB415286, caused DUSP1 expression to wane with the same time course as that shown here [6]. This waning effect following GSK-3α/β inhibition by phosphorylation occurred because active nonphosphorylated GSK-3α/β mediates DUSP1 phosphorylation, which protects DUSP1 from being degraded by endosomal activity. Our finding that PDTC inhibited GSK-3α/β dephosphorylation is consistent with two different reports in which: 1) this antioxidant reduced hypoxia-induced Akt and GSK-3α/β dephosphorylation in the brain [37]; 2) PDTC-induced GSK-3α/β inactivation in enterocytes resulting in prolonged MAPK activation [12].

Taken together, this study suggests that EGF and PKC-induced increases in proliferation are essentially dependent on increases in $[Ca^{2+}]_i$ levels mediating p-ERK1/2-induced NKCC1 phosphorylation through protein-protein interaction between ERK1/2 and NKCC1. The mitogenic responses induced by such interaction are modulated through negative feedback control by changes in the expression levels of DUSP1 and DUSP6. DUSP1 expression levels are determined by changes in NF-κB activity as well as previously described modulation of ERK1/2 and p38 MAPK phosphorylation [6].

Acknowledgements

References

1 Yu FS, Yin J, Xu K, Huang J: Growth factors and corneal epithelial wound healing. Brain Res Bull 2010;81:229-235.

2 Reinach PS, Pokorny KS: The corneal epithelium: Clinical relevance of cytokine-mediated responses to maintenance of corneal health. Arq Bras Oftalmol 2008;71:80-86.

3 Lu L, Wang L, Li T, Wang J: Nf-kappab subtypes regulate ccctc binding factor affecting corneal epithelial cell fate. J Biol Chem 2010;285:9373-9382.

4   Wang Z, Reinach PS, Zhang F, Vellonen KS, Urtti A, Turner H, Wolosin JM: Dusp5 and dusp6 modulate corneal epithelial cell proliferation. Mol Vis 2010;16:1696-1704.

5   Wang Z, Yang H, Tachado SD, Capo-Aponte JE, Bildin VN, Koziel H, Reinach PS: Phosphatase-mediated crosstalk control of Erk and p38 mapk signaling in corneal epithelial cells. Invest Ophthalmol Vis Sci 2006;47:5267-5275.

6   Wang Z, Yang H, Zhang F, Pan Z, Capo-Aponte J, Reinach PS: Dependence of EGF-induced increases in corneal epithelial proliferation and migration on GSK-3 inactivation. Invest Ophthalmol Vis Sci 2009;50:4828-4835.

7   Capo-Aponte JE, Wang Z, Akinci MA, Wolosin JM, Pokorny KS, Iserovish P, Reinach PS: Potassium-chloride cotransporter mediates cell cycle progression and proliferation of human corneal epithelial cells. Cell Cycle 2007;6:2709-2718.

8   Roderick C, Reinach PS, Wang L, Lu L: Modulation of rabbit corneal epithelial cell proliferation by growth factor-regulated K^+ channel activity. J Membr Biol 2003;196:41-50.

9   Yang H, Wang Z, Miyamoto Y, Reinach PS: Cell signaling pathways mediating epidermal growth factor stimulation of Na:K:Cl cotransport activity in rabbit corneal epithelial cells. J Membr Biol 2001;183:93-101.

10   Okada Y, Saika S, Shirai K, Yamanaka O, Kitano A, Wang Z, Yang H, Reinach P: JNK MAPK signaling contributes in vivo to injury-induced corneal epithelial migration. Ophthalmic Res 2009;42:185-192.

11   Owens DM, Keyse SM: Differential regulation of map kinase signalling by dual-specificity protein phosphatases. Oncogene 2007;26:3203-3213.

12   Wang J, Ford HR, Grishin AV: NF-kappab-mediated expression of MAPK phosphatase-1 is an early step in desensitization to tlr ligands in enterocytes. Mucosal Immunol 2010;3:523-534.

13   Hoffmann EK, Lambert IH, Pedersen SF: Physiology of cell volume regulation in vertebrates. Physiol Rev 2009;89:193-277.

14   Lang F, Foller M, Lang K, Lang P, Ritter M, Vereninov A, Szabo I, Huber SM, Gulbins E: Cell volume regulatory ion channels in cell proliferation and cell death. Methods Enzymol 2007;428:209-225.

15   Bildin VN, Wang Z, Iserovich P, Reinach PS: Hypertonicity-induced p38MAPK activation elicits recovery of corneal epithelial cell volume and layer integrity. J Membr Biol 2003;193:1-13.

16   Bildin VN, Yang H, Crook RB, Fischbarg J, Reinach PS: Adaptation by corneal epithelial cells to chronic hypertonic stress depends on upregulation of Na:K:Cl cotransporter gene and protein expression and ion transport activity. J Membr Biol 2000;177:41-50.

17   Capo-Aponte JE, Iserovich P, Reinach PS: Characterization of regulatory volume behavior by fluorescence quenching in human corneal epithelial cells. J Membr Biol 2005;207:11-22.

18   Capo-Aponte JE, Wang Z, Bildin VN, Pokorny KS, Reinach PS: Fate of hypertonicity-stressed corneal epithelial cells depends on differential MAPK activation and p38 MAPK/Na-K-2Cl cotransporter1 interaction. Exp Eye Res 2007;84:361-372.

19   Wu X, Yang H, Iserovich P, Fischbarg J, Reinach PS: Regulatory volume decrease by sv40-transformed rabbit corneal epithelial cells requires ryanodine-sensitive Ca^{2+}-induced Ca^{2+} release. J Membr Biol 1997;158:127-136.

20   Delpire E, Gagnon KB: Spak and osr1, key kinases involved in the regulation of chloride transport. Acta Physiol (Oxf) 2006;187:103-113.

21   Smith L, Smallwood N, Altman A, Liedtke CM: Pkcdelta acts upstream of SPAK in the activation of NKCC1 by hyperosmotic stress in human airway epithelial cells. J Biol Chem 2008;283:22147-22156.

22   Kahle KT, Rinehart J, Lifton RP: Phosphoregulation of the Na-K-2Cl and K-Cl cotransporters by the wnk kinases. Biochim Biophys Acta 2010;1802:1150-1158.

23   Andersen GO, Skomedal T, Enger M, Fidjeland A, Brattelid T, Levy FO, Osnes JB: Alpha1-ar-mediated activation of nkcc in rat cardiomyocytes involves Erk-dependent phosphorylation of the cotransporter. Am J Physiol Heart Circ Physiol 2004;286:H1354-1360.

24   Yang H, Mergler S, Sun X, Wang Z, Lu L, Bonanno JA, Pleyer U, Reinach PS: TRPC4 knockdown suppresses epidermal growth factor-induced store-operated channel activation and growth in human corneal epithelial cells. J Biol Chem 2005;280:32230-32237.

25   Yang H, Sun X, Wang Z, Ning G, Zhang F, Kong J, Lu L, Reinach PS: EGF stimulates growth by enhancing capacitative calcium entry in corneal epithelial cells. J Membr Biol 2003;194:47-58.

26   Panet R, Eliash M, Pick M, Atlan H: $Na^+/K^+/Cl^-$ cotransporter activates mitogen-activated protein kinase in fibroblasts and lymphocytes. J Cell Physiol 2002;190:227-237.

27   Flemmer AW, Gimenez I, Dowd BF, Darman RB, Forbush B: Activation of the Na-K-Cl cotransporter nkcc1 detected with a phospho-specific antibody. J Biol Chem 2002;277:37551-37558.

28   Xu KP, Dartt DA, Yu FS: EGF-induced erk phosphorylation independent of PKC isozymes in human corneal epithelial cells. Invest Ophthalmol Vis Sci 2002;43:3673-3679.

29   Brondello JM, Pouyssegur J, McKenzie FR: Reduced map kinase phosphatase-1 degradation after p42/p44MAPK-dependent phosphorylation. Science 1999;286:2514-2517.

30   Kucharska A, Rushworth LK, Staples C, Morrice NA, Keyse SM: Regulation of the inducible nuclear dual-specificity phosphatase DUSP5 by Erk MAPK. Cell Signal 2009;21:1794-1805.

31   Islam M, Akhtar RA: Upregulation of phospholipase cgamma1 activity during EGF-induced proliferation of corneal epithelial cells: Effect of phosphoino-sitide-3 kinase. Invest Ophthalmol Vis Sci 2001;42:1472-1478.

32   Kang SS, Li T, Xu D, Reinach PS, Lu L: Inhibitory effect of pge2 on EGF-induced map kinase activity and rabbit corneal epithelial proliferation. Invest Ophthalmol Vis Sci 2000;41:2164-2169.

33   Kang SS, Wang L, Kao WW, Reinach PS, Lu L: Control of sv-40 transformed rce cell proliferation by growth-factor-induced cell cycle progression. Curr Eye Res 2001;23:397-405.

34   Cai L, Du T, Song D, Li B, Hertz L, Peng L: Astrocyte erk phosphorylation precedes k^+-induced swelling but follows hypotonicity-induced swelling. Neuropathology;31:250-264.

35   Hannemann A, Flatman PW: Phosphorylation and transport in the Na-K-2Cl cotransporters, nkcc1 and NKCC2a, compared in HEK-293 cells. PLoS One 2011;6:e17992.

36   Hodges RR, Horikawa Y, Rios JD, Shatos MA, Dartt DA: Effect of protein kinase C and Ca^{2+} on p42/p44 MAPK, PYK2, and SRC activation in rat conjunctival goblet cells. Exp Eye Res 2007;85:836-844.

37   Nurmi A, Goldsteins G, Narvainen J, Pihlaja R, Ahtoniemi T, Grohn O, Koistinaho J: Antioxidant pyrrolidine dithiocarbamate activates AKT-GSK signaling and is neuroprotective in neonatal hypoxia-ischemia. Free Radic Biol Med 2006;40:1776-1784.

Appendix C

NF-κB feedback control of JNK1 activation modulates TRPV1-induced increases in IL-6 and IL-8 release by human corneal epithelial cells

Z. Wang[1], Y. Yang[1], H. Yang[1], J.E. Capó-Aponte[2], S.D. Tachado[4], J.M. Wolosin[3], P.S. Reinach[1].

[1] Department of Biological Sciences, State University of New York, State College of Optometry, New York, NY10036
[2] Visual Sciences Branch, U.S. Army Aeromedical Research Laboratory, Fort Rucker, AL 36362
[3] Department of Ophthalmology and the Black Family Stem Cell Institute, Mount Sinai School of Medicine, New York, NY 10029
[4] Department of Medicine, Beth Israel Deaconess Medical Center and Harvard Medical School, Boston, MA 02215

*Correspondence to: Dr. Peter S. Reinach, Department of Biological Sciences, State University of New York, State College of Optometry, New York, NY 10036, USA; Tel: 212-938-5785; Fax 212-938-5794; Email: preinach@sunyopt.edu

Abstract

Background: In mice, corneal wound healing in response to severe injury can lead to dysregulated inflammation and opacity due to transient receptor potential vanilloid type1 (TRPV1) ion channel activation [1]. Accordingly, we characterized in human corneal epithelial cells (HCEC) the signaling pathways mediating TRPV1-induced increases in inflammatory cytokine (IL-6) and chemoattractant (IL-8) release.

Methods: SV40 immmortalized HCEC were transduced with lentiviral vectors to establish stable JNK1, NF-κB1 and DUSP1 shRNAmir sublines. Immunoblotting evaluated the expression of NF-κB1, DUSP1, PKCδ and the phosphorylation status of cell signaling mediators. ELISA evaluated IL-6 and IL-8 release.

Results: Capsaicin (CAP), a selective TRPV1 agonist, induced time-dependent activation of transforming growth factor activated kinase 1 (TAK1) and mitogen activated protein kinase (MAPK) cascades followed by IκBα phosphorylation and rises in IL-6 and IL-8 release. All responses were blocked by the TAK1 inhibitor 5z-7-oxozeaenol (5z-OX). Ablation of either JNK1 or NF-κB1 expression abolished increased IL-6 and IL-8 release. However, JNK1 knockdown only partially suppressed CAP-induced NF-κB activation while 5z-OX eliminated it. On the other hand, loss of NF-κB1 expression diminished CAP-induced JNK1 activation as a result of increases in DUSP1 expression whereas PKCδ expression concomitantly declined. In contrast, in the DUSP1 knockdown subline, IL-6/8 release by CAP was augmented due to enhanced and prolonged JNK1 phosphorylation.

Conclusions: TRPV1 activation elicits increases in IL-6 and IL-8 release through two

TAK1-dependent signaling pathways leading to NF-κB activation. One of them depends on JNK1 activation while the other is JNK1 independent. Positive feedback control of JNK1 activation by NF-κB is required for CAP to elicit IL-6 and IL-8 rises. NF-κB mediates such regulation through changes in DUSP1 expression, which in turn modulate JNK1 phosphorylation. NF-κB may control DUSP1 expression by altering PKCδ expression.

Introduction

In mice, the corneal wound healing outcome to severe injuries is unfavorable due to dysregulated inflammation and scarring induced by transient receptor vanilloid type1 (TRPV1) channel activation [1]. This channel is the archetypal member of the vanilloid TRP family and was first identified as the receptor for capsaicin, the pungent ingredient of chili pepper. This receptor integrates noxious thermal and chemical stimuli to induce pain and inflammation in a host of different tissues [2, 3]. Different endogenous fatty acid amides lipid ligands released by injury can also activate TRPV1 [4]. Accordingly, extensive effort is being exerted to develop TRPV1-related therapeutic strategies to mitigate these stress-induced responses.

The signaling events mediating TRPV1-induced increases in interleukin (IL)-6 and IL-8 release include transient intracellular Ca^{2+} rises leading to p38, ERK1/2 and JNK1/2 mitogen activated protein kinase (MAPK) pathway phosphorylation as well as NF-κB activation in human corneal epithelial cells (HCEC) [5-7]. In addition, TRPV1 stimulation elicits increases in cell proliferation through stimulation of the ERK1/2 pathway whereas increases in IL-6 and IL-8 occur through stimulation of the global MAPK cascades. Their joint involvement in eliciting increases in IL-6 and IL-8 release was based on the finding that each of the described inhibitors of these pathways only partially suppressed these responses. As drugs can have limited selectivity, genetic approaches are required to validate which of these pathways elicit such control [8]. This concern coupled with recent reports that toll-like receptor (TLR) activation induces inflammation solely through JNK1 phosphorylation prompted us to reevaluate in

HCEC which MAPK pathways elicit TRPV1 control of IL-6 and IL-8 release [9].

The JNK-family consists of three isoforms, JNK1, JNK2 and JNK3. JNK1 is the major player mediating biological functions [10]. In some tissues, the JNK signaling pathway selectively mediates receptor control of inflammatory responses [11]. On the other hand, in the corneal epithelium, the JNK signaling pathway also contributes to growth factor-induced increases in cell migration, but suppresses mitogenic responses [12-14]. The functional importance of the JNK pathway in mediating epithelial renewal prompted us to determine in HCEC if selective suppression of JNK1 signaling could inhibit TRPV1-induced increases in IL-6 and IL-8 release.

Activation of NF-κB entails phosphorylation of its inhibitor IκBα by IκB kinase (IκK), which signals its degradation by ubiquitination [15]. Once NF-κB activation occurs, its individual subunits in unique dimeric configurations translocate into the nucleus to interact with gene promoters mediating transcription. TNFα, IL-1 and TLR activation as well as exposure to UV light are also known to induce in the cornea NF-κB activation [16-18]. Therefore, modulation of NF-κB activation plays an important role in controlling inflammatory responses to a number of different stresses.

Receptor-induced responses elicited through MAPK signaling are dependent on the magnitude and duration of terminal kinase (TK) phosphorylation. Such regulation is elicited by a family of TK-targeting dual specificity phosphatases (DUSPs) through negative feedback control of TK activation [19]. In HCEC, three out of ten active DUSP members are constitutively expressed at relatively high levels. They include DUSP1, DUSP5 and DUSP6 [14]. DUSP5 and DUSP6 are essentially ERK1/2

selective whereas DUSP1 is relatively nonselective since it inhibits ERK1/2, p38 and JNK1/2 MAPK activation, but its selectivity for p38 and JNK1/2 is greater than that for ERK1/2 [20]. There is evidence suggesting that NF-κB can elicit control of JNK1 phosphorylation status through modulation of DUSP1 expression [21]. However, the role of DUSP1 in mediating interactions between NF-κB and JNK1 has not been addressed in HCEC. Such insight could help better understand how to control increases in IL-6 and IL-8 release induced by TRPV1 activation during exposure to chemical or thermal stresses.

Transforming growth factor-β activated kinase-1 (TAK1) is a serine/threonine kinase in the MAPK kinase kinase (MAP3K) family. TAK1 bridges receptor activation to downstream signaling cascade events leading to cellular responses evoked by various pro-inflammatory cytokines that include IL-1, transforming growth factor-β (TGF-β), TNF-α as well as TLR, CD40 and B cell receptors [22-24]. TAK1 activation can lead to global MAPK and NF-κB activation. Even though it is apparent that receptors mediating inflammatory responses link their activation to downstream events through TAK1 activation, its role has not been determined in HCEC in mediating TRPV1 control of IL-6 and IL-8 release.

We show here that TRPV1 activation induces IL-6 and IL-8 release through TAK1 phosphorylation in HCEC, which leads to global MAPK and NF-κB activation. TAK1 elicits NF-κB activation through both JNK1-dependent and -independent pathways. JNK1 is the sole mediator of CAP-induced increases in IL-6 and IL-8 release. IL-6 and IL-8 release is modulated by changes in DUSP1 expression levels since they affect the

magnitude and duration of JNK1 activation. Declines in NF-κB activation are associated with declines in PKCδ expression, which are inversely related to increases in DUSP1 stabilization. Therefore, NF-κB activity modulates JNK1/2 phosphorylation through positive feedback control which determines the magnitude of CAP-induced increases in IL-6 and IL-8 release.

Materials and Methods

Reagents

Capsaicin (CAP), capsazepine (CPZ), TAK1 inhibitor 5z-7-oxozeaenol (5z-OX), and pyrrolidinedithiocarbamate (PDTC) were purchased from Sigma-Aldrich (St. Louis, MO). Antiphospho-ERK, total-ERK, total-p38, total-JNK, and β-actin antibodies were from Santa Cruz Biotechnology (Santa Cruz, CA). Anti-phospho-TAK1, phospho-p38, phospho-JNK/SAPK, phospho-IκBα, total TAK1, total-NF-κB1 and PKC-δ antibodies were purchased from Cell Signaling Technology (Danvers, MA). The anti-DUSP1 antibody was obtained from ABNOVA (Walnut Creek, CA). IL-6 and IL-8 ELISA kits were from R&D Systems (Minneapolis, MN).

Cell Culture

SV40 adenovirus-immortalized HCEC, a generous gift from Araki-Sasaki (Kagoshima Miyata Eye Clinic, Kagoshima, Japan), were cultured in supplemented Dulbecco's modified Eagle's medium (DMEM/F12). After reaching 80% to 90% confluence, cells were detached with 0.05% trypsin-EDTA and were subcultured in DMEM/F12 medium supplemented with 10% fetal bovine serum (FBS), 5 ng/mL EGF, 5 μg/mL insulin, and

40 µg/mL gentamicin in a humidified incubator with 5% CO_2, 95% atmosphere air at 37°C.

Lentiviral vectors

Lentiviral vectors for stable expression of shRNAmir sequences against DUSP1, JNK1, and NF-κB1 were generated using pGIPz plasmids clones V3LHS_352110, V2LHS_61931, and V3LHS_170502, respectively (Open Biosystems, Hunstville, AL). Blast analysis of the 20-mer antisense sequences expressed by these clones demonstrated that in each case only the intended target RNA was a full sequence match. The expression cassette incorporated into the host cell DNA by these lentiviral vectors drives the expression of a turbo-GFP protein, the shRNAmir sequence and a puro gene from a single CMV promoter. Viral particles were generated by transducing HEK293T cells cultured in 100 mm dishes with 2 µg active plasmid, 8 µg of packing plasmid mix (UMIX™, Rockville, MD) in 10 ml medium (DMEM with 10% FBS) containing 20 µl HEKFectin (BioRad, Richmond, CA). The culture medium was refreshed after overnight incubation and virus-rich supernatant was collected 48 h later after confirming that most HEK293 cells developed strong GFP fluorescence. Transduced cells were selected with puromycin (5 µg/ml) using the disappearance of all GFP negative cells and elimination of all cells from an untransduced control culture as selection end points. To generate a control subline for evaluating any non-specific effects of shRNAmirs, viral particles incorporated a cassette for the simultaneous expression of a non-coding shRNAmir and puromycin resistance. After puromycin selection, these cells were used to determine if transfection had non-specific effects on

cell-line functional properties.

Western Blot Analysis

After HCEC reached about 80% confluence, they were gently washed twice in cold
phosphate-buffered saline (PBS) and harvested in 0.5 ml cell lysis buffer containing 20
mM Tris, 150 mM NaCl, 1 mM EDTA, 1 mM EGTA, 1% Triton X-100, 2.5 mM
sodium pyrophosphate, 1 mM ß-glycerol phosphate, and 1 mM Na_3VO_4, pH 7.5, with a
protease inhibitor mixture (1 mM PMSF, 1 mM benzamidine, 10 µg/mL leupeptin, and
10 µg/mL aprotinin). Cells were scraped with a rubber policeman, followed by
sonication and centrifugation (13,000 rpm for 15 min at 4°C). The protein
concentration of each lysate was determined by bicinchoninic acid assay (micro BCA
protein assay kit; Pierce Biotechnology, Rockford, IL). After boiling samples for 5 min,
20-50 µg denatured protein was electrophoresed onto 10% polyacrylamide sodium
dodecylsulphate (SDS) minigels, followed by electrophoresis and blotting onto
Immun-Blot PVDF membrane (Bio-Rad, Hercules, CA). Membranes were blocked
with blocking buffer, 5% fat-free milk in 1x PBS buffer with 0.1% Tween-20 for 1 h at
room temperature and then probed overnight at 4°C with primary antibodies of interest.
Membranes were incubated with 1:2000 dilution of a secondary antibody with goat
anti-rabbit or mouse IgG for 1 h at room temperature. Immunobound antibody was
visualized using an enhanced chemiluminescence detection system (ECL Plus; GE
Healthcare, Piscataway, NJ). Images were analyzed by densitometry (SigmaScan Pro;
Sigma). All experiments were repeated at least three times in triplicate (n = 3) unless
otherwise indicated.

ELISA

ELISA for IL-6 and IL-8 was performed according to the manufacturer's instructions.

The amount of IL-6 or IL-8 in the culture medium was normalized according to the total

amount of cellular protein lysed with 2% SDS and 0.5 N NaOH. Results are expressed

as mean ± SEM of picograms of IL-6 or IL-8 per milligram protein of cell lysate. Each

experiment was performed in triplicate with three replicates (n = 3).

Data analysis: All results are reported as means ± SEM. Results were analyzed using

non-paired Students t-test. They were considered significant if $p < 0.05$.

Results

TRPV1-induces phosphorylation of TAK1

TAK1 activation plays a major role in mediating responses to a host of different

cytokines. Figure 1A shows the time-dependent effects of CAP on TAK1

phosphorylation status. Phosphorylated-TAK1 (p-TAK1) increased by 130% after 2.5

min and progressively declined to the baseline after 30 min. Figure 1B shows that either

capsazepine (CPZ), a TRPV1 antagonist, or 5z-7-oxozeaenol (5z-OX), a TAK1

inhibitor, suppressed the rise by 90% and 100% respectively ($p < 0.001$). Therefore,

CAP induces TAK1 phosphorylation.

**TRPV1-induced TK phosphorylation and IL-6/8 release depend on TAK1
activation**

Figure 1C provides the dose-dependent inhibitory effects of 5z-OX on TAK1 activation after exposure to CAP. Simultaneously, phosphorylation levels of all TKs were completely inhibited by 1 μM 5z-OX (p<0.001). Figure 1D indicates that either 5z-OX or CPZ completely blocked CAP-induced rises in IL-6 and IL-8 release (p<0.001). Taken together, TRPV1-induced increases in IL-6 and IL-8 release are elicited through TAK1-mediated stimulation of MAPK signaling.

TRPV1-induced IL-6 and IL-8 release requires JNK1 activation

The role of JNK1 activation in mediating CAP-induced increases in IL-6 and IL-8 was determined in the JNK1 subline whose JNK1 protein levels were reduced by more than 90% in comparison to a scrambled shRNA (Figure 2A). The latter expression level was identical to that in the wildtype (WT) cells (data not shown). JNK1 phosphorylation in the WT cells increased by 270% after 15 min exposure to CAP (Figure 2B, p<0.001). This rise was suppressed by 82% in the JNK1 subline. Such a decline in JNK1 activation obviated CAP-induced increases in IL-6 and IL-8 release relative to those in the WT cells (Figure 2C, p<0.001), demonstrating the central role of JNK1 activity in these responses. In contrast, CAP-induced increases in cell proliferation were unaffected in the JNK1 subline (data not shown).

TRPV1-induced IL-6 and IL-8 release requires NF-κB activation

To determine the involvement of NF-κB in CAP-induced IL releases, we developed a NF-κB1 subline. Figure 3A shows that the knockdown was nearly complete (p<0.001 versus scrambled) and Figure 3B (left and right) shows that in this subline, CAP failed to cause any increases in IL-6 and IL-8 release.

TAK1 and JNK1 activities are essential for NF-κB activation

In some tissues NF-κB activity has been shown to be dependent on TAK1 and JNK1 activity [25, 26]. To establish the validity of these dependences in the HCECs, we measured the phosphorylation status of IκBα, the stoichiometric inhibitor of NF-κB. Each unit of IkBa phosphorylation is expected to equal one unit of released active NF-κB. In the JNK1 subline, CAP-induced IκBα phosphorylation was reduced only by 50% from that in the WT cells whereas 5z-OX further eliminated the remaining 50% of this response (Figure 4A). The partial suppression of IκBα phosphorylation in the JNK1 subline suggests that TAK1 can activate NF-κB through another pathway not involving JNK1.

NF-κB activity modulates JNK1 phosphorylation status via a positive feedback loop involving DUSP1 and PKCδ

In addition to the effect of JNK1 activity on NF-κB, other robust evidence shows that in several cell systems NF-κB modulates the duration and magnitude of JNK1 phosphorylation [21]. To determine if this occurs in HCEC, we compared the effects of CAP on TK phosphorylation in WT cells with that in the NF-κB1 subline. Figure 4B shows the time-dependent effects of CAP on JNK1/2 phosphorylation in the NF-κB1 subline and those in the WT cells. In these cells, p-JNK1 formation initially increased 2.7-fold at 15 min followed by waning towards control levels after 90 min whereas in the NF-κB1 subline CAP could no longer induce evident changes in p-JNK1 throughout the observation period. This indicates NF-κB activity can regulate JNK1 phosphorylation status. Interestingly, similar suppression patterns were also observed

in p-ERK1/2 and p-p38 formation.

The inability of CAP to induce global MAPK phosphorylation in the absence of NF-κB1 expression prompted us to investigate if DUSP1 is mediating the feedback control, since it is a pan MAPK inhibitor. Figure 4C shows that DUSP1 expression in the NF-κB1 subline was around 300% of the level in the WT cells during 90 min. Furthermore, we determined if rises in DUSP1 expression are associated with changes in PKCδ expression since in murine embryonic fibroblasts loss of NF-κB activity by knocking down RelA resulted in declines in PKCδ expression [27]. In another study, this loss was associated with increases in DUSP1 phosphorylation (i.e., stabilization) [28]. The corresponding changes in PKCδ expression (Figure 4C) show that during this period the changes in its expression in the WT cells and NF-κB1 subline were the reciprocal of those occurring in the WT cells (p<0.001). Therefore, the apparent inverse relationship between increases in DUSP1 and declines in PKCδ expression suggests NF-κB-dependent increases in PKCδ expression contributes to DUSP1 degradation.

DUSP1 modulates TRPV1-induced IL-6/8 release through control of JNK phosphorylation

To determine the significance of DUSP1 expression in the control of IL release induced by CAP, we used a DUSP1 subline. In this subline, DUSP1 protein expression was reduced by 85% (Figure 5A, p<0.001). Figure 5B compares, the time-dependent changes in TK phosphorylation in the WT cells and the DUSP1 subline. In the WT cells, the TKs underwent rapid phosphorylation and reached a peak within 15 min, which gradually waned down during the next 60 min. On the other hand, in the DUSP1

subline all TKs underwent larger increases at the beginning and remained invariant for a longer period, particualarly in the case of JNK1/2. Figure 5C shows the impact of enhanced JNK1 phosphorylation on IL-6 and IL-8 release. After 24 h exposure to CAP, IL-6 and IL-8 release was 140% and 255% more, respectively, in the DUSP1 subline than in the WT cells ($p<0.001$).

Discussion

Figure 6 provides a working model describing TRPV1-mediated signaling control of IL-6 and IL-8 release. TRPV1-induced Ca^{2+} influx results in TAK1 phosphorylation followed by transient pan MAPK and NF-κB activation. NF-κB activation occurs through both JNK1-dependent and JNK1-independent pathways. The IL-6 and IL-8 responses to CAP are dependent on the magnitude and duration of both TAK1 and JNK1 activation as well as positive feedback control of JNK1 phosphorylation by NF-κB. Such regulation by NF-κB is elicited through an inverse relationship between increases in NF-κB activation and declines in DUSP1 expression levels. Increases in NF-κB and PKCδ expression occur in parallel with one another. Taken together, CAP-induced increases in IL-6 and IL-8 release can occur provided NF-κB is fully activated by TAK1, so as to keep DUSP1 expression levels low enough to allow p-JNK1 to sufficiently accumulate for a long enough time.

TAK1 was originally described as a key MAPK activation mediator in response to TGF-β [29]. Recently, TAK1 has also been linked to IL-1 receptor, TLR, TNF-a receptor, T-cell receptor and B-cell receptor stimulation mediating inflammatory

responses to extracellular stresses through activating p38, JNK and NF-κB [22]. Our results indicate that TAK1 phosphorylation by TRPV1 induced global MAPK and NF-κB activation since: 1) transient activation of TAK1 (Figure 1A) preceded MAPK phosphorylation (Figure 4B and 5B); 2) TAK1 inhibition completely abolished CAP-induced global MAPK and NF-κB activation (Figures 1C and 4A) as well as increases in IL-6 and IL-8 release (Figure 1D). Recently, we found that TRPV1 elicits TAK1 phosphorylation through an interaction with an adaptor protein, myeloid differentiation primary response gene 88 (MyD88). This TRPV1-linked signaling pathway bears close resemblance to the described MyD88-dependent pathways linked to all TLRs described in the cornea except TLR3 [30,31].

Unlike our previous report that all TKs are contributing to TRPV1-induced increases in IL-6 and IL-8 release [5], we showed here that JNK1 knockdown alone was sufficient to eliminate this response (Figure 2C). This difference is attributable to our earlier use of inhibitors to resolve how this response is mediated. More recently other studies employed knockdown strategies to show that JNK1 plays a central role in mediating corneal inflammatory responses to TLR activation both in vitro and vivo [9]. In HCEC, TLR2-induced NF-κB activation and CXC (C-X-C motif) chemokine production were only dependent on JNK1 activation. Furthermore, JNK1$^{-/-}$ (knockout) mice showed impairment of TLR2-induced neutrophil recruitment and corneal stroma haze development.

NF-κB mediates transcription of pro-inflammatory cytokine and chemokine release in HCEC in response to various pathological conditions such as infections

[32-35] and hyperosmolar challenges [7, 36, 37]. Its involvement in mediating IL-6 and IL-8 release is evident since: 1) IκBα phosphorylation preceded this response (Figure 4A); 2) NF-κB1 knockdown eliminated CAP-induced increases in IL-6 and IL-8 release (Figure 3B). CAP-induced NF-κB activation is under dual control by both TAK1 and JNK1, since IκBα phosphorylation was only reduced by 50% in the JNK1 knockdown subline whereas complete suppression required TAK1 inhibition in this subline (Figure 4A). Dual pathway activation of NF-κB through both MAPK-dependent and -independent pathways has been described in some other tissues [25, 26, 38]. Interestingly, although NF-κB was 50% activated in the JNK1 subline, CAP failed to elicit any increases in IL-6 and IL-8 release, indicating other transcription factors directly activated by JNK1, such as AP-1, may also play a role.

It is possible that the correspondence between increases in NF-κB and JNK1 activation is due to positive feedback control of JNK1 phosphorylation by NF-κB [21], which in turn modulates the level of IL-6 and IL-8 release. Such control is provided through an inverse relationship between increases in NF-κB activation and declines in DUSP1 expression through increases in PKCδ expression. DUSP1 expression only rose in the NF-κB subline whereas in the WT cells it remained essentially invariant (Figure 4C). In the NF-κB1 subline, large increases in DUSP1 expression obviated JNK1 phosphorylation (Figure 4B). These results have clinical relevance since it is known that the anti-inflammatory effects of glucocorticoids are attributable to their upregulation of DUSP1 expression [39]. Direct targeting DUSP1 may provide a more selective anti-inflammation strategy and remove concerns about described side effects

arising from prolonged glucocorticoids usage.

In HCEC, TRPV1 transactivation by epidermal growth factor receptors (EGFR) induces increases in cell proliferation and migration through the same signaling pathways linked to EGFR [6]. The current study provides an explanation for why activation of TRPV1 by CAP induces also increases in IL-6/8 whereas EGF does not induce this response even though both agonists activate TAK1. A reason for this difference may be that TAK1 activation by CAP was 2.3-fold larger and more prolonged than that induced by EGF (data not shown). This effect by CAP is consistent with the larger increase in NF-κB activation resulting in stronger positive feedback control by NF-κB of JNK1 phosphorylation, compared to that by EGF. This difference may account for the increases in IL-6 and IL-8 release induced by CAP.

Our finding that loss of NF-κB1 expression has an opposite effect on DUSP1 expression disagrees with a study using enterocytes in which increases in NF-κB activation had a corresponding rather than an opposite effect on LPS-induced DUSP1 expression [40]. This disagreement may be accounted for by differences in the cell type, stimuli and/or experimental approaches. We silenced NF-κB1 whereas the other study deleted IκBα. Nevertheless, our results are consistent with another study in which loss of RelA expression caused PKCδ levels to decline along with phosphorylated JNK1 [27]. In addition, it has been shown knocking down PKCδ expression in neurons caused DUSP1 levels to rise [28].

In conclusion, CAP-induced increases in IL-6 and IL-8 release are dependent on TAK1 activation. Consequently, TAK1 activates NF-κB through both

JNK1-dependent and JNK1-independent pathways. CAP-induced NF-κB activation

provides a positive feedback control of JNK1 phosphorylation to maintain its activation

level. Such interactions are mediated through reciprocal modulation of PKCδ and

DUSP1 expression levels.

Disclaimer

The views, opinions and/or findings contained in this report are those of the author(s)

and should not be construed as an official Department of the Army position, policy or

decision, unless so designated by other official documentation. Citation of trade names

in this report does not constitute an official Department of the Army endorsement or

approval of the use of such commercial items.

References

1. Okada Y, Reinach PS, Shirai K, Kitano A, Kao WW, Flanders KC, Miyajima M, Liu H, Zhang J, Saika S. TRPV1 Involvement in Inflammatory Tissue Fibrosis in Mice. Am J Pathol. 2011 ;178:2654-64.

2. Caterina MJ, Leffler A, Malmberg AB, Martin WJ, Trafton J, Petersen-Zeitz KR, et al. Impaired nociception and pain sensation in mice lacking the capsaicin receptor. *Science*. 2000;288:306-13.

3. Davis JB, Gray J, Gunthorpe MJ, Hatcher JP, Davey PT, Overend P, et al. Vanilloid receptor-1 is essential for inflammatory thermal hyperalgesia. *Nature*.

2000;405:183-7.

4. Ross RA. Anandamide and vanilloid TRPV1 receptors. *Br J Pharmacol*. 2003;140:790-801.

5. Zhang F, Yang H, Wang Z, Mergler S, Liu H, Kawakita T, Tachado SD, Pan Z, Capó-Aponte JE, Pleyer U, Koziel H, Kao WW, Reinach PS. Transient receptor potential vanilloid 1 activation induces inflammatory cytokine release in corneal epithelium through MAPK signaling. J Cell Physiol. 2007; 213:730-9.

6. Yang H, Wang Z, Capó-Aponte JE, Zhang F, Pan Z, Reinach PS. Epidermal growth factor receptor transactivation by the cannabinoid receptor (CB1) and transient receptor potential vanilloid 1 (TRPV1) induces differential responses in corneal epithelial cells. Exp Eye Res. 2010; 91:462-71.

7. Pan Z, Wang Z, Yang H, Zhang F, Reinach PS. TRPV1 activation is required for hypertonicity-stimulated inflammatory cytokine release in human corneal epithelial cells. Invest Ophthalmol Vis Sci. 2011;52:485-93.

8. Bain J, Plater L, Elliott M, Shpiro N, Hastie CJ, McLauchlan H, Klevernic I, Arthur JS, Alessi DR, Cohen P. The selectivity of protein kinase inhibitors: a further update. Biochem J. 2007; 408:297-315.

9. Adhikary G, Sun Y, Pearlman E. C-Jun NH2 terminal kinase (JNK) is an essential mediator of Toll-like receptor 2-induced corneal inflammation. J Leukoc Biol. 2008;83:991-7.

10. Liu J, Minemoto Y, Lin A. c-Jun N-terminal protein kinase 1 (JNK1), but not JNK2, is essential for tumor necrosis factor alpha-induced c-Jun kinase activation and

apoptosis. Mol Cell Biol. 2004; 24:10844-56.

11. Salh B. c-Jun N-terminal kinases as potential therapeutic targets. Expert Opin Ther Targets. 2007; 11:1339-53.

12. Kimura K, Teranishi S, Yamauchi J, Nishida T. Role of JNK-dependent serine phosphorylation of paxillin in migration of corneal epithelial cells during wound closure. Invest Ophthalmol Vis Sci. 2008; 49:125-32.

13. Okada Y, Saika S, Shirai K, Yamanaka O, Kitano A, Wang Z, Yang H, Reinach P. JNK MAPK signaling contributes in vivo to injury-induced corneal epithelial migration. Ophthalmic Res. 2009; 42:185-92.

14. Wang Z, Reinach PS, Zhang F, Vellonen KS, Urtti A, Turner H, Wolosin JM. DUSP5 and DUSP6 modulate corneal epithelial cell proliferation. Mol Vis. 2010; 16:1696-704.

15. Wullaert A, Bonnet MC, Pasparakis M. NF-κB in the regulation of epithelial homeostasis and inflammation. Cell Res. 2011; 21:146-58.

16. Sun Y, Karmakar M, Roy S, Ramadan RT, Williams SR, Howell S, Shive CL, Han Y, Stopford CM, Rietsch A, Pearlman E. TLR4 and TLR5 on corneal macrophages regulate Pseudomonas aeruginosa keratitis by signaling through MyD88-dependent and -independent pathways. J Immunol. 2010; 185:4272-83.

17. Ritchie MH, Fillmore RA, Lausch RN, Oakes JE. A role for NF-kappa B binding motifs in the differential induction of chemokine gene expression in human corneal epithelial cells. Invest Ophthalmol Vis Sci. 2004; 45:2299-305.

18. Wang L, Reinach P, Lu L. TNF-alpha promotes cell survival through stimulation of

K$^+$ channel and NFkappaB activity in corneal epithelial cells. Exp Cell Res. 2005; 311:39-48.

19. Slack DN, Seternes OM, Gabrielsen M, Keyse SM. Distinct binding determinants for ERK2/p38alpha and JNK map kinases mediate catalytic activation and substrate selectivity of map kinase phosphatase-1. J Biol Chem. 2001; 276:16491-500.

20. Dickinson RJ, Keyse SM. Diverse physiological functions for dual-specificity MAP kinase phosphatases. J Cell Sci. 2006; 119:4607-15.

21. Liu J, Lin A. Wiring the cell signaling circuitry by the NF-kappa B and JNK1 crosstalk and its applications in human diseases.Oncogene. 2007;26:3267-78.

22. Landström M. The TAK1-TRAF6 signalling pathway. Int J Biochem Cell Biol. 2010;42:585-9.

23. Pearlman E, Johnson A, Adhikary G, Sun Y, Chinnery HR, Fox T, Kester M, McMenamin PG. Toll-like receptors at the ocular surface. Ocul Surf. 2008; 6:108-16.

24. Skaug B, Jiang X, Chen ZJ. The role of ubiquitin in NF-κB regulatory pathways. Annu Rev Biochem. 2009;78:769-96.

25. Chen ZJ, Bhoj V, Seth RB. Ubiquitin, TAK1 and IKK: is there a connection? Cell Death Differ. 2006; 13:687-92.

26. Ear T, Fortin CF, Simard FA, McDonald PP. Constitutive association of TGF-beta-activated kinase 1 with the IkappaB kinase complex in the nucleus and cytoplasm of human neutrophils and its impact on downstream processes. J Immunol. 2010; 184:3897-906.

27. Liu J, Yang D, Minemoto Y, Leitges M, Rosner MR, Lin A. NF-kappaB is required for UV-induced JNK activation via induction of PKCdelta. Mol Cell. 2006;21:467-80.

28. Choi BH, Hur EM, Lee JH, Jun DJ, Kim KT. Protein kinase C delta-mediated proteasomal degradation of MAP kinase phosphatase-1 contributes to glutamate-induced neuronal cell death. J Cell Sci. 2006;119:1329-40.

29. Yamaguchi K, Shirakabe K, Shibuya H, Irie K, Oishi I, Ueno N, Taniguchi T, Nishida E, Matsumoto K. Identification of a member of the MAPKKK family as a potential mediator of TGF-beta signal transduction. Science. 1995;270:2008-11.

30. Redfern RL, McDermott AM. Toll-like receptors in ocular surface disease. Exp Eye Res.90:679-87.

31. Ren MY, Wu XY. Toll-like receptor 4 signalling pathway activation in a rat model of Acanthamoeba Keratitis. Parasite Immunol. 2011; 33:25-33.

32. Ren M, Gao L, Wu X. TLR4: the receptor bridging Acanthamoeba challenge and intracellular inflammatory responses in human corneal cell lines. Immunol Cell Biol. 2010; 88:529-536.

33. Kumar A, Yin J, Zhang J, Yu FS. Modulation of corneal epithelial innate immune response to pseudomonas infection by flagellin pretreatment. Invest Ophthalmol Vis Sci. 2007;48:4664-70.

34. Kumar A, Zhang J, Yu FS. Toll-like receptor 2-mediated expression of beta-defensin-2 in human corneal epithelial cells. Microbes Infect. 2006;8:380-9.

35. Zhang J, Wu XY, Yu FS. Inflammatory responses of corneal epithelial cells to

Pseudomonas aeruginosa infection. Curr Eye Res. 2005;30:527-34.

36. Lee JH, Kim M, Im YS, Choi W, Byeon SH, Lee HK. NFAT5 induction and its role in hyperosmolar stressed human limbal epithelial cells. Invest Ophthalmol Vis Sci. 2008;49:1827-35.

37. Chen M, Hu DN, Pan Z, Lu CW, Xue CY, Aass I. Curcumin protects against hyperosmoticity-induced IL-1beta elevation in human corneal epithelial cell via MAPK pathways. Exp Eye Res. 2010; 90:437-43.

38. Fortin CF, Cloutier A, Ear T, Sylvain-Prévost S, Mayer TZ, Bouchelaghem R, McDonald PP. A class IA PI3K controls inflammatory cytokine production in human neutrophils. Eur J Immunol. 2011;41:1709-19.

39. Shipp LE, Lee JV, Yu CY, Pufall M, Zhang P, Scott DK, Wang JC. Transcriptional regulation of human dual specificity protein phosphatase 1 (DUSP1) gene by glucocorticoids. PLoS One. 2010; 5:e13754.

40. Wang J, Ford HR, Grishin AV. NF-kappaB-mediated expression of MAPK phosphatase-1 is an early step in desensitization to TLR ligands in enterocytes. Mucosal Immunol. 2010;3:523-34.

Legends

Figure 1. CAP induces TAK1 activation

    (A) TRPV1-induced TAK1 phosphorylation: CAP (20µM) in HCECs caused time

dependent changes in TAK1 phosphorylation as revealed by Western blot analysis. TAK1 levels validate protein loading equivalence. Results shown are representative of three independent experiments.

(B) Inhibition of TAK1 phosphorylation: Preincubation for 60 min with either CPZ (10μM) or 5z-OX (0.1μM) suppressed CAP (20μM)-induced TAK1 activation. TAK1 levels validate protein loading equivalence.

(C) Dose dependent inhibitory effects of 5z-OX on TAK1 and MAPK phosphorylation. HCECs were preincubated with 5z-OX (0.01-1μM) for 1 h before exposure to CAP (20μM) for 5 min. JNK1/2 levels validate protein loading equivalence.

(D) Dependence of IL-6 and IL-8 increases on TRPV1 and TAK1 activation. ELISA was performed after 24 h in presence or absence of CAP (20μM). Following 60 min exposure to CPZ (10 μM) or 5z-OX (0.1μM), the effects of CAP (20μM) were determined on the release of IL-6 and IL-8. Results are from three independent experiments each performed in triplicate. Significant relative to the control (**)

Figure 2. Dependence of CAP-induced increases in IL-6 and IL-8 release on JNK1 activation

(A) Validation of JNK1 knockdown: Western blot analysis compares total JNK1 protein expression in resting scrambled HCEC and JNK1 subline. The expression level of scrambled and WT HCEC were the same. (Data not shown)β-actin levels validate protein loading equivalence.

(B) Time dependence of CAP-induced changes in p-JNK1/2 formation: WT HCEC and JNK1 subline were exposed to CAP (20μM) for the indicated periods. β-actin levels validate protein loading equivalence.

(C) Loss of JNK1 expression obviates IL-6/8 responses to TRPV1 activation: ELISA was performed on WT and JNK1 subline after 24 h in presence or absence of CAP (20μM) for both WT HCEC and JNK1 subline. Results are from three independent experiments each performed in triplicate. Significant relative to the control (**)

Figure 3.Dependence of TRPV1-induced increases in IL-6/8 release on NF-κB activation

(A) NF-κB1/p50 protein expression levels in scrambled HCEC and NF-κB1 subline were compared by Western blot analysis.Protein loading equivalence validated based on GAPDH expression.

(B) CAP fails to induce IL-6 and IL-8 rises after gene knockdown. ELISA was performed after 24 h in the presence or absence of CAP (20μM) for both WT cells and JNK1 subline. (Results are from three independent experiments each performed in triplicate. Significant relative to the control (**)

Figure 4. Positive feedback control of JNK1 phosphorylation by NF-κB through DUSP1

(A) Contribution by JNK1 to IκBα phosphorylation: Western blots compare CAP (20μM) induced IκBα phosphorylation in WT HCECs and JNK1 subline at 60 min. Preincubation with either 5z-OX (0.1μM), CPZ (10μM) or PDTC

(50μM) for 60 min suppressed CAP-induced IκBα phosphorylation.

(B) Positive feedback control by NF-κB of JNK1/2 activation: Loss of NF-κB activation reduces transient JNK1/2 , p38 and ERK1/2 MAPK activation induced by CAP (20μM) for up to 90 min. Summary plots contrast time dependent patterns of MAPK activation in WT (left) cells with those in NF-κB1 subline (right).

(C) Inverse relationship between changes in PKCδ and DUSP1 expression. WT cells and NF-κB1 subline were exposed to CAP (20μM) as described in B. Summary plot (left) indicate that in WT cells CAP-induced increases in PKCδ expression whereas DUSP1 remained invariant (left). Summary plot (right) reveals converse responses by PKCδ and DUSP1 to CAP in NF-κB1 subline.

Figure 5. Changes in MAPK activation patterns and IL-6/8 release in DUSP1 gene knockdown cells

(A) Western blot analysis of total DUSP1 protein expression in resting scrambled HCEC and DUSP1 subline.

(B) Comparison of time dependent changes in MAPK phosphorylation in WT cells and DUSP1subline. Cells were exposed to CAP (20μM) for indicated times. Changes are compared in p-ERK1/2, p-JNK1/2 and p38 MAPK in WT HCEC and DUSP1 subline. Protein loading equivalence validated based on invariant ERK1/2 expression levels.

(C) DUSP1 gene knockdown enhances CAP-induced IL-6 and IL-8 release.

ELISA was performed on WT HCECs and DUSP1subline after 24 h exposure to CAP (20 μM). Three independent experiments each performed in triplicate. Significant relative to the control (**)

Figure 6. TRPV1-linked signaling pathways mediating IL-6 and IL-8 release

TRPV1 stimulation leads to TAK1 dependent JNK1 and NF-κB activation. Activated JNK1 potentiates NF-κB activation by TAK1. NF-κB provides a positive feedback control of JNK1 phosphorylation through inhibition of DUSP1 expression, which is possibly controlled by PKCδ. Activated NF-κB translocates to nucleus, along with other transcription factors activated by p-JNK1 (e.g. AP-1), promote IL-6 and IL-8 mRNA expression. Solid line indicates established interaction. Broken line represents unproven interaction. Arrowhead means stimulation whereas hammerhead represents inhibition. For example, arrow pointing from TAK1 to NF-κB is broken since it is not yet known if interaction is direct or there are signaling intermediates mediating NF-κB activation by TAK1.
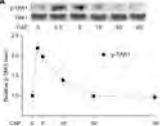
A

B

p-TAK1
TAK1

Relative p-TAK1 level

OxLP	−	+	−	+
GRE	−	−	+	+
siSIRT	−	−	−	−

C

CAP	-	+	+	+	+	+	+
5z-OX	-	-	0.01	0.05	0.1	0.5	1μM

D

IL-6, IL-8 (pg/mg of protein)

Legend: ☐ IL-6 ☐ IL-8

A JNK1 / β-actin — scrambled, JNK1 subline

B p-JNK1/2 — Wildtype, JNK1 subline, β-actin

Relative p-JNK1/2 level vs CAP (0', 6', 15', 30', 60', 90')
— WT, JNK1 subline

C IL-6 (pg/mg protein) — Con, CAP, CAP + CPZ; Wildtype, JNK1 subline
IL-8 (pg/mg protein) — Con, CAP, CAP + CPZ; Wildtype, JNK1 subline

A

B

A

p-IκBα   WT
α-IκBα   JNK1 subline
β-actin

Relative p-IκBα level

**

Groups: CON, CAP, Sc-OX + CAP, CPZ + CAP, PDTC + CAP

Legend: WT, JNK1 subline

A

DUSP1

β-actin

scrambled   DUSP1 subline

B

p-p38

p38

p-JNK1/2

p-ERK1/2

ERK1/2

CAP   0   5'   15' 30' 60'   0   5'   15' 30' 60'

WT   DUSP1 subline

Relative phosphorylation level

WT   DUSP1 subline

0 5' 15' 30' 60'   0 5' 15' 30' 60'

- p-JNK1/2
- p-ERK1/2
- p-p38

C

IL-6 (pg/mg protein)

CON   CAP   CAP + CPZ

WT   DUSP1 subline

**   **

IL-8 (pg/mg protein)

CON   CAP   CAP + CPZ

WT   DUSP1 subline

**   **
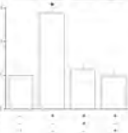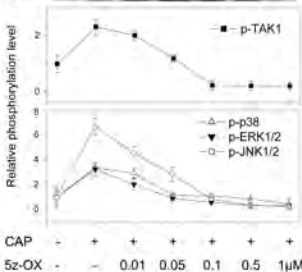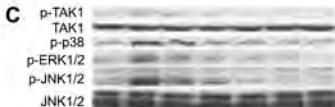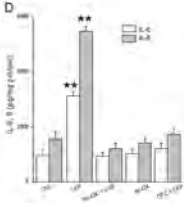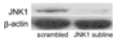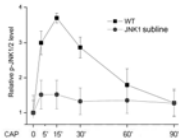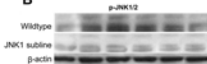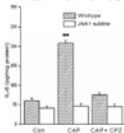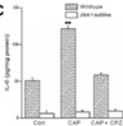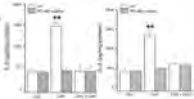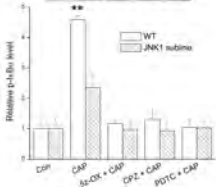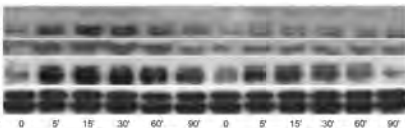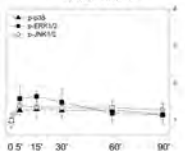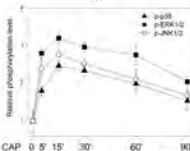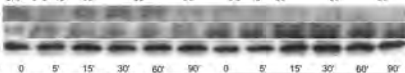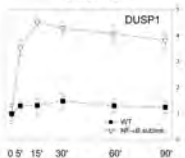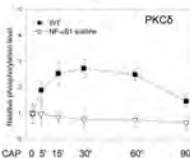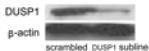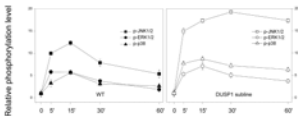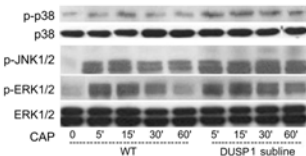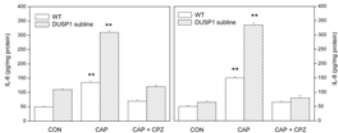
Figure 6
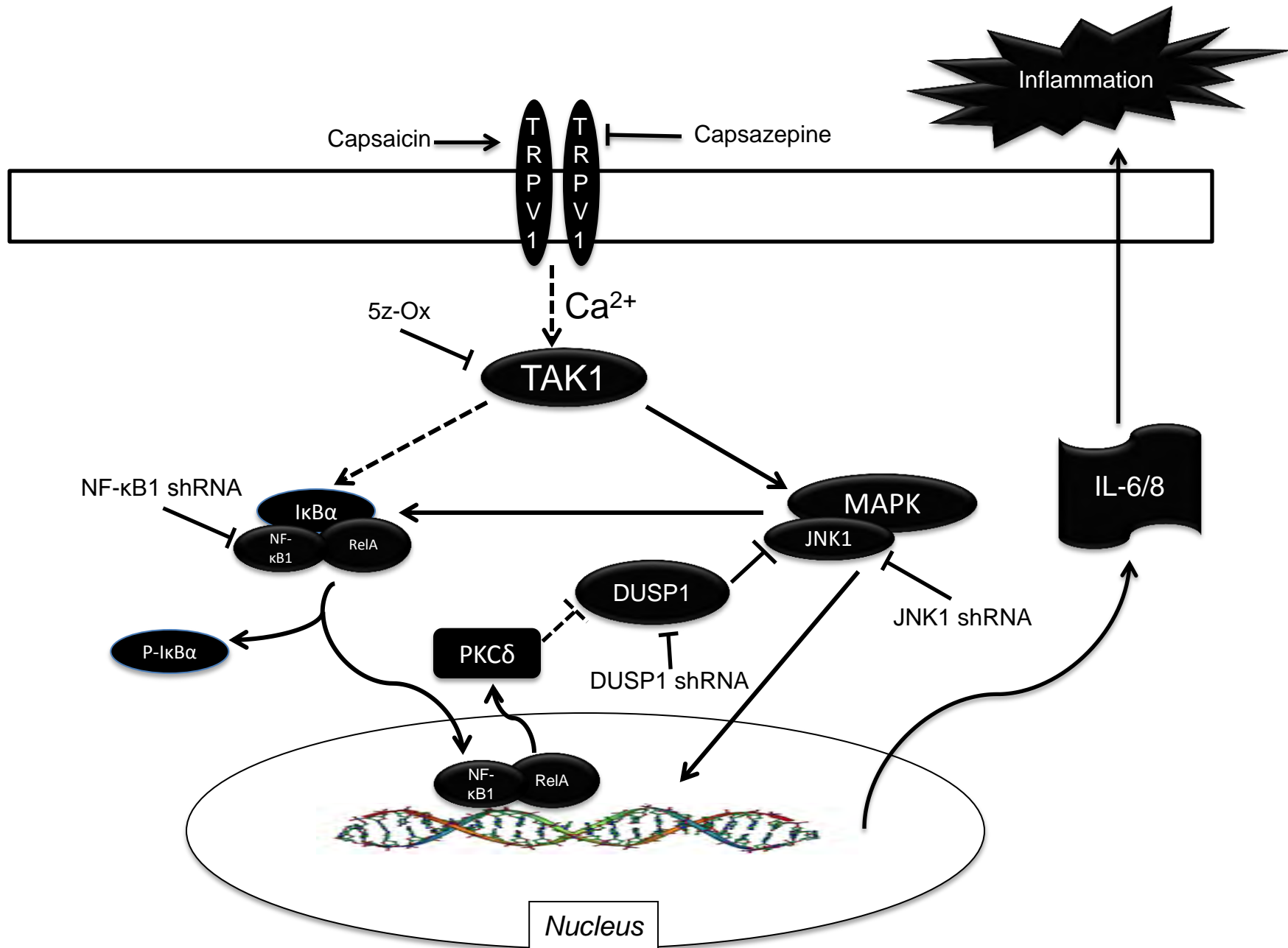
Appendix D

Print this Page

1. Genetics and Gene Expression	4. Processing and Perception	7. Repair, Regeneration and Restoration
2. Development	5. Inflammation, Infection and Ischemia	8. Imaging and Other Methods
3. Physiology and Pathology	6. Degenerations, Dystrophies and Death	9. Diagnosis and Treatment

CME Session

Presentation Abstract

Abstract Title: **Tak1 Interactions With TRPV1 and CB1 Control IL-6 and IL-8 Release in Human Corneal Epithelial Cells**

Presentation Start/End Time: Sunday, May 01, 2011, 8:30 AM -10:15 AM

Session Number: 115

Session Title: Cytokines/Growth Factors

Location: Hall B/C

Reviewing Code: 389 signal transduction: receptors - PH

Author Block: Zheng Wang[1], Hua Yang[1], Jose E. Capo-Aponte[2], Nili Parekh[1], Peter S. Reinach[1]. [1]Biological Sciences, SUNY College of Optometry, New York, NY; [2]Visual Sciences Branch, US Army Aeromedical Rsrch Lab, Fort Rucker, AL.

Keywords: 482 cornea: epithelium; 556 inflammation; 712 signal transduction: pharmacology/physiology

Abstract Body: **Purpose:** Corneal epithelial injury-induced transient receptor potential vanilloid 1 (TRPV1) channel activation provokes inflammation through increases in IL-6 and IL-8 release whereas costimulation of the cannabinoid receptor subtype 1 (CB1) blunts this response. We determined in SV40-immortalized human corneal epithelial cells (HCEC) if the opposing effects elicited by TRPV1 and CB1 activation on IL-6 and IL-8 release are elicited through differential modulation of JNK1/2 and NF-κB activation through changes in transforming growth factor-β-activated kinase 1 (TAK1) phosphorylation.
Methods: HCEC lysates were coimmunoprecipated with either anti TRPV1, TAK1, CB1 or TAB1 antibodies followed by Western blotting with an appropriate antibody to probe for protein-protein interactions. Changes in I-κB phosphorylation status provided readout

of NF-κB activation. ELISA determined the individual effects of TRPV1 and CB1 activation as well as TAK1 inhibition on IL-6 and IL-8 release.

Results: Ten μM capsaicin or 5 μM WIN55,212-2 induced transient activation through interactions between TRPV1 and CB1. These receptors also had the same effects on TAK1 as well as its associated partner, TAB1. TRPV1 and CB1-induced TAK1 phosphorylation (i.e. activation) was larger and invariant during exposure to 1 μM okadaic acid. Capsaicin induced larger increases in TAK1 phosphorylation than those caused by 10 μM WIN55,212-2. These effects were eliminated by either 5 μM capsazepine or AM251, respectively. Receptor-induced TAK1, JNK1/2, I-κB phosphorylation and increases in IL-6 and IL-8 release were fully blocked by a selective TAK1 inhibitor, 10 nM (5Z)-7-oxozeaenol.

Conclusions: Capsaicin-induced TAK1-TAB1 complexation mediates IL-6 and IL-8 increases through JNK1/2 and NF-κB phosphorylation. Differences in the magnitude of TAK1 activation induced by either TRPV1 or CB1 stimulation may help explain why only capsaicin induced rises in IL-6 and IL-8 release. TAK1 may be a drug target to reduce injury-induced corneal inflammation without compromising TRPV1-induced increases in corneal wound healing.

CommercialRelationships: **Zheng Wang**, None; **Hua Yang**, None; **Jose E. Capo-Aponte**, None; **Nili Parekh**, None; **Peter S. Reinach**, None

Support: EY04795 and W81XWH-09-2-0162

Appendix E

Print this Page

1. Genetics and Gene Expression   4. Processing and Perception   7. Repair, Regeneration and Restoration

2. Development   5. Inflammation, Infection and Ischemia   8. Imaging and Other Methods

3. Physiology and Pathology   6. Degenerations, Dystrophies and Death   9. Diagnosis and Treatment

CME Session

Presentation Abstract

Abstract Title: **CB1 Activation Reduces TRPV1-induced Responses in Human Corneal Epithelial Cells**

Presentation Start/End   Monday, May 02, 2011, 1:45 PM - 3:30 PM
Time:

Session Number: 270

Session Title: Signal Transduction

Location: Hall B/C

Reviewing Code: 389 signal transduction: receptors - PH

Author Block: *Hua Yang[1], Stefan Mergler[2], Zheng Wang[1], Kulandaiappan Varadaraj[3], Sindhu S. Kumari[3], Peter S. Reinach[1].* [1]Biological Sciences, SUNY College of Optometry, New York, NY; [2]Department of Ophthalmology, University Medicine Charite Berlin, Berlin, Germany; [3]Physiology & Biophysics, SUNY, Stony Brook, Stony Brook, NY.

Keywords: 482 cornea: epithelium; 711 signal transduction; 556 inflammation

Abstract Body: **Purpose:** In primary sensory neurons, cannabinoid 1 (CB1) receptors suppress transient receptor potential vanilloid type 1 (TRPV1) channel activation. As TRPV1 is expressed in the mouse corneal epithelium and human corneal epithelial cells (HCEC), we determined in both tissue types if protein-protein interaction is associated with CB1 suppression of TRPV1 function.
Methods: Immunostaining and Western blot analysis probed for CB1 and TRPV1 colocalization and interaction. The CB1 agonist/antagonist pair: WIN55, 212-2 (WIN) and AM251 (AM) was used along with the mixed endogenous TRPV1/CB1 agonist, anandamide (AEA). The TRPV1 agonist/antagonist pair: capsaicin (CAP) and capsazepine (CPZ) was also used. ELISA determined proinflammatory cytokine release. TRPV1 channel activity was

characterized with the planar-patch clamp technique.

Results: In the mouse corneal epithelium, CB1 and TRPV1 colocalization was identified. Furthermore, coimmunoprecipitation analysis of HCEC identified protein-protein interaction between CB1 and TRPV1. CAP (10 µM)-induced 2.1, 2.5, 1.8-fold increases in IL-6, IL-8 and TNF-α release, respectively, Joint CB1/TRPV1 activation with 10 µM AEA induced rises that were 30-50% smaller than those obtained by CAP alone. However, these rises induced by AEA were restored to CAP obtained levels by initially blocking AEA activation of CB1 with AM251. CAP in HCEC induced 2.1-fold increases in cation channel current at a holding potential of 0 mV. This response to CAP could be suppressed during exposure to WIN.

Conclusions: Protein-protein interaction between CB1 and TRPV1 is consistent with our findings that CB1 activation can dampen both CAP-induced increases in current, proinflammatory cytokine and chemoattractant release. These effects indicate that changes in CB1 activity modulate TRPV1 activation. Taken together, CB1 may be a potential drug target to reduce corneal epithelial inflammation resulting from injury-induced TRPV1 activation by release of endogenous metabolites.

CommercialRelationships: **Hua Yang**, None; **Stefan Mergler**, None; **Zheng Wang**, None; **Kulandaiappan Varadaraj**, None; **Sindhu S. Kumari**, None; **Peter S. Reinach**, None

Appendix F

Print this Page

1. Genetics and Gene Expression   4. Processing and Perception   7. Repair, Regeneration and Restoration

2. Development   5. Inflammation, Infection and Ischemia   8. Imaging and Other Methods

3. Physiology and Pathology   6. Degenerations, Dystrophies and Death   9. Diagnosis and Treatment

CME Session

Presentation Abstract

Abstract Title: **CB1 Receptor Activation Elicits Human Corneal Epithelial Layer Barrier Function Restoration During Exposure To A Hypertonic Stress**

Presentation Start/End Time: Wednesday, May 04, 2011, 2:45 PM - 3:00 PM

Session Number: 444

Session Title: Corneal Epithelium / CME

Location: Floridian BCD

Reviewing Code: 164 corneal epithelium - CO

Author Block: *Jing Yuan, Fan Zhang, Hua Yang, Peter Reinach.* Biological Science, SUNY State College of Optometry, New York, NY.

Keywords: 482 cornea: epithelium; 663 pump/barrier function; 671 receptors

Abstract Body: **Purpose:** The effects of CB1 stimulation on (HCEC) tight junctional permeability have not been determined. We characterized the effects of CB1 activation on translayer electrical resistance during exposure to a hypertonic stress described in some types of dry eye disease. **Methods:** SV40-immortalized HCEC were seeded on 0.4 μm pore size Transwell® inserts. They were air lifted and reached confluence after about 5 days. Transepithelial layer electrical resistance (TEER) assessed tight junctional integrity. **Results:** After 5 h exposure to a 300 mOsm isotonic medium, TEER slightly declined to reach 200 ± 3.7 (n=3) ohm*cm2 and remained stable during the subsequent 15 h. On the other hand, replacement at 5 h with a 375 mOsm medium caused TEER to initially fall by 31% with partial restoration to a level at 20 h that was still 16 % below the isotonic control. However, inclusion of the mixed CB1/TRPV1 agonist, anandamide (AEA), at concentrations ranging from 1 to 10 μM, in the 375 mOsm medium, hastened complete TEER restoration to its isotonic control level. It occurred as early as 5 h after imposition

of this stress. Under isotonic conditions, 1 µM AEA blocked the initial 31% decline in the baseline TEER. In 375 mOsm medium, the TEER decreased from 20% to 25% despite the presence of either 10 or 20 µM AEA if HCEC were instead preexposed for 30 min to either 5µM or 10 µM AM 251, a selective CB1 antagonist. Furthermore, in isotonic medium, AM251 prevented TEER recovery from its 5 h suppressed level to its baseline levels. The TEER in isotonic medium was unchanged with either 5 or 10 µM AM251.

Conclusions: During exposure of HCEC to a hypertonic stress simulating tear film osmolarity in some types of dry eye disease, TEER initially declined and failed to fully recover with time. However, CB1 activation by AEA instead caused the TEER to fully recover more rapidly to its isotonic level. These AEA effects were solely due to CB1 activation since AM 251 fully inhibited both of them. Taken together, endocannabinoids may have therapeutic potential in reducing declines in epithelial barrier function occurring in some types of dry eye disease.

CommercialRelationships: **Jing Yuan**, None; **Fan Zhang**, None; **Hua Yang**, None; **Peter Reinach**, None

Appendix G

CHAPTER:	Transient Receptor Potential (TRP) Channels in the Eye
AUTHORS:	Zan Pan, Jose Capo-Aponte and Peter Reinach
BOOK EDITOR:	Shimon Rumelt
STATUS:	ACCEPTED

FULL CHAPTER REVIEW

September 25, 2011

Editor's comments

This is a fine chapter on transient receptor potential (TRP) channels in the eye. You are to be congratulated for this nice contribution.

To have the best study ever published on the topic:

General requests

1. An abstract is not required for the chapter. Please omit it.
2. Please provide a figure that demonstrates the pathways and activity of the different TRPs and a table of the location of the different TRPs and their activity.
3. Please limit the use of abbreviations to 2-3. Please spell-out all abbreviations (e.g., EGFR, INMP, MMP, HB-EGF, EGF, DES, HCEC, ICS, PIP2, IP3, ON, etc.) when first appear in the text and write the abbreviations in parentheses.
4. Please explain terms like pseudogene, EGF dream stream signaling, etc.
5. Please omit capital letters when not required (page 12, paragraph 2, line 2 from "Muller").
6. Please spell-out numbers when appear at the beginning of a sentence.
7. Please use the same tense (present tense).
8. Some citations are missing (e.g., page 8, paragraph 2, lines 1,2, page 11, paragraph 1, lines 4-6, etc.). Please add them.
9. The chapter contains spelling, syntax and grammar errors (e.g., "neovascularization" and not "neovascularisation," missing commas, misplacing "the," etc.). Please review the English before uploading your updated chapter.

The Book Editor requires you to make the suggested changes.

Sincerely yours,

Aleksandar Lazinica, CEO

Lazinica Aleksandar **INTECH**
d.o.o. Rijeka

Transient Receptor Potential (TRP) Channels in the Eye

Zan Pan,[1] José E. Capó-Aponte,[2,3] and Peter S. Reinach[3]

[1] Margaret Dyson Vision Institute, Weill Cornell Medical College,

1300 York Avenue, New York, NY 10065, USA

[2] Visual Sciences Branch, U.S. Army Aeromedical Research Laboratory,

Fort Rucker, AL 36362, USA

[3] Department of Biological Science, State University of New York, College of Optometry,

33 West 42nd Street, New York, NY 10036, USA

Correspondence to: E-mail: zap2001@med.cornell.edu

Phone: +1-212-746-3093

Fax: +1-212-746-8101

Word count: 4100

Abstract

Transient receptor potential (TRP) channels represent a superfamily of non-selective cation channels which contains 28 different genes. They are divided into subfamilies based on amino acid sequence homology between gene products. In mammals, there are six subfamilies. Cation selectivity for calcium and sodium varies by subfamilies and even between members of each sub-group. Some studies indicate that TRP channel subunits form part of store-operated calcium channels. TRP channels are expressed in the nervous systems as well as non-nervous systems such as lung, cardiovascular system and the urinary bladder. TRP channels present diverse sensitivities to an ample collection of stimuli, such as light, temperature, smell, taste, sound, acidity, osmolar and mechanical pressures. Recently, some TRP channels were found to be involved in mediating cellular events including proliferation, migration, apoptosis, inflammation and cell volume regulation. Mutation or activation of some TRP channels has been related to disease pathogenesis, indicating TRP channels play a great role beyond as physiological sensors.

The importance of TRP channels function in the eye has been recognized in ophthalmology and vision research. Eyes have a rich expression of various TRP channel subtypes in the cornea, trabecular meshwork, ciliary muscle, crystalline lens, and retina. Their roles in ocular diseases including corneal wound healing, glaucoma, cataract, and retinopathy have been documented. This chapter reviews the TRP channel superfamily nomenclature and highlights their critical roles in ocular homeostatic and pathological states. The chapter will also shed light on TRP channels as a potential drug target for treating various eye diseases.

1. Introduction

The first member of transient receptor potential (TRP) channel superfamily was discovered in photoreceptors of *Drosophila* over 30 years ago.[1] Since then this protein superfamily has been extensively characterized based on exponential increases in the number of publications related to TRP channels. With 28 TRP homologous genes identified in mammals, TRP channels have been detected in both neural and non-neural tissues.

In humans, 27 different TRP genes are classified into two groups and six different subfamily based on their amino acid homology and phenotypes associated with mutant genes. The genes of TRP channel in Group 1 and Group 2 are only distally related. The Group 1 of TRP genes are comprised of TRPC (canonical), TRPM (melastatin), TRPV (vanilloid) channel subfamilies, with TRPA (ankyrin) being more recently assigned to this group.[2] Such categorization is based on their resemblance to the amino acid sequence of the *Drosophila* TRP channel. The nomenclature of TRP channel genes in Group 2 is based on the human phenotypes generated by the mutation of the founding genes of each subfamily, including polycystic kinase disease (PKD) and mucolipidosis type IV (MCOLN, mucolipin). Their encoded proteins have also been referred to as TRPP (polycystin) and TRPML (mucolipin), respectively (Figure 1).

The TRP superfamily is evolutionarily conserved from nematodes to mammals.[3] The common features of TRP channels are six putative transmembrane spanning domains and a cation-permeable pore formed by a short hydrophobic region between transmembrane domains 5 and 6. They are configured as homo- or hetero-tetramers to form non-selective cation channels (Figure 2). Their permeability ratios to Ca^{2+}/Na^+ vary

significantly among individual members. TRPV5 and TRPV6 channels exhibit a

Ca^{2+}/Na^+ permeability ratio of greater than 100, indicating high Ca^{2+} selectivity.[4] In

contrast, TRPM4 and TRPM5 channels are impermeable to Ca^{2+} but are selective for

monovalent cations (Na^+, K^+).[5, 6] Such intra-family variability is unique to the TRP

channel superfamily whereas most other ion channel families have little difference in

ionic permeability within a family.[7]
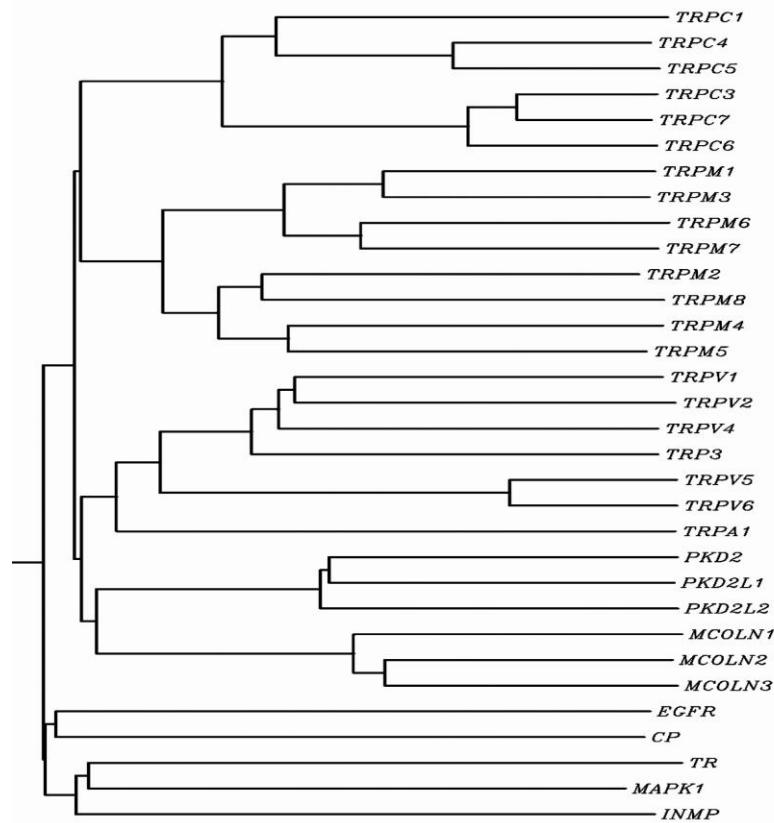
**Figure 1.** *Human TRP channel superfamily dendrogram. Random proteins bound to the*

plasma membrane (i.e., EGF receptor, EGFR), endoplasmic reticulum (i.e., calreticulin

precursor, CP), mitochondria (thioredoxin reductase, TR), cystolic protein (i.e., mitogen-

activated protein kinase 1, MAPK1) and nuclear membrane (i.e., inner nuclear

membrane protein, INMP) are shown to illustrate that PKD and MCOLN are

evolutionarily related to TRP channels or are the results of convergent evolution. The dendrogram shows that PKD and MCOLN belong to the TRP channel superfamily, since random genes extend from branches distinct from the TRP channel superfamily.[8]

TRP channel subfamilies in Group1 share substantial sequence homology in the transmembrane domains 6. What divides each subfamily is differences in their intracellular domains. TRPC, TRPV and TRPA channels contain ankyrin repeats near the intracellular N-terminal domain, whereas the TRPC and TRPM channels subfamilies possess proline-rich 'TRP domain' in the region of the C-terminal near the putative transmembrane segment. TRPM6 and TRPM7 channels have a protein kinase domain in the C-terminal.

The TRPC channels subfamily consists of seven genes (TRPC1–7) in mammals, but TRPC2 channel is pseudogene in humans. TRPC channels are widely expressed in multiple systems. TRPC4, TRPC5, TRPC6 and TRPC7 channels are identified in the various ocular tissues of mammals.[9-12] The TRPM channel subfamily comprises eight genes (TRPM 1–8), of which three encode channel-like proteins and five non-channel proteins. TRPM1 channels are expressed in retinas and TRPM8 channels in corneas.[13, 14] The TRPV channels subfamily contains six members (TRPV1–6). TRPV1, TRPV2, TRPV3 and TRPV4 channels are expressed in the cornea whereas TRPV1, TRPV2, TRPV5 and TRPV6 channels are expressed in the retina.[15-20] The TRPA channels subfamily has only one member, TRPA1.
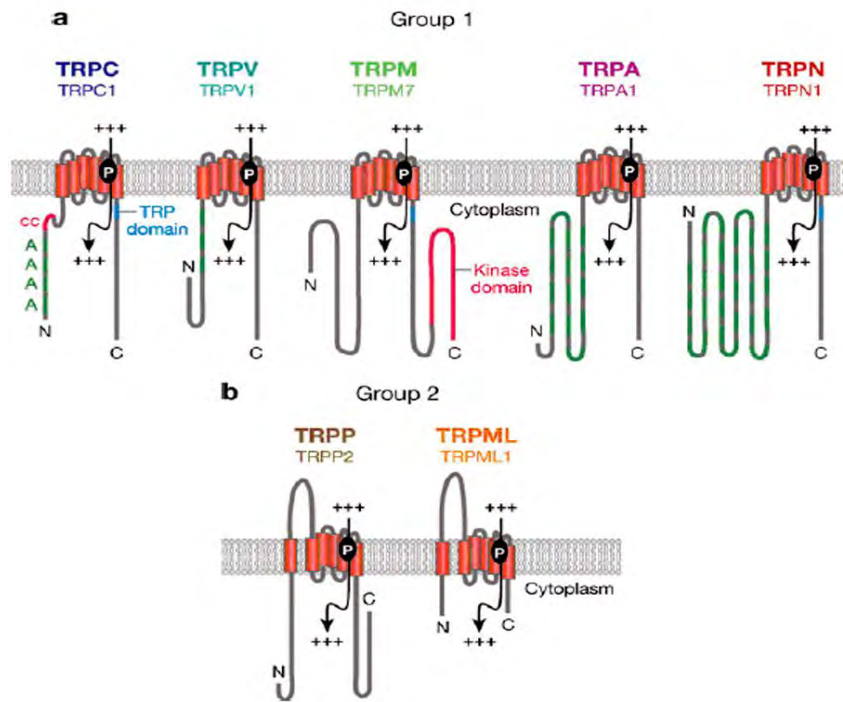
Figure 2. *Domain structure of the TRP channel superfamily. There are five TRP channel subfamilies in Group 1 (TRPN , no mechanoreceptor potential C, channels are not expressed in mammals) (a) and two TRP channel subfamilies in Group 2 (b). All subfamilies contain a six-transmembrane domain unit with a cation-permeable pore between domains 5 and 6. Four of such units are assembled as a homo- or hetero-tetramer to form a TRP channel. Domain indications: ankyrin repeats (A), coiled-coil domain (cc), protein kinase domain (TRPM6 and TRPM7 channels only), cation-permeable pore (P), transmembrane (TM) domain, cation-permeable (+++), TRP channels domain (TRPC and TRPM channels only), large extracellular loop between TM I and TM II (TRPP and TRPML channels only). Adapted with permission from Venkatachalam and Montell.*[21]

TRPP and TRPML channel subfamilies belong to Group 2. They contain limited sequence homology to TRP channels in Group 1, although such resemblance to classical TRP channels is still larger than those of random genes (e.g., EGFR, INMP) (Figure 1). TRPP channels proteins share 25 percent amino acid sequence homology to TRPC3 and TRPC6 channels over a region including transmembrane domains 4 and 5 and the hydrophobic pore loop between domains 5 and 6. TRPML channel proteins consist of three small proteins compared with other TRP channel proteins. Homology of their amino acid sequence with TRPC channels proteins is restricted to the region spanning transmembrane domains 4 to 6 (amino acids 331 to 521). TRP channels in Group 2 have a unique large extracellular loop between their first and second transmembrane domains. They are named as TRP channels based on the six transmembrane domains that they contain and function as cation-permeable channels.

The activation mechanisms of TRP channels are unique in that there are a diverse host of stimuli that can activate TRP channels and exhibit sharp differences in stimulatory modes even within each TRP channels subfamily. TRP channels are initially recognized as sensory mechanisms to a variety of stimuli, ranging from light, temperature, osmotic pressure, smell, taste, mechanical stress and acidity. There is also increasing awareness of their roles in mediating wound healing, inflammation, apoptosis and excretion. These channels are sensitive to intracellular and extracellular messengers, as well as declines in the calcium content of intracellular calcium stores (ICS).

Their activation following conformation changes increases Ca^{2+}/Na^{+} cell permeability ratios, which is dependent on TRP channel subunit composition. Transient increases in intracellular calcium concentration trigger intracellular activation of

mediators including: 1) phospholipase C (PLC) by coupled GTP-binding protein, leading to stimulation of store-operated Ca^{2+} channels ; 2) transactivation of EGF tyrosine receptors through MMP-mediated HB-EGF shedding.[4, 10, 16] The physiological significance of TRP channel expression is indicated by the finding that TRP channel mutations are linked to human diseases.[22]

Similarly, there is compelling evidence that the TRP channel superfamily plays a critical role in ocular homeostasis and pathogenesis. Functional importances of TRP isotypes expressed in different ocular tissues are multi-faceted. Their activation is essential for retaining corneal deturgescence and clarity, mediating aqueous humor outflow in trabecular meshwork and ciliary body as well as inducing light sensation in retina. Mutation of TRP channels is associated with ocular pathological phenotypes either due to loss of its homeostatic role or over-activation of its function. The realization of the importance of TRP channels has prompted much research effort to investigate novel strategies for regulating TRP channels function in a number of ocular diseases.

2. Roles of TRP Channels in Corneal Sensation and Wound Healing

Continuous renewal of corneal epithelial layer is essential to maintain corneal transparency. The intact epithelium not only offers a smooth and clear optical surface, but also provides corneal barrier function. This property protects the underlying stroma from swelling and pathogenic invasion. Should such protection mechanism become compromised by ocular surface diseases, outcomes can range from mild symptoms, such as irritation, photophobia, to severe consequences including corneal opacity, ulceration and even perforation. TRP channel functions have been indicated to associate with

maintaining corneal sensation and integrity. Functional expressions of TRPC1, TRPC 3, TRPC4, TRPC6 and TRPC as well as TRPV1–4 channels are identified in the corneal epithelium, TRPV1-4 in the corneal endothelium, TRPV1, TRPA1, and TRPM8 in the corneal nerve varying in different species.[10, 15-17, 23, 24, 25-27] These channels are involved in corneal regenerative, protective and sensory mechanisms.

TRPC4 channels protein was localized in plasma membranes of cultured human corneal epithelial cells and is responsible for epidermal growth factor (EGF)-promoted epithelial proliferation. TRPC4 channel is activated by EGF-induced depletion of ICS content in the endoplasmic reticulum. This depletion occurs as a consequence of stimulation of PLC activity which results in increases in inositol 1,4,5-trisphosphate (IP3) formation. This response leads to declines in ICS content and activation of TRPC4 store operated channel (SOC) function. Its activation induces intracellular Ca^{2+} influx leading to stimulation of downstream signalling cascades. They include the mitogen activated protein kinase (MAPK) cascade composed of ERK, JNK and p38 casettes as well as protein kinase A (PKA), protein kinase C (PKC), JAK/STAT and PI3-K/AKT/GSK-3. All of their activations contribute to the control of increases in cell survival and proliferation elicited by this mitogen. The importance of TRPC4 channels activation to mediate EGF-induced mitogenic responses is indicated by the finding that knockdown of its gene expression in HCEC eliminated the mitogenic response to EGF.[10]

TRPV1 channel expression was first identified on the ophthalmic branch of the trigeminal nerve. More recently, the functional expression of this channel was also identified in the corneal epithelial and endothelial layers. A hallmark of its activity is that the cannabinoid compounds (such as capsaicin isolated from hot chilli pepper),

hyperosmolarity, acidity (pH below 6) and high temperatures (above 43°C) stimulate TRPV1 channels. In the corneal epithelium, severe chemical injury to mice corneal epithelium induces TRPV1 channel activation leading to dysregulated inflammation, scarring and loss of corneal transparency. On the other hand, its activation stimulates in HCEC proliferation and migration through EGF receptor (EGFR) transactivation.[28] The involvement of TRPV1 channel activation in inducing these diverse responses is indicated by the finding that in homozygous TRPV1 knockout mice the wound healing response to an alkali burn does not result in losses of corneal transparency. Similarly, TRPV1 channel activation in some types of dry eye disease resulting from exposure to hyperosmolar tears may account for chronic inflammation since TRPV1 channels activation caused by exposure to a hyperosmolar challenge induced large increases in a host of proinflammatory cytokines (e.g. IL-6, IL-8, TNF α and IL-1 β) and chemoattractants (e.g., MCP-1) in HCEC. On the other hand, pre-exposure to a selective TRPV1 channels antagonist obviated all of these responses suggesting that TRPV1 channel is a potential drug target for the treatment of dry eye syndrome because suppression of its activation may reduce ocular surface inflammation.[16, 23]

In contrast with TRPV1, its cohort TRPV4 channel reacts to a different spectrum of stresses. Unlike TRPV1 channel which is thought to only be activated by a hyperosmolar stress, TRPV4 channels may instead be an osmosensor for a hypoosmolar challenge.[17] Such a stress is encountered by the cornea during exposure to fresh water (e.g., swimming, bathing, use of some eye drops). This hypotonic exposure results initially in corneal epithelial swelling due to obligatory water influx resulting in equilibration between the cell interior and surface tears. However, excessive swelling can

lead to cell lysis. To counter the initial swelling, corneal epithelial cells mediate

regulatory volume decrease (RVD) behavior by stimulating volume-sensitive potassium

and chloride channels as well as potassium-chloride co-transporter (KCC) activity to

restore isotonic cell volume through osmotically coupled net fluid efflux.

TRPV1–4 channel isoforms also serve as thermosensors over defined temperature

ranges in the corneal epithelium. In addition, TRPV3 channel activation, either by

temperatures above 33°C or by its selective agonist, carvacrol, not only contributes to

thermosensation, but also accelerate epithelial wound recovery by enhancing cell survival,

proliferation and migration.[15, 29] TRPV1–3 and TRPC4 channels are also expressed in

corneal endothelial cells.[9, 30] TRPV1–3 channels are sensitive to temperatures from 25 to

40°C, similar to their epithelial counterparts.

TRP channels play an important role in corneal sensations. The cornea has the

highest sensory nerve density of any tissue in the body. The corneal sensory nerves

originate from the ophthalmic branch of the trigeminal ganglion and are responsible for

eliciting nociception to thermal, chemical and mechanical stimuli.[31] TRPV1 channels

were co-localized with substance P (SP) and calcitonin-gene-related peptide (CGRP) in

the ophthalmic branch of the trigeminal nerve indicating its role in eliciting nociceptive

perception. This realization makes TRPV1 channel tenable as a potential drug target for

treating neurotrophic keratopathy.[31, 32] Additionally, TRPM8 channel contributes to

corneal cold sensation and basal tear secretion required to maintain corneal surface

hydration.[14, 33]

Taken together, these studies on the corneal epithelial, endothelial cells and

corneal nerves indicate that functional expressions of TRP channels are essential for

maintaining corneal transparency and eliciting adaptive responses to stresses. This indicates the importance of further studies on TRP channel regulation since such insight may lead to novel strategies for treating corneal diseases and better management of ocular surface inflammatory pain.

3. Roles of TRP Channels in Glaucoma

Some members of the TRPC and TRPV channels subfamilies are expressed in trabecular meshwork, ciliary muscle and retinal ganglion cells.[34, 35] Their roles have been associated with regulating intraocular pressure through modulation of aqueous humor flows and ganglion cell survival. The trabecular meshwork contains contractile elements whose tension modulation changes fluid drainage rate from the anterior chamber into the Canal of Schlemm. The contractile state of trabecular meshwork is governed by tension imparted from the ciliary muscle and possibly trabecular meshwork itself.[35, 36] The trabecular meshwork and the ciliary muscle act as functional antagonists. Such opposition is evident since ciliary muscle contraction leads to relaxation of the trabecular meshwork with subsequent increases in fluid outflow whereas trabecular meshwork contraction has the opposite effect.[35] Malfunction of trabecular meshwork and ciliary muscle contractility often leads to ocular hypertension and glaucoma.[37] Their contractile states are modulated by changes in intracellular Ca^{2+} concentration and Ca^{2+} channel activity. Specifically, increases in cytoplasmic Ca^{2+} resulting from the stimulation of TRP channels enhance contractility. Other types of Ca^{2+} channels that regulate intracellular Ca^{2+} concentration include L-type voltage-gated Ca^{2+} channels, receptor operated Ca^{2+} channels and store-operated calcium entry (SOCE) pathways. In

bovine trabecular meshwork cells, TRPC1 and TRPC4 channels are implicated in the formation of heteromeric SOCE channels which contribute to rises in cytoplasmic Ca^{2+} store and therefore trabecular meshwork contractility during exposure to bradykinin or endothelin-1.

Similarly TRPC1, TRPC3, TRPC4 and TRPC6 channels are also present in ciliary muscle cells. The ciliary muscle is densely innervated by parasympathetic neurons that stimulate muscle contraction through acetylcholine-mediated muscarinic receptor stimulation on neighboring muscle cells. Such activation leads to a surge in intracellular Ca^{2+} concentration resulting in membrane voltage depolarization via receptor-operated non-selective cation channels. TRPC1, TRPC3, TRPC4 and TRPV6 channels are considered as potential candidates for such channels as they are co-localized with muscarinic receptor type 3 in ciliary muscle fibres.[38, 39]

Modulation of TRPC channel activity in turn alters aqueous humor outflow and therefore intraocular pressure through changes in trabecular meshwork contractility. The dual localization of TRPC channels on ciliary muscles and trabecular meshwork cells suggests that strategies targeted towards their selective modulation may be prove to be advantageous in providing better control of intraocular pressure in patients with ocular hypertension or glaucoma. Such an outcome is possible once there is definitive identification of the TRP channels subtypes on each of these tissues. At this point it may be possible to maximize fluid outflow rates by selectively decreasing trabecular meshwork resistance through an increase in its contractile state. Accordingly, additional studies are needed to map the TRP channels subtypes and characterize their mechanisms of regulation in the ciliary muscle and trabecular meshwork.

Chronic intraocular hypertension is a risk factor which in some cases can induce glaucoma due to damage to retinal ganglion cells. Such damage can result from either increased hydrostatic pressure, declines in retrograde neutrophin flow, ischemic or oxidative stress. Irreversible loss of retinal ganglion cells leads to gradual and often insidious vision impairment and possible blindness. Elevated intraocular pressures can activate TRP channels in retinal ganglion cells . TRP channel sensitivity to hydrostatic pressure has been described in bladder, lung and skin.[40-42] Sappington et al. have shown *in vitro* that exposure of retinal ganglion cell to elevated hydrostatic pressure induced transient rises intracellular Ca^{2+} accumulation due to TRPV1 channel activation. This effect promoted apoptosis of retinal ganglion cell whereas suppression of TRPV1 channel activation protected retinal ganglion cell from pressure-induced death.[34] Recently, similar stresses were identified to stimulate TRPV4 channel and induce apoptosis in retinal ganglion cell.[43] The increased levels of cytoplasmic Ca^{2+} is the underlying mechanism of leading to retinal ganglion cell apoptosis.[44] Ca^{2+}-dependent calcineurin and calpain are a phosphatase and a protease, respectively, that trigger apoptosis signalling. Both of them induce cytochrome c release from mitochondria and trigger pro-apoptotic signalling. In contrast, TRPV1 channel in the retinal microglia appears to have a retinoprotective effect. Retina microglia cells are essential to neuronal homeostasis and provide innate immunity for retina to defense pathogenic infiltration. Exposure of microglia to chronic stress is associated with various neurodegenerative diseases, including retinal dystrophies. TRPV1 channel activation in the cultured retinal microglia cells by the hydrostatic pressure induces increases in IL-6 and TNF-α release through transient rises in intracellular Ca^{2+} levels. Rises in IL-6 suppress pro-apoptotic signalling pathways and cell death[45]

Therefore, provided strategies can be devised to selectively induce microglial TRPV1 channels expression, TRPV1 channels may be a potential drug target in managing pressure-induced retinal ganglion cell loss in glaucoma.

4. Possible Roles of TRP Channels in Cataract Development

Maintenance of intracellular Ca^{2+} levels is imperative to crystalline lens clarity.[46] Lenses with cortical cataracts have intracellular Ca^{2+} levels that are above those in the physiological range.[47] Accordingly, a better understanding of the mechanisms mediating control of lens intracellular Ca^{2+} levels is pertinent for identifying economical and novel drug strategies to preserve lens transparency or slow cataract progression.

As previously described,

Store operated calcium entry channels (SOCE) are composed of TRP subunits and are heterogeneously expressed in the lens epithelial cells. Equatorial Epithelial cells in the lens equatorial region have the higher SOCE expression than is those in the central anterior region. This difference is attributable to the fact that the size of the intracellular calcium storage is larger in the equatorial than the central anterior epithelial cells.[48] The higher intracellular Ca^{2+} load in the equatorial epithelium is required for its more rapid proliferative rate than other parts of the lens epithelium. However, the equatorial epithelium is more susceptible to damage that can induce cortical cataracts since the development of such cataracts is associated with Ca^{2+} overload in the lens epithelial cells. The identity of the TRP channels isoforms constituting SOCE is elusive since drugs that modulate SOCE activity have poor selectivity for each of the different TRP subunits in the TRPV and TRPC channels subfamilies. For example, the inhibitory effects of

lanthanum are used as a criterion to distinguish between SOCE and TRPC channel involvement in the development of cataract. At lower concentrations (i.e., in the nanomolar range), lanthanum inhibits SOCE, whereas at higher concentrations it blocks TRPC-containing channels.[49, 50] However, this approach is problematic because the cut-off between lanthanum concentration ranges having the inhibitory effect to either SOCE or TRPC channel is poorly defined. Another complication is that, in the micromolar range, Ca^{2+} influx is potentiated through TRPC4- and TRPC5-containing pathways. Nevertheless, the current understanding is that SOCE is the major pathway for Ca^{2+} influx in the lens. Better insight into the specific involvement of TRP channels dysfunction in cataractogenesis will be clarified once either more selective Ca^{2+} channel modulators become available or genetic approaches are employed to selectively modulate levels of TRP channels isoform expression.

5. Roles of TRP Channels in Retinopathy

TRP channels are abundantly expressed in the entire retinal layer including the retinal pigment epithelium (RPE), photoreceptors, retinal ganglion cells, Mϋller cells, and microglia. Initially, TRP channels mediated phototransduction was identified in *Drosophila* and 13 of the known 28 homologues of the mutant insect channel were next identified in the mammalian retina.[51] For example, the TRPC channels in mammals are most closely related to the *Drosophila* TRP channels. The difference is that in mammals the six TRPC subfamily genes (i.e., trpc 1, 3–7) encode seven proteins (TRPC1–7 channels), since TRPC2 is a pseudogene.

In *Drosophila* retinal photoreceptors, TRPC channels lead to photoexcitation. Light absorption converts rhodopsin to active metarhodopsin, which activates phospholipase C (PLC). PLC hydrolyses phosphatidylinositol 4,5-bisphosphate (PIP$_2$) to inositol 1,4,5-triphosphate (IP$_3$) and diacylglycerol (DAG). DAG can be degraded to release polyunsaturated fatty acids and protons. TRPC channel activation occurs as a consequence of phosphoinositide depletion and acidification resulting from PLC-induced PIP$_2$ hydrolysis and proton release associated with IP$_3$ formation.[34] TRPC channel activation by phosphoinositide metabolites suggests that these channels are part of the light-sensing mechanism for *Drosophila,* but their role in humans is still unclear.

TRP channels dysfunction has been implicated in mammalian retinopathy. Mutation of TRPM1 channels in ON bipolar cells has been linked to autosomal-recessive congenital stationary night blindness (CSNB), a heterogeneous group of retinal disorders characterized by non-progressive impaired night vision and variable decreased visual acuity.[52] On the other hand, Wang et al. reported that TRPC6 channel activation has a neuroprotective effect on retinal ischemia-reperfusion (IR) injury in the rat.[53] Following IR, the expression of TRPC6 channels decreases in retinal ganglion cells. Activation of TRPC6 channels before IR reduces retinal ganglion cells losses whereas suppression of TPC6 channels has an opposite effect. Such protection by TRPC6 channels on retinal ganglion cells is dependent on brain-derived neurotrophic factor (BDNF) signalling.

The RPE layer has essential roles in sustaining normal retinal function. It regulates the hydration and ionic composition of the subretinal space, as well as rod outer segment function. RPE also secretes cytokines that are essential for retinal health. TRPV5 and TRPV6 expression was identified *in vitro* in the human RPE, implicating that these

two most calcium-selective channels of the TRP channel superfamily contribute to the

regulation of the subretinal space calcium composition accompanying light/dark

transitions.[19] TRPV2 channels were shown in another study to control RPE release of

vascular endothelial growth factor (VEGF). Insulin-like growth factor-1 (IGF-1) is a

TRPV2 channel activator that selectively induces the intracellular Ca^{2+} transients

required for inducing VEGF release. Control of this response is needed to reduce retinal

neovascularization, since wet age-related macular degeneration (AMD) is decreased or

stabilized by treatment with anti-VEGF antibodies. These results suggest that reducing

TRPV2 channels activity may provide another option for managing wet AMD.[54]

6. Summary

TRP channels are involved in ocular sensory and cellular functions. In mammals,

TRP channel subunit proteins are encoded by 27 genes and are classified into two groups

and six different subfamilies, based on differences in amino acid sequence homology.

Group 1 and Group 2 of TRP channels are only remotely related, but share similar cation

channel-forming structures of six transmembrane domains. Their cation selectivity and

activation mechanisms are very diverse and depend on individual TRP channel. TRP

channel activation induces a host of responses to variations in ambient temperature,

pressure, osmolarity and pH. In addition, their activation by injury induces inflammation,

neovascularization, pain and cell death, as well as wound healing. There is emerging

interest in characterising their roles in inducing ocular surface disease, glaucoma,

cataracts and retinopathy. Such efforts could lead to the identification of novel drug

targets for improving disease therapeutic management.

References

1.   Minke B. Drosophila mutant with a transducer defect. *Biophys Struct Mech* 1977;3:59-64.

2.   Clapham DE. TRP channels as cellular sensors. *Nature* 2003;426:517-524.

3.   Harteneck C, Plant TD, Schultz G. From worm to man: three subfamilies of TRP channels. *Trends Neurosci* 2000;23:159-166.

4.   Montell C. The TRP superfamily of cation channels. *Sci STKE* 2005;2005:re3.

5.   Launay P, Fleig A, Perraud AL, Scharenberg AM, Penner R, Kinet JP. TRPM4 is a Ca2+-activated nonselective cation channel mediating cell membrane depolarization. *Cell* 2002;109:397-407.

6.   Hofmann T, Chubanov V, Gudermann T, Montell C. TRPM5 is a voltage-modulated and Ca(2+)-activated monovalent selective cation channel. *Curr Biol* 2003;13:1153-1158.

7.   Voets T, Janssens A, Droogmans G, Nilius B. Outer pore architecture of a Ca2+-selective TRP channel. *J Biol Chem* 2004;279:15223-15230.

8.   Pan Z, Yang H, Reinach PS. Transient receptor potential (TRP) gene superfamily encoding cation channels. *Hum Genomics* 2011;5:108-116.

9.   Xie Q, Zhang Y, Cai Sun X, Zhai C, Bonanno JA. Expression and functional evaluation of transient receptor potential channel 4 in bovine corneal endothelial cells. *Exp Eye Res* 2005;81:5-14.

10.   Yang H, Mergler S, Sun X, et al. TRPC4 knockdown suppresses epidermal growth factor-induced store-operated channel activation and growth in human corneal epithelial cells. *J Biol Chem* 2005;280:32230-32237.

11.   Warren EJ, Allen CN, Brown RL, Robinson DW. The light-activated signaling pathway in SCN-projecting rat retinal ganglion cells. *Eur J Neurosci* 2006;23:2477-2487.

12.   Da Silva N, Herron CE, Stevens K, Jollimore CA, Barnes S, Kelly ME. Metabotropic receptor-activated calcium increases and store-operated calcium influx in mouse Muller cells. *Invest Ophthalmol Vis Sci* 2008;49:3065-3073.

13.   Oancea E, Vriens J, Brauchi S, Jun J, Splawski I, Clapham DE. TRPM1 forms ion channels associated with melanin content in melanocytes. *Sci Signal* 2009;2:ra21.

14.   Madrid R, Donovan-Rodriguez T, Meseguer V, Acosta MC, Belmonte C, Viana F. Contribution of TRPM8 channels to cold transduction in primary sensory neurons and peripheral nerve terminals. *J Neurosci* 2006;26:12512-12525.

15.   Mergler S, Garreis F, Sahlmuller M, Reinach PS, Paulsen F, Pleyer U. Thermosensitive transient receptor potential channels (thermo-TRPs) in human corneal epithelial cells. *J Cellular Physiol (in press)* 2010.

16.   Pan Z, Wang Z, Yang H, Zhang F, Reinach PS. TRPV1 Activation is Required for Hypertonicity Stimulated Inflammatory Cytokine Release in Human Corneal Epithelial Cells. *Invest Ophthalmol Vis Sci (in press)* 2010.

17.   Pan Z, Yang H, Mergler S, et al. Dependence of regulatory volume decrease on transient receptor potential vanilloid 4 (TRPV4) expression in human corneal epithelial cells. *Cell Calcium* 2008;44:374-385.

18.   Sappington RM, Calkins DJ. Contribution of TRPV1 to microglia-derived IL-6 and NFkappaB translocation with elevated hydrostatic pressure. *Invest Ophthalmol Vis Sci* 2008;49:3004-3017.

19.	Kennedy BG, Torabi AJ, Kurzawa R, Echtenkamp SF, Mangini NJ. Expression of transient receptor potential vanilloid channels TRPV5 and TRPV6 in retinal pigment epithelium. *Mol Vis* 2010;16:665-675.

20.	Leonelli M, Martins DO, Kihara AH, Britto LR. Ontogenetic expression of the vanilloid receptors TRPV1 and TRPV2 in the rat retina. *Int J Dev Neurosci* 2009;27:709-718.

21.	Venkatachalam K, Montell C. TRP channels. *Annu Rev Biochem* 2007;76:387-417.

22.	Nilius B, Voets T, Peters J. TRP channels in disease. *Sci STKE* 2005;2005:re8.

23.	Zhang F, Yang H, Wang Z, et al. Transient receptor potential vanilloid 1 activation induces inflammatory cytokine release in corneal epithelium through MAPK signaling. *J Cell Physiol* 2007;213:730-739.

24.	Yang H, Sun X, Wang Z, et al. EGF stimulates growth by enhancing capacitative calcium entry in corneal epithelial cells. *J Membr Biol* 2003;194:47-58.

25.	Yamamoto Y, Hatakeyama T, Taniguchi K. Immunohistochemical colocalization of TREK-1, TREK-2 and TRAAK with TRP channels in the trigeminal ganglion cells. *Neurosci Lett* 2009;454:129-133.

26.	Salas MM, Hargreaves KM, Akopian AN. TRPA1-mediated responses in trigeminal sensory neurons: interaction between TRPA1 and TRPV1. *Eur J Neurosci* 2009;29:1568-1578.

27.	Bang S, Kim KY, Yoo S, Kim YG, Hwang SW. Transient receptor potential A1 mediates acetaldehyde-evoked pain sensation. *Eur J Neurosci* 2007;26:2516-2523.

28.	Yang H, Wang Z, Capo-Aponte JE, Zhang F, Pan Z, Reinach PS. Epidermal growth factor receptor transactivation by the cannabinoid receptor (CB1) and transient receptor potential vanilloid 1 (TRPV1) induces differential responses in corneal epithelial cells. *Exp Eye Res* 2010;91:462-471.

29.	Yamada T, Ueda T, Ugawa S, et al. Functional expression of transient receptor potential vanilloid 3 (TRPV3) in corneal epithelial cells: involvement in thermosensation and wound healing. *Exp Eye Res* 2010;90:121-129.

30.	Mergler S, Valtink M, Coulson-Thomas VJ, et al. TRPV channels mediate temperature-sensing in human corneal endothelial cells. *Exp Eye Res* 2010;90:758-770.

31.	Murata Y, Masuko S. Peripheral and central distribution of TRPV1, substance P and CGRP of rat corneal neurons. *Brain Res* 2006;1085:87-94.

32.	Okada Y, Reinach PS, Kitano A, Shirai K, Kao WW, Saika S. Neurotrophic keratopathy; its pathophysiology and treatment. *Histol Histopathol* 2010;25:771-780.

33.	Parra A, Madrid R, Echevarria D, et al. Ocular surface wetness is regulated by TRPM8-dependent cold thermoreceptors of the cornea. *Nat Med* 2010;16:1396-1399.

34.	Sappington RM, Sidorova T, Long DJ, Calkins DJ. TRPV1: contribution to retinal ganglion cell apoptosis and increased intracellular Ca2+ with exposure to hydrostatic pressure. *Invest Ophthalmol Vis Sci* 2009;50:717-728.

35.	Wiederholt M, Thieme H, Stumpff F. The regulation of trabecular meshwork and ciliary muscle contractility. *Prog Retin Eye Res* 2000;19:271-295.

36.	Wiederholt M. Direct involvement of trabecular meshwork in the regulation of aqueous humor outflow. *Curr Opin Ophthalmol* 1998;9:46-49.

37.	Weinreb RN, Khaw PT. Primary open-angle glaucoma. *Lancet* 2004;363:1711-1720.

38.   Salmon MD, Ahluwalia J. Discrimination between receptor- and store-operated Ca(2+) influx in human neutrophils. *Cell Immunol* 2010;265:1-5.

39.   Sugawara R, Takai Y, Miyazu M, Ohinata H, Yoshida A, Takai A. Agonist and antagonist sensitivity of non-selective cation channel currents evoked by muscarinic receptor stimulation in bovine ciliary muscle cells. *Auton Autacoid Pharmacol* 2006;26:285-292.

40.   Goto M, Ikeyama K, Tsutsumi M, Denda S, Denda M. Calcium ion propagation in cultured keratinocytes and other cells in skin in response to hydraulic pressure stimulation. *J Cell Physiol* 2010;224:229-233.

41.   Yin J, Kuebler WM. Mechanotransduction by TRP channels: general concepts and specific role in the vasculature. *Cell Biochem Biophys* 2010;56:1-18.

42.   Birder LA. TRPs in bladder diseases. *Biochim Biophys Acta* 2007;1772:879-884.

43.   Ryskamp DA, Witkovsky P, Barabas P, et al. The polymodal ion channel transient receptor potential vanilloid 4 modulates calcium flux, spiking rate, and apoptosis of mouse retinal ganglion cells. *J Neurosci* 2011;31:7089-7101.

44.   Qu J, Wang D, Grosskreutz CL. Mechanisms of retinal ganglion cell injury and defense in glaucoma. *Exp Eye Res* 2010;91:48-53.

45.   Sappington RM, Chan M, Calkins DJ. Interleukin-6 protects retinal ganglion cells from pressure-induced death. *Invest Ophthalmol Vis Sci* 2006;47:2932-2942.

46.   Duncan G, Williamsa MR, Riacha RA. Calcium, cell signalling and cataract. *Progress in Retinal and Eye Research* 1994;13:623-652.

47.   Duncan G, Bushell AR. Ion analyses of human cataractous lenses. *Exp Eye Res* 1975;20:223-230.

48.   Rhodes JD, Russell SL, Illingworth CD, Duncan G, Wormstone IM. Regional differences in store-operated Ca2+ entry in the epithelium of the intact human lens. *Invest Ophthalmol Vis Sci* 2009;50:4330-4336.

49.   Gwack Y, Srikanth S, Feske S, et al. Biochemical and functional characterization of Orai proteins. *J Biol Chem* 2007;282:16232-16243.

50.   Nilius B, Owsianik G, Voets T, Peters JA. Transient receptor potential cation channels in disease. *Physiol Rev* 2007;87:165-217.

51.   Gudermann T, Mederos y Schnitzler M. Phototransduction: keep an eye out for acid-labile TRPs. *Curr Biol* 2010;20:R149-152.

52.   van Genderen MM, Bijveld MM, Claassen YB, et al. Mutations in TRPM1 are a common cause of complete congenital stationary night blindness. *Am J Hum Genet* 2009;85:730-736.

53.   Wang X, Teng L, Li A, Ge J, Laties AM, Zhang X. TRPC6 channel protects retinal ganglion cells in a rat model of retinal ischemia/reperfusion-induced cell death. *Invest Ophthalmol Vis Sci* 2010;51:5751-5758.

54.   Cordeiro S, Seyler S, Stindl J, Milenkovic VM, Strauss O. Heat-Sensitive Trpv Channels Regulate Vegf-a Secretion in Retinal Pigment Epithelial Cells. *Invest Ophthalmol Vis Sci* 2010;51:6001-6008.
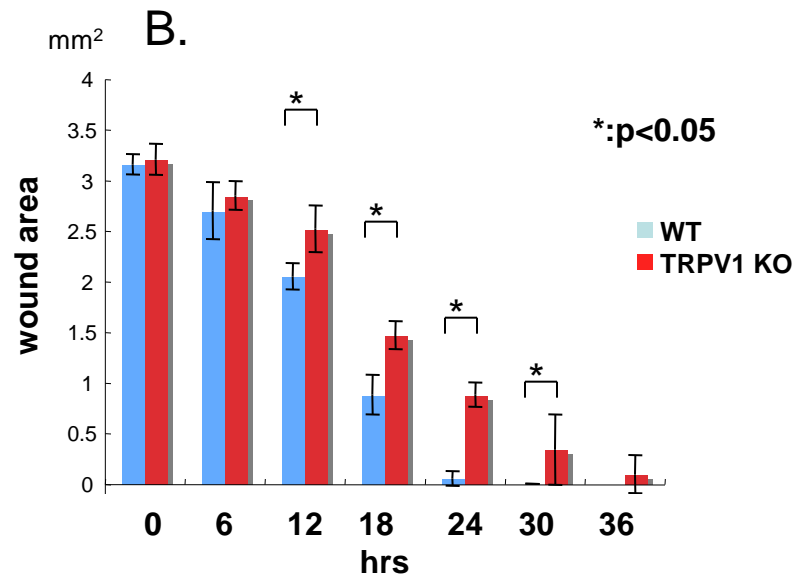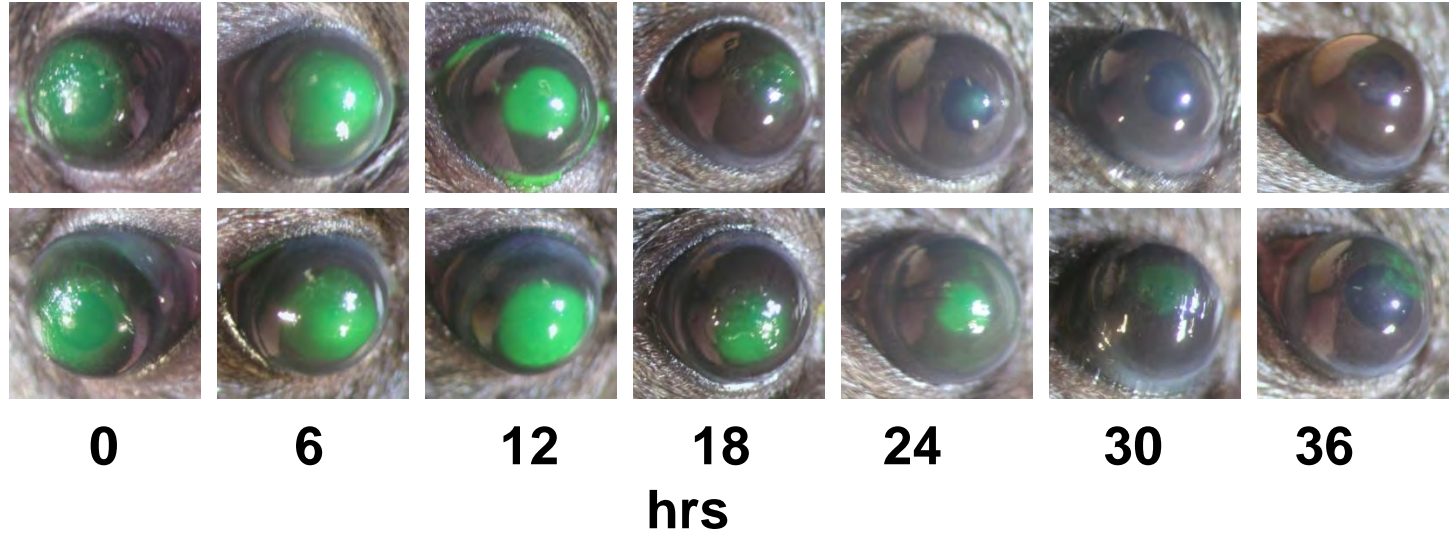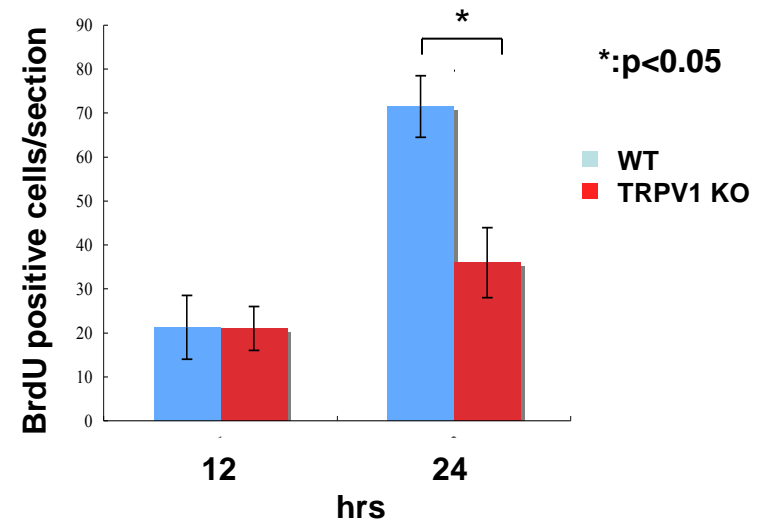
Appendix H

Epithelial defect

A.

WT

TRPV1 KO

0   6   12   18   24   30   36

hrs

B.

mm²

wound area

*:p<0.05

■ WT
■ TRPV1 KO

0   6   12   18   24   30   36

hrs

C.

BrdU positive cells/section
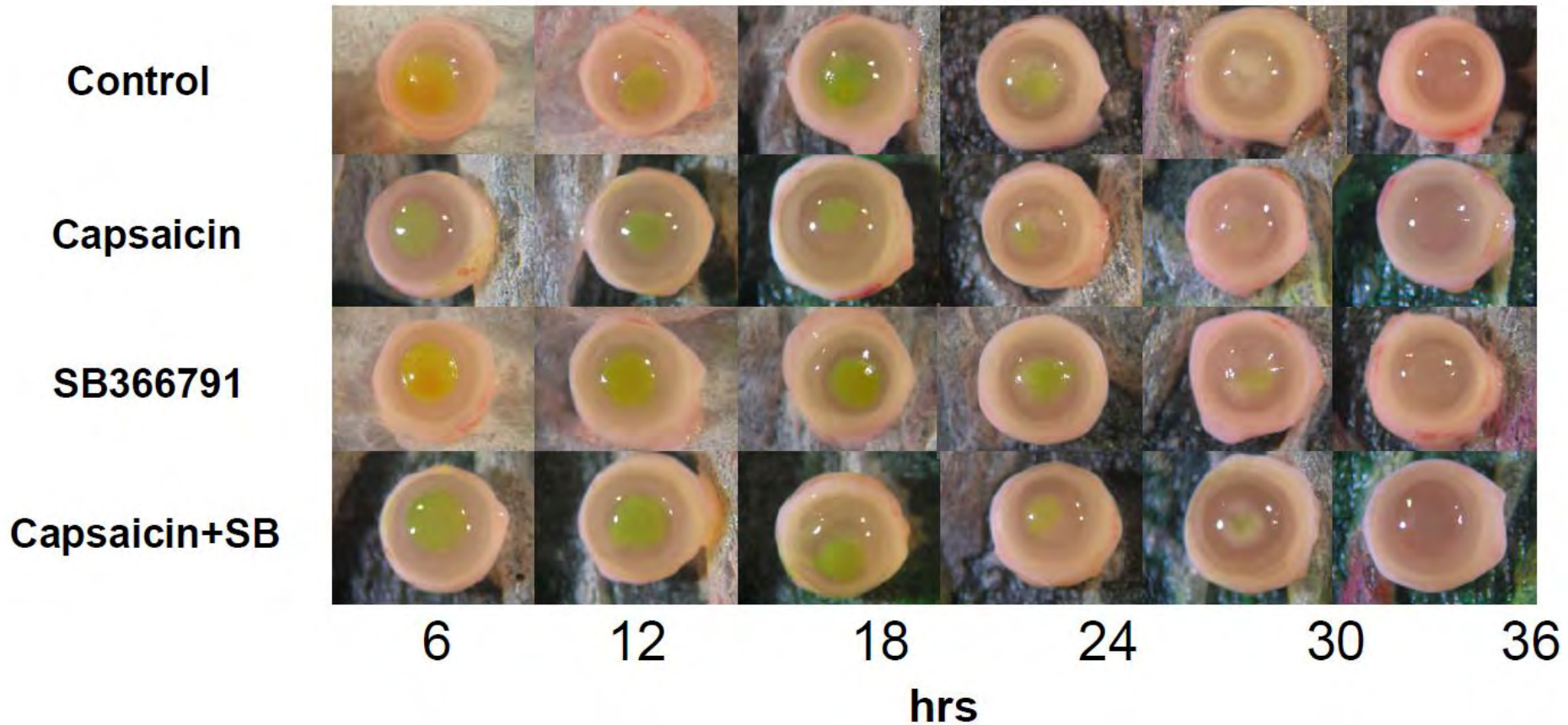
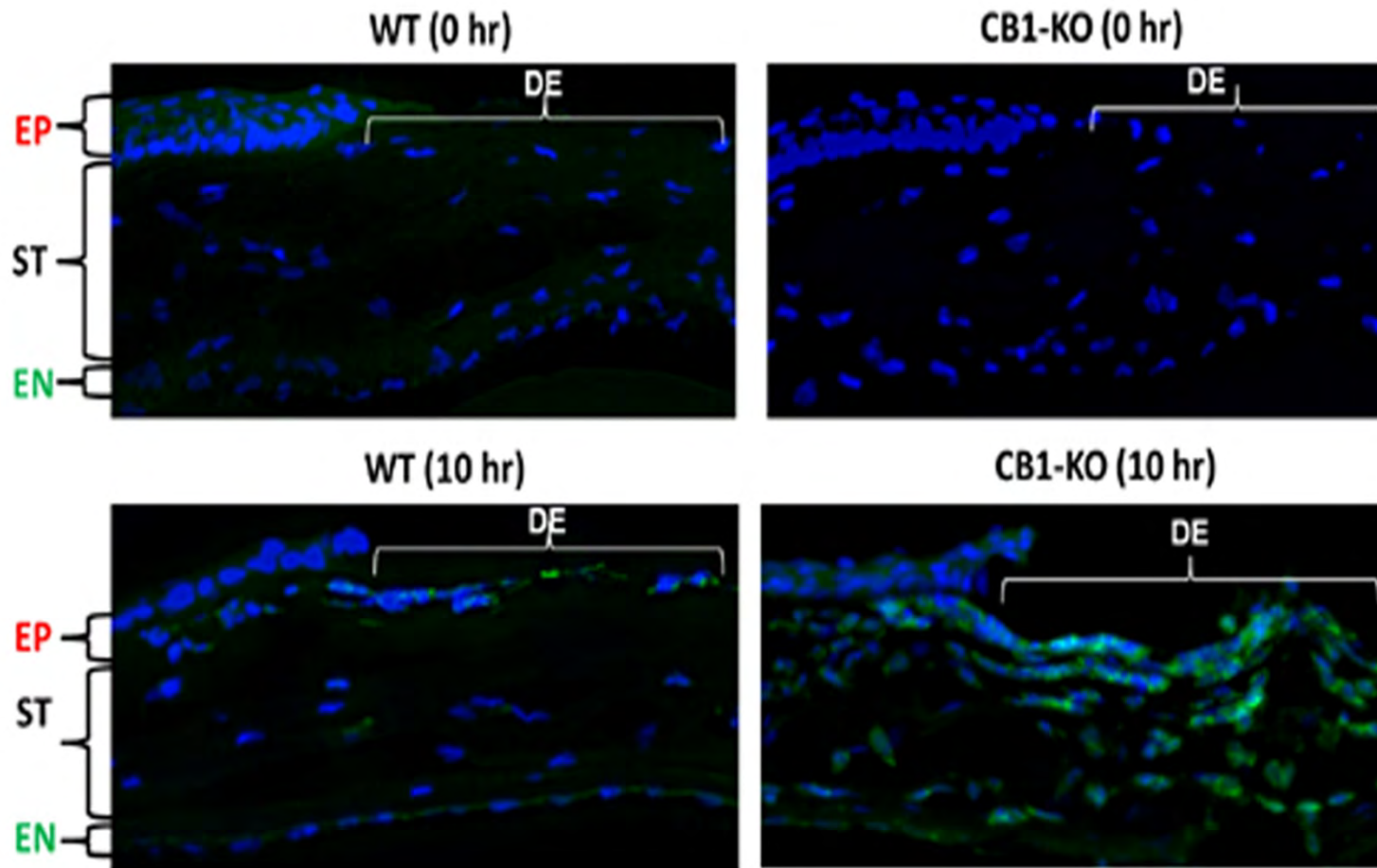*:p<0.05

■ WT
■ TRPV1 KO

12   24

hrs

Appendix I
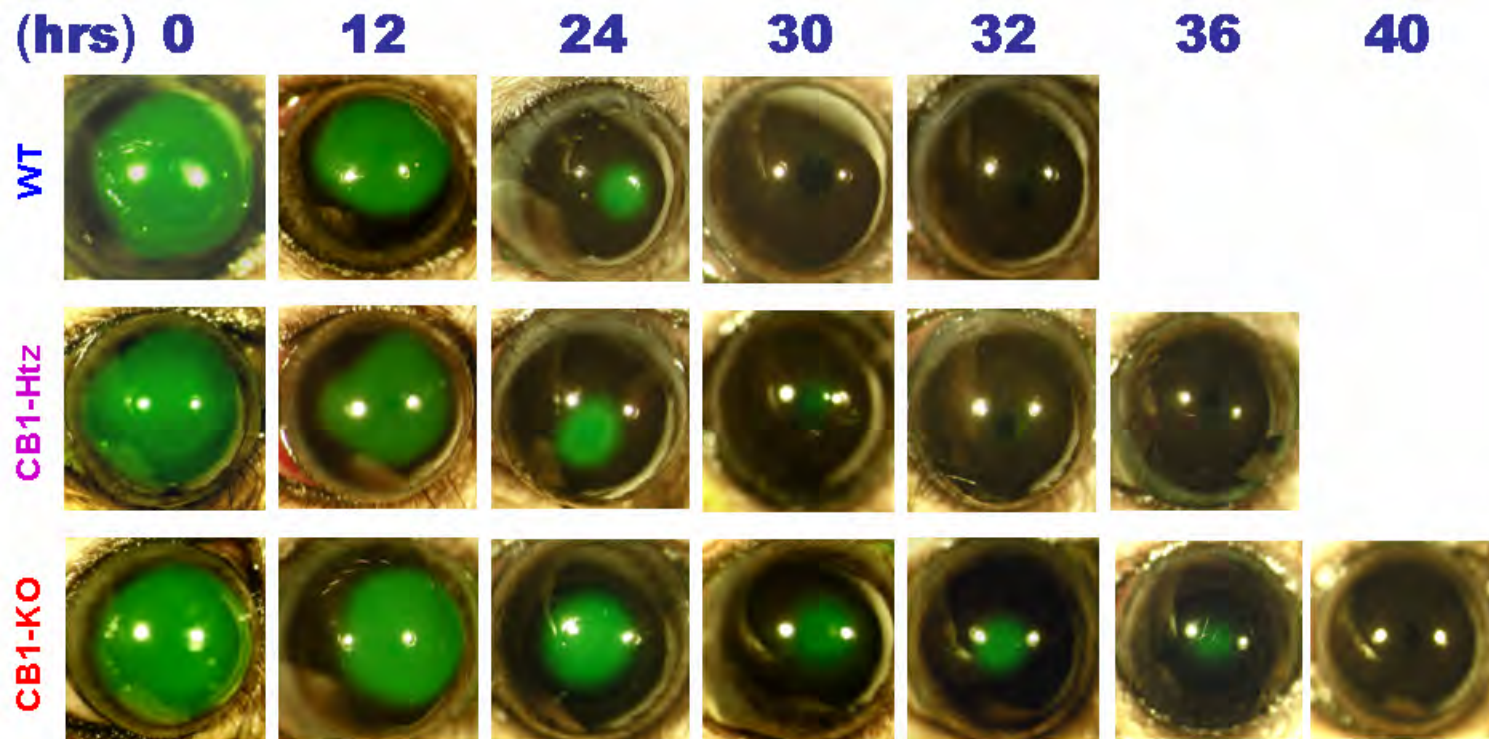
Epithelial defect

Appendix J

CB1 activation reduces stroma neutrophil recruitment

Appendix K

CB1 ablation delays mouse corneal epithelial wound healing

WT- Wild Type ~32h
Htz- CB1 heterozygous Knockout ~36 h
KO- CB1 homozygous Knockout ~40 h